Maximizing Performance from Loudspeaker Ports

Alex Salvatti and Doug Button, JBL Professional
Allan Devantier, Infinity systems
Northridge, California

There is a current trend in the marketplace for loudspeaker ports to have a more aerodynamic appearance. This may be as much for appearance as for performance reasons. However the sharp discontinuity at the end of a traditional port does create turbulence at high drive levels as air is drawn into the port. As well, the axial cross-sectional shape of the port can have an influence on the turbulence generated on the air as it exits the port. Ports altered to provide a more aerodynamic shape to minimize turbulence for inlet and exit air streams show performance improvements in efficiency, compression, maximum output and distortion reduction and will be outlined herein. The ideal shapes for high velocity inlet and exit air streams are different and the best solution is one that balances both. Additionally, turbulence is actually preferred in matters of cooling the box through heat exchange via the air in the port.

0. Introduction

Loudspeaker ports are generally used to augment the low frequency acoustic output by supplying a Helmholtz resonator via a port/vent. At resonance, the inertance of the vent resonates with the compliance of the air in the cabinet and the system acts as an acoustic impedance transformer presenting a high impedance to the rear of the loudspeaker cone and a low impedance to the air [1]. This increases acoustic output over a limited low frequency range over a sealed box design. Several complications occur in vented designs as output is increased beyond the point where the air in the port is able to respond in a linear fashion. These include undesirable extraneous noises generated within the port as well as acoustic compression and distortion. These generally broadband "chuffing" noises due to fast moving air have been dealt with in recent years (actually since the late seventies, see ref [2]) by rounding the port ends with various radii which leads to the now common flared port.

Recent studies by Vanderkooy [3,4], Backman [5] and Roozen et al [6] suggest performance advantages can be achieved by providing a more aerodynamic profile through the length of the port. Additionally, having this aerodynamic profile on both the entrance and exit of the port is important.

The tapered port also behaves as if it is longer than a straight ducted port, which is very useful for use in compact systems when port length is often restricted. Our investigational method for measuring port performance utilizes a microphone for pressure measurements and a hot wire anemometer for velocity. Extensive bench-marking of current designs reveals that current attempts at high output ports suffer from compression effects at high drive, showing that at very high levels all ports eventually 'lock up' limiting maximum

output. At very high drive levels the air in the port becomes turbulent. The measurements show the velocity and pressure moving from a reactive relationship to a resistive one at high levels. At these levels the output from the port is 180 degrees out of phase with the output of the cone creating a nearly complete cancellation of low frequency energy.

The document herein will include a preliminary discussion on the history of loudspeaker port performance and theoretical issues. Then 10 studies will follow leading to some general conclusions about designing ports for maximum performance.

Study #1 will examine port compression in straight vs. radiused ports, showing that the former compresses to a much greater degree.
Study #2 expands on the first by developing the utility of the Reynold's number as a general description of flow dynamics and proposes the "Wall".
Study #3 introduces a novel method to model a generalized flared port and presents an empirical formula to accurately predict the tuning of any flared port.
Study #4 explores port compression among various flare rates showing that there is a tradeoff between greater output at low levels vs. output at high levels.
Study #5 examines how port profiles affect distortion, finding that once again there exists a tradeoff between good performance at low SPL and high SPL. We discuss the effect of port profile on odd order distortion and the implications of port symmetry on even harmonic distortion.
Study #6 discusses velocity profile measurements made across different ports and how the results point to one profile as a preferred condition.
Study #7 tests the hypothesis that port wall roughness imparts some performance improvements, finding that in fact roughness is detrimental to distortion and compression.
Study #8 presents the same type of data as studies #4 and #5 using a different mathematical port profile but shows that the same conclusions and tradeoffs apply.
Study #9 expands on the importance of port symmetry for lowest even order distortion.
Study #10 concludes the work by discussing the thermal implications of port design and placement, introducing the concept of port turbulence as beneficial to cooling.

1. History

As early as 1980 (Laupman [2]) patents started surfacing suggesting that flaring the end of ports was beneficial (figure 1). As well, there are many good studies on turbulent effects in pipes dating back much further. Ingard [7] 1968 shows the nature of compression and distortion on orifices. Figure 2 From Ingard shows the compression effects on the SPL with increasing input. Figure 3a shows the harmonic content from a symmetrical orifice driven at high level. Note that the odd harmonics are much stronger. Figure 3b also shows how at very high velocities the quadrature (reactive) relationship between the velocity and pressure in the orifice disappears and the two are nearly in phase at high levels. This is particularly interesting because if the port pressure is in phase with velocity, the output of the port (which is now in phase with the back side of

the cone) will be 180 degrees out of phase with the front of the cone. *In this condition the output in the far field could approach zero in a bass reflex speaker.*

Extensive studies by Young [8] in 1975 and Harwood [1] in 1972 outline expected performance limitations of traditional straight ports. Young points to a maximum velocity of about 10 m/s before serious sonic detriment to the signal. In figure 4, Harwood shows the maximum allowable SPL vs. pipe diameter before appreciable distortion ensues. Both authors point to a need for ports to be large in order that they produce greater SPL before losses and distortion become intolerable, the bottom line being to limit the velocity to below about 10 m/s. Both allude to turbulence being generated as the Reynolds number becomes too high, this being the cause for onset of performance degradation. The degradation takes on the form of broadband noise, harmonic distortion and compression.

More recently Backman [5] 1995 shows the effects of adding very small radii to the ends of ports. The study shows a reduction of the distortion even by adding this small change. Figures 5 & 6 show the difference in distortion and compression measured by Backman by radiusing the ends of the ports. Recent patents by Roozen et al [6] show a rather slow taper as being optimum. As well, Roozen displays some very informative FEA plots in figures 7 & 8 showing the vortex shedding on a highly radiused port and an slow taper port. The more flared port shows the vortices being generated inside the port, while the straighter port shows the vortex shedding occurring nearer the port ends. Also, the magnitude of the vortices is less in the slow taper port.[1] This study shows that for high *exit* velocities a slower taper may be required but it neglects to take into account that as an *inlet* a more extreme flare might actually be preferred. Granowski's patent [9] 1998 (figure 9) claims that an ellipsoidal flare is preferred. A further invention outlined in patents by Polk et al [10] (figure 10) and Goto [11] (figure 11) describe radiused ports with a plunger on the exit that smoothly directs the port velocity 90 degrees in all directions to the outer periphery of the port. The previous study by Backman [5] showed that forcing the air to make any kind of turn will cause turbulence to occur at lower levels and is to be avoided if possible. However, these designs may have the great benefit in making the port effectively longer and useful in redirecting the airflow that might otherwise shoot straight into a wall or floor.

Figures 12 and 13 are from a patent by Gahm [12]. The basic invention is a modular kit for making port tubes with radiused ends. Figure 13 is particularly interesting as it shows a method for using the port velocity to cool the loudspeaker driver directly.

The most recent (and extensive) work on the topic comes from Vanderkooy [3,4,13]. This work shows detailed measurements of port velocity & pressure waveforms and waveform analysis, as well as outlining a detailed methodology for taking the data. In figures 14 and 15 we see the waveform distortion at progressively higher levels of a straight vs. radiused port. Note that the straight port develops a rather asymmetrical waveform with high levels of both odd and even harmonics. The radiused (at both ends) port however generates a more symmetrical wave resembling a square wave with largely only odd harmonics. In figure 16 Vanderkooy reports on compression effects on several ports with

[1] For more information on vortex shedding see reference [6].

a variety of interesting mathematical descriptions. While no one profile stands out as superior, an interesting observation of the data shows (also shown by Backman) that at medium to higher levels, a small amount of gain takes place before compression sets in. This might suggest that boundary layer separation is beginning but is very small and provides a more aerodynamic flow situation for the air in the center of the port that is still laminar. Vanderkooy was also able to develop a model and supporting measurements that show that at high SPL's the in-box pressure and port throat velocity in the port come in phase, supporting Ingard. This clearly supports the earlier contention that at high levels the output from port will be out of phase with the front of the driver in a bass reflex enclosure and will add additional compression, possibly completely canceling the fundamental. *The port is now simply a leak in the box*. As the cone moves inward, air exits the port in the opposite direction and the resulting volume of air displaced is reduced. Vanderkooy shows detailed measurement and analysis of the *exit* jet formation at high levels that support much of the analysis of Roozen. It is also important to closely examine the dynamics of the air during the *inlet* stroke.

2. Fluid flow Theory

Fluid flow is a very complex field and rigorous solutions to some problems, such as the fine scale random fluctuations in turbulent flow, defy closed form solutions. In fact, there are no analyses, not even computer solutions which exist to completely describe turbulent flow. Luckily, there are some simplifications which can be made for the flow in loudspeaker ports. The most important is the assumption of ***incompressible flow***, i.e. density fluctuations are negligible. This simplifies the general continuity equation:

$$\frac{\partial r}{\partial t} + \nabla \cdot r\tilde{v} = 0 \qquad (1)$$

where;

r = Density of air
v = Velocity

to:

$$\nabla \cdot \tilde{v} = 0 \qquad (2)$$

For air at standard temperature and pressure, this is a valid assumption when the velocity is less than the commonly accepted limit of *Mach number* **Ma** < 0.3, or a velocity of less than about 100m/s. This is the case for all loudspeaker applications.

The definition of a *Newtonian fluid* is that forces due to viscosity are proportional to rate of deformation. Toothpaste is Non-Newtonian because one must apply a large amount of force to get the flow started, but then it flows easily. Air and water are Newtonian. The

primary parameter used to describe the behavior of all Newtonian fluids is the dimensionless *Reynolds number*, **Re**. For flow in a circular pipe, the pipe Reynolds number is:

$$\mathrm{Re}_d = \frac{rvD}{m} = \frac{inertial\_forces}{viscous\_forces} \tag{3}$$

where;

D = the diameter of the pipe.
m = viscosity of air

In oscillating flows, the dimensionless *Strouhal number* **St** is also important and is defined as:

$$St = \frac{wL}{v} = \frac{frequency}{mean\_speed} = \frac{port\_radius}{particle\_displacement} \tag{4}$$

Where:

w = Angular frequency
L = characteristic length (i.e. port radius)

According to Peters et al. [14] values of $St \leq 1$ lead to flow separation, vortices, and jets.

Flow can be laminar or turbulent, with the commonly accepted transition between the two occurring near Re_d = 2300 for pipes. This value is accurate for commercial pipes, but the critical Re can be much higher if the pipe has flared ends or has smooth walls. For example, even for a rather large 4" port tube, this would predict that turbulence would commence at velocities above 0.35 m/s, a very low velocity indeed. A practical upper limit for Reynolds number obtainable in loudspeaker ports is on the order of 100,000.

Turbulence can be defined as an eddy-like state of fluid motion where inertial vortex forces of eddies are larger than other forces such as viscous or buoyant which arise to damp the eddies out. It leads to random fluctuations in the flow velocity, with amplitude variations up to 20% of nominal with a very wide frequency bandwidth of "noise" components up to 10kHz. What physically causes turbulence? It occurs when viscous forces are unable to damp out the non-linear inertial vortex forces $\tilde{v} \times \tilde{w}$ that arise in the pipe:

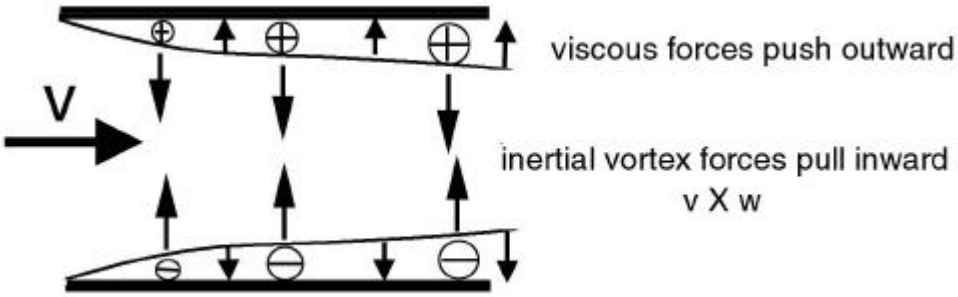

In the diagram above which shows viscous pipe flow, the flow is to the right, and the vortex rings appear clockwise looking downstream. Note that the direction of the vortex forces is inward and these are balanced by the viscous forces which are directed outward as shown. This equilibrium is delicate and can be upset as velocity increases. Beyond a critical value of Re_d any small perturbation will cause eddies to form which are too large to be damped. These tiny eddies will cause other eddies to form in the opposite direction which will then pair up. The swirling eddy pair will similarly lead to other eddy pairs, the two of which will pair, etc., from small scale to large, growing larger until the entire pipe is full of eddies of all sizes and the flow is fully turbulent.

At high Reynolds numbers viscosity can generally be neglected except in the thin layer of fluid that forms along solid boundaries which is aptly called the "boundary layer". Here, viscosity effects are significant. The velocity profile across the boundary layer varies from 0 (there is no slip between the boundary and the layer of fluid immediately adjacent) to 99% of the free stream velocity at the edge. The typical width of a boundary layer in ports would be on the order of 1mm.

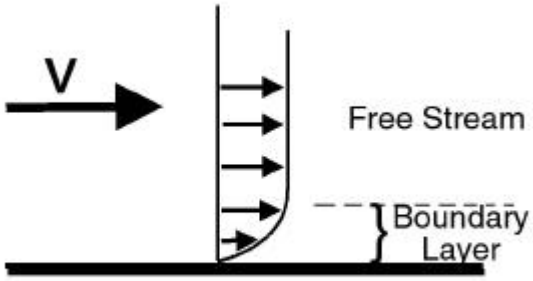

When the fluid boundary converges, such as through a nozzle, the flow is essentially squeezed down into a smaller area. The velocity increases and the pressure decreases. This is called *a favorable pressure gradient,* such as the inlet of a flared port. When the boundary diverges, such as the exit of a gently flared port, (a so called unfavorable or *adverse pressure gradient*) the fluid is forced to lose velocity and gain pressure as the boundary layer hugs the wall. If the flare is too extreme, however, the deceleration of the flow is too great and causes the shear stress at the wall to approach 0. If this happens, the flow runs out of momentum at the boundary and local flow reversal occurs.

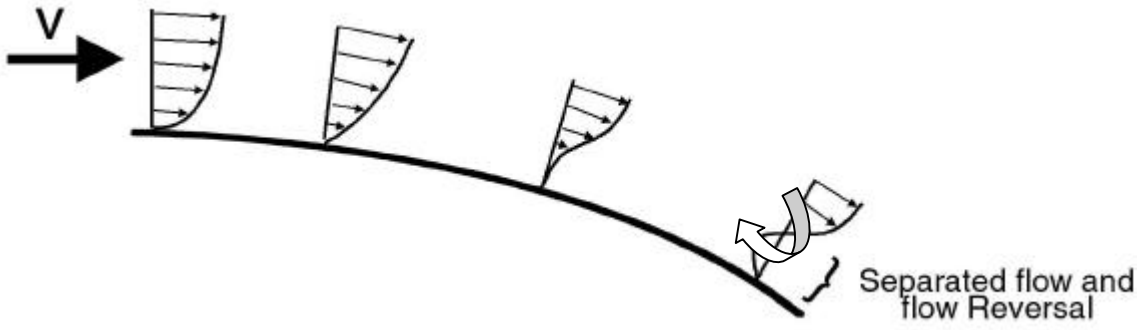

When the momentum goes to zero, the pressure gradient becomes so large that undesirable flow separation occurs along with the localized reversal. Theoretically, this separation of the acoustic flow leads to output-robbing vortices which sink the acoustical energy into the kinetic energy of the vortex. This energy is then uselessly dissipated by friction instead of acoustic propagation [14]. Note that the above situation cannot occur on the other half of the period when the flow is going in the opposite direction because *flow separation cannot occur when there is a favorable pressure gradient* (area is decreasing).

Boundary layers may be laminar or turbulent as well. Turbulent boundary layers have the desirable quality of being able to withstand higher pressure gradients without becoming separated. This is because the turbulent layer has the larger wall shear stress and higher momentum near the wall. This extra momentum near the wall allows a turbulent layer to withstand the unfavorable pressure gradient without separation. How does one cause the boundary layer to become turbulent? Some of the factors which would tend to cause transition to turbulence include free stream disturbances, boundary roughness, pressure gradients, or vibration. Obstructions in the boundary layer also hasten the onset of transition.

Some experiments performed by Merkli [15] found that for oscillating flow, turbulence does not occur over an entire cycle, rather it occurs in the form of periodic bursts followed by "relaminarization" during the same cycle. They plot a factor

$$A = \frac{2v}{\sqrt{\frac{mw}{r}}} \tag{5}$$

and find a critical value $A_c = 400$ above which transition into turbulence occurs. Their study was limited to the frequency range away from the resonance of the pipe ($1.1 < \frac{f}{f_{res}} < 0.9$), while we are mainly interested near resonance where acoustic port output is greatest.

Vorticity Ω is defined as the curl of the velocity vector. Physically it is equivalent to the rate of angular deformation. If $\nabla \times \tilde{V} = 0$ then there is no angular deformation in any plane at any point. Circulation Γ is defined as $\Gamma = \oint \tilde{V} \bullet dl$. Physically, circulation is

the flux of vorticity. If $\Omega = 0$ then the flow is irrotational. This is the case outside the boundary layer if we neglect the coriolis force and gravity. The boundary layer is definitely NOT irrotational. These assumptions simplify the momentum equation to the unsteady Bernoulli equation.

To make a detailed analysis of airflow in a port and develop a design approach it is important to understand the fluid flow dynamics in both directions. The preferred geometry for each may be in conflict as the intake stroke would be well served with a large radius providing a *slow head loss* and *favorable pressure gradient,* and exit would be well served with a more gradual flare to avoid an excessive *adverse pressure gradient.*

3. Study #1: Power Compression on Straight vs. Radiused ports

The first study done several years ago by the authors was to simply make a side by side comparison of the power compression of a straight vs. radiused port. Previous work by Gander [16], Harwood [1] and Young [8] clearly pointed out that all ports do power compress at high levels. As mentioned before, radiused ports have become something of a fashion and the authors intuitively concluded that they should also have superior fluid flow properties (at least on the inlet air stream) and subsequently less compression. Shown in figures 17, 18 and 19 are the compression vs. level of a straight 6" long, 3" diameter port vs. the same port with large radii on the inside and outside. The different plots are at different frequencies 25, 30 and 35 Hz. The port was driven by two 12" high excursion woofers in a 2 ft^3 box. The tuning frequency was about 30 Hz. The input voltage and current were monitored to account for thermal compression effects and the output is plotted vs. actual input drive power. The microphone was a small ¼" B & K microphone spaced about 4 inches away from the port on axis. This was determined to not interfere with the airflow yet give a high enough port-to-driver output ratio that good results could be seen. A number of observations can be made from this simple experiment.

The first and most obvious is that the radiused port compresses substantially less at moderate levels of operation than the straight one. As well, at lower frequencies (higher velocities) the effect is much more pronounced. There also appears to be a "wall" which neither port is able to go beyond. The conclusion is that this wall exists at the point where the air in the port becomes completely turbulent. Another observation is that about 8 dB more output can be obtained before 1 to 2 dB of compression sets in. A close examination of the curves suggests an increase or expansion in the medium area of operation of a half dB or so. This implies that at medium levels the radiused port might have a small boundary layer separation that acts as an 'air bearing' and actually reduces losses in the port.

Most of these conclusions are basically correct but need some adjustment. Previous work by Strahm [17] following from Young [8] show that the impedance minimum at port resonance rises as a port compresses. This means that the power delivered to the speaker will go down even if the drivers do not thermally power compress. Since the plot is based

on the real power to the drivers, and the straight port begins to compress very early on, the impedance will rise and the compression will appear to be worse. The rise in output in the middle range was also witnessed by Vanderkooy [3] confirming that this data is correct. The bottom line is that the difference between the two may not be as much as this experiment suggests, but the radiused port is still much better. Nevertheless, the issue is clearly velocity related, and boundary layer separation is quite possibly involved at lower levels.

4. Study #2: Port Compression vs. Reynold's number

The previous study and historical work suggest that port performance and maximum output capability is related to the velocity in the port. In the process of working toward developing ports with optimum performance, the next step is to confirm that turbulence is in fact the culprit and to develop a simple measure of when that turbulence is too great for desirable acoustical performance.

This study involved the measurement of the velocity of the airflow in three large subwoofers with two 18" drivers in each. A hot wire anemometer was placed in the center of the port of three very different port designs. The SPL was again measured with a small ¼" microphone a few inches from the port. Of the enclosures tested, one had a large single rectangular port, one had 3 circular ports and one had 4 rectangular ports. None had any radii. The area of each port was different in all cases, the boxes tuned differently, and each had differing volumes. The question was, what figure of merit could be applied to all subwoofers that would clearly show a relationship to power compression that would be independent of design?

The conclusion was to take data on the velocity in the middle of the port. The velocity measurements would then be converted to a Reynolds number for each of the designs and then plotted vs. compression. Figures 21, 22 and 23 show the compression vs. Reynold's number of each of the designs. What stands out is, for the most part, all three designs show nearly the exact same compression curve at all frequencies tested. All designs seem to hit a wall near a Reynold's number of about 50,000-100,000. This number was also confirmed by Vanderkooy [3]. The Moody chart (figure 20) shows this to be in the transition zone. The conclusion is that compression is clearly related to turbulence and that a Reynold's number of about 50,000 is good indicator of when the system begins to degrade.

5. Study # 3: Modeling flared ports and prediction of tuning

Everyone from piping system engineers to carburetor designers know that pipe entrance losses are highly dependent on geometry. Interestingly, exit losses are independent of geometry. However, audio signals by definition are oscillating and therefore both sides of a loudspeaker port are "entrances" and would benefit from rounding of the edges. *A well rounded entrance (**radius = 0.2 x diameter**) yields a very low 5% loss, while a sharp entrance asymptotically reaches 50% loss.* (Figure 24)

The main difficulty in modeling flared loudspeaker ports is the infinite variety of profiles that will yield the same port tuning. Many loudspeaker designers choose not to experiment with flared ports because without a well-defined diameter to plug into the standard port tuning formula, they are left to design by trial and error. There are no CAD programs which incorporate the ability to design flared ports as of yet, however there is a growing demand to take advantage of flared ports and a need to predict their performance is required.

The tuning of a port, flared or otherwise, is a function of the port cross sectional area to port length ratio. For a standard straight cylindrical port and neglecting end corrections, there are several equivalent embodiments of the port tuning equation:

$$f = \frac{1}{2p}\sqrt{\frac{gP_0A}{rV_bL}} = \frac{c}{2p}\sqrt{\frac{A}{LV_b}} = \frac{c}{2p}\sqrt{\frac{r}{m_{ap}V_b}} \qquad (6)$$

where g=7/5 for air, P_0=101000 Pa, r =1.2 kg/m^3, V=box volume, L = port length, m_{ap} = acoustic mass of air in port[2]. Notice the A/L ratio enters directly with other non-port parameters.

For the generalized case of ports with any cross section, one only needs to find the *effective* A/L ratio to find the actual tuning frequency. Vanderkooy has shown the formula for this to be

$$\left[\frac{A}{L}\right]_{eff} = \frac{1}{\int_{-\frac{L}{2}}^{\frac{L}{2}} \frac{dx}{A(x)}} + E_c \qquad (9)$$

Where A(x) is the area function and E_c are any end corrections. The difficulty for flared ports arises in finding the correction E_c. End corrections are needed because the radiation impedance of a port is not zero, the free ends of which act as a vibrating diaphragm. Since the radiation impedance is small, however, the effect is merely to increase the effective length of the tube by an amount d. This d is relatively constant over a wide range of driving amplitudes. For traditional straight ports, d is a well-known quantity, equal to 0.61a for a free end and 0.85a for a flanged end, where a is the port radius [18] (p.131)

[2] The acoustic mass reactance in the port m_{ap} in units of kg/m^4 is given by:

$$m_{ap} = \int_{-\frac{L}{2}}^{\frac{L}{2}} \frac{r}{A(x)}dx + E_c \qquad (7)$$ which simplifies to $$m_{ap} = \frac{rL_{eff}}{pa^2} \qquad (8)$$

for a standard cylindrical port.

Flared ports, however, do not have a well-defined diameter and so d is not so simple. In effect, the end correction is a measure of the inertia of the flow at the exit. Given that each port shape has a different correction, is there any hope of developing a generalized port tuning equation? Some method of approximating a general port flare would need to be devised so that the effect of "amount of flare" could be studied. For simplicity, we chose to investigate flare profiles described by a simple radius. Using this simplification we can define a "Normalized Flare Rate" or NFR as the ratio of overall port length to flare radius:

$$NFR = \frac{port\_length}{2(flare\_radius)} \qquad 0 < NFR < 1 \qquad (10)$$

Thus a straight port would have a NFR of 0.0 and very extreme port with a full radius would have an NFR of 1.0 (figure 25). Most port profiles can be approximated with an NFR in this range. This normalization of scale allows the results to be generalized to any size port.

An initial samples of 6 port tubes, all of length 120mm and minimum diameter of 60mm were made with NFR's of 0, 0.125, 0.25, 0.5, 0.667, and 1.0. In addition, all profiles had a small 12mm blend radius on both ends to avoid sharp edges, as well as a 140mm inner baffle for symmetry.

Unexpectedly, port tuning frequency was only weakly dependent on flare. Clearly, *the port length and minimum throat diameter appear to be the main determinates of tuning.* As port flare becomes more pronounced, the end correction, as typically calculated based on the radius at the mouth, overestimates the reactive air mass present. A better way to predict tuning appears to be basing the length correction on minimum throat diameter instead of maximum diameter. Following this path, fitting the experimentally determined tuning frequencies to a function of the flare radius leads to a striking linear relationship (r^2=0.98) between NFR and effective port area. (figure 26). The data fit yields port tuning predictions within 2% for all 6 ports made, and within 5% for all other port profiles yet tested including elliptical and exponential profiles. Of course, the prediction accuracy is better the closer a given profile can be approximated by a simple radius. The formula is:

$$f = \frac{c}{2p}\sqrt{\frac{A_{eff}}{L_{eff}V_b}} \quad \text{where} \quad Aeff = \left[1 + 0.576\underbrace{\left(\frac{L_{act}}{2r_{fit}}\right)}_{\text{“NFR”}}\right]A_{\min} \quad \text{and} \quad L_{eff} = L_{act} + D_{\min} \qquad (11)$$

where c = speed of sound, L_{act} = actual port length, r_{fit} = best fit flare radius, A_{min} = minimum throat area, D_{min} = minimum throat diameter, and V_b = net box volume

The only difficulty in using this formula is finding the best fit flare radius to a given profile, but even this is relatively easy using the built in optimizers in most spreadsheet software.

6. Study #4: Acoustic Compression

As SPL demanded of a port is increased, there is no escaping some degree of port compression. The question becomes how port flare affects this compression, if at all. As previously described in earlier sections, turbulence is most likely the culprit. One effect of turbulence in a port is a reduction of the Q of the resonance. This causes a drop in the acoustical output at resonance.

In order to explore this phenomenon, another test enclosure was constructed as a bandpass box with a ported chamber volume of 0.201 cubic meters, and a sealed chamber volume of 0.1113 cubic meters. Constructed of 1" MDF with a single high throw 18" woofer, testing conducted with this box would effectively remove acoustic contributions from the transducer (as it is buried within the box), leaving only port output (figure 27) Box loss Q_L was measured by the Thiele method at over 14, indicating a very rigid, low loss box.

Initial trials were made to find the best microphone placement to measure compression (see Vanderkooy [13] for an extensive investigation). The tests were conducted with the microphone at the port mouth, inside the box, and at 2m measured on a ground plane. The data shows that the compression measurements are very similar in all cases (figure 28). The cleanest data is the inbox measurement, so this method was chosen for the experiment. In-box acoustic measurements were performed using a B&K 4136 ¼" microphone, which has a 3% distortion limit of >170dB SPL. To prevent transducer power compression from contaminating the results, a very high power driver with minimum power compression in the test range was employed. The transducer was driven using a large power amplifier in bridged mode which can provide 2kW of output into 4 ohms. Most measurements were made over a frequency range of 10Hz to 100Hz using a 15 second sweep. Each port was driven at successively higher voltages in 6dB increments beginning at 1.25V and ending at 40V. The curves were then mathematically lowered by the amount the input power was increased so that the curves would overlap, except for compression effects. The results from all ports are shown in Figure 29. These results show that there is no compression at the end of the sweep so we can be sure that all compression shown is solely due to the port. Despite the fact that all ports compress, the way they compress appears to be different. The largely radiused ports not only compress in level but the frequency of the resonance shifts. It is suspected this happens because the port becomes effectively shorter as it starts to be come turbulent, a confirmation of Vanderkooy's contention that end correction change with level. The section of the port area near the ends has severe boundary separation due to the *adverse pressure gradient* as predicted by Roozen. The air in this section is largely turbulent and is not part of the acoustic mass of the port. The port is thus effectively shorter and tunes higher. Of additional interest is that the largely radiused ports have higher output at low levels. The

Q of the port is clearly higher and losses are less. The straighter ports show less frequency shift, but in the straight port the compression and losses are relatively high, especially at low levels. An optimum solution strikes a balance of minimizing frequency shift and compression. The port with an NFR of 0.5 appears to find this balance.

In addition to the set of 6 ports made for the study of section 5, other profiles were measured for compression, including elliptical, exponential, and polynomial flares. All ports tested had the same minimum throat diameter of 60mm and length of 120mm so that a legitimate comparison could be made. Figure 30 shows the compression measurements of all ports. Without exception, all ports measured showed severe compression of about 10dB at port tuning at 40 Volts. Despite how closely grouped the data is, suggesting that any moderate amount of flaring is good and that there is no clear winner, there were some differences noted. The most obvious conclusion is that a large amount of radius is clearly better at lower levels. Also, it appears the more extreme the port flare, the worse the compression at high levels. In addition, the straight port starts out with about 2dB less output than any flared port but compresses less dramatically than would be expected. A close examination points to a "sweet spot" where a moderate amount of flare (NFR near 0.5) works better than all others.

7. Study #5: Distortion Measurements

Probably the single most remarkable characteristic of flared ports over straight is the marked reduction in distortion which can be achieved. It is clear that aerodynamic profiles are much quieter than their straight counterparts, but once again we can question whether a particular profile has advantages over any other.

To answer the question, another enclosure was built as a bandpass box that could be mounted in a 2π anechoic chamber to maximize S/N ratio, as shown in figure 31. A very long throw 15" woofer was used to excite the ports. Harmonic distortion was measured using a sine source set to the tuning frequency of each port in the vented test enclosure. MLSSA was used as a digital storage scope to capture several cycles of the acoustic output from a distance of 1m to the port. The microphone was placed 45 degrees off axis to avoid contamination from jets. An FFT was applied to the captured waveform and the amount of energy at the desired frequency multiples was calculated. The test was repeated for increasing input voltage in 1dB increments until the limit of the amplifier was reached at 40V. Results were examined for odd harmonics, even harmonics, and THD (all harmonics). Although noise is the most obvious artifact, non-harmonic noise was not considered for this experiment because early testing showed that port differences are captured well with harmonic analysis (figure 32a). In all cases, most harmonic distortion occurs in the odd harmonics, with all ports examined having about the same low amount of even harmonics (figure 32). Examination of these results shows that port symmetry (i.e. adding a baffle on the inside port end) is important for minimizing this type of distortion. As expected, a low even harmonic content is found in symmetrical ports. Odd harmonic content, however, is strongly affected by port flare geometry. In these experiments, straight ports are clearly inferior to ports with even the gentlest flare.

As for flared ports, the results generally show that at lower acoustic levels, greater port flares yields lower distortion, with the NFR=1.0 port performing best as it is the least lossy as shown in the previous section.

At higher levels near 100dB at 1m, ports with moderate flare lead the pack with NFR=0.5 optimum.

At very high levels (over 100dB at 30Hz from a 2.5" port), however, it is apparent that *too much flare causes more distortion than gentler flares*. Surprisingly, standard straight ports do not fare as poorly at high levels as would be expected. In fact, very gentle flares are worse than no flare at all!

There appears to be an optimum. A moderate amount of flare for best overall distortion performance is required. This profile is a compromise for best performance over the entire amplitude range. Once again, the optimum normalized flare rate is near 0.5.

8. Study # 6: Velocity Measurements and Jet Formation

As discussed in earlier sections the air velocity in ports is intimately related to performance. In order to explore the velocity magnitude and distribution across the face of flared ports to see the change in profile toward formation of jets, a hot wire anemometer (TSI model 8360) was used to measure air velocity across the 6 ports mentioned. Measurements were mainly performed at the mouth in the baffle plane. Velocity profile across each port mouth was measured for increasing input power into a test enclosure which was a 24" cube made of 1" MDF with four 18" high power woofers, as shown in figure 33. One side was fitted with a cutout to accept interchangeable baffles. Based on the 2-3" minimum port throat diameter selected, the four woofers undoubtedly would be sufficient to create the required volume velocity needed to fully characterize each port for air velocity measurements. The transducers were driven using a large power amp in bridged mode which can provide 2kW of output into 4 ohms. Measurements were made near port tuning were velocity would be greatest. As can be seen in figure 34 and 35, the measurements tend to confirm previous work indicating that at low to medium levels, the air velocity is greatest near the port walls and a ring of high velocity is forming with less on the port axis. At high levels when jets form, however, this behavior is not present and velocity magnitude is greatest at the port center. What is interesting to note in figure 35 is that at high velocities the straight port and the most gently flared ports have the highest velocity across an area that maps to the center hole diameter and then rapidly drops off suggesting a clear jet has formed. They seem to exhibit very similar maximum velocity numbers and this transition is at about 10 m/s as predicted by Young. On the other hand the most radiused ports have a much more evenly distributed velocity profile with a lower maximum velocity possible suggesting more compression, but maybe not, as the total area under curve looks to be similar. The one port profile that stands out as having the best of both worlds is the port with the 120mm radius (NFR of 0.5). The "area under the curve" approaches a maximum suggesting the

least amount of total compression and most maximum output. This study as well points to a balance of conditions for inlet and outlet airflow preferences in geometry.

9. Study #7: Roughness experiment

One might think that smoother surface textures in ports would directly result in higher performance. However, since Coulomb's experiments from the 1800's it has been known that surface roughness has an effect on friction resistance. Interestingly, the effect is negligible in laminar flow but not if the flow is turbulent, i.e. surface roughness effects would be evident only at the higher port velocities. If reduced drag is desired, a rough surface will actually perform better due to boundary layer effects. This is the reason why golf balls have dimples – the surface roughness is intended to "trip" the boundary layer so it will go turbulent at a lower Reynolds number (in flight the Re of golf balls is about 100,000). The turbulence causes the separation point to move from the front to the back of the golfball, thereby reducing drag and allowing a farther flight. There are now even commercially available subwoofer loudspeakers which use a flared port with dimples, similar to a golf ball. Figure 36 of a bowling ball entering the water at 25 ft/s demonstrates how much larger the wake is on the smooth ball, vs. that of the surface roughened ball on the right. Notice also that the separation point has moved farther back.

Another example of intentionally induced turbulence is often seen on the top surface of airplane wings near the leading edge. These "vortex generators" are also used to prevent boundary layer separation, which could cause the wing to stall under high lift conditions such as during landing.

In fluid mechanics, surface roughness is characterized by the dimensionless *Roughness ratio:*

$$\frac{e}{d} = \frac{Wall\_roughness}{diameter} \tag{12}$$

Small changes in the roughness ratio can lead to very large effects in the turbulent flow region. To test the hypothesis, we constructed 5 copies of the best performing port (NFR=0.5) then affixed precision glass beads of various sizes ranging from 1mm to 2.5mm to the inside port walls using a spray adhesive. This corresponds to a roughness ratio range from approximately 0.01 to 0.042 on the Moody chart. These ports were manufactured such that the volume occupied by the beads was accounted for, see figure 37 for picture of a typical textured port from the study. These ports were then subjected to the same distortion and compression tests described earlier. Contrary to expectation, over the range of roughness examined, rough ports were generally inferior to the smooth walled port. Rough ports had more harmonic distortion above 95dB at 1m . Only in a very narrow range between 90-95dB did wall roughness give a marginal improvement in odd harmonic distortion. At all other levels, the smooth walled port performed better (see figure 38)

Based on the fluid mechanics literature [22], we expected to see the benefit of rough walls in the acoustic compression measurement. Unfortunately, roughened port walls failed to show any advantages here as well. In fact, figure 39 shows all rough ports were consistently compressing about 1-1.5dB more than the smooth port. These negative results may be explained by noting that even at the highest Reynolds numbers near 100,000, the Moody chart predicts that we are only just entering the transition region and have not reached the fully turbulent region where roughness would be expected to make a large impact. Based on these results, it does not appear that roughening the wall in this range buys any extra performance.

10. Study #8: Polynomial Flare Rate

Taking a slightly different approach to defining the flare rate we chose to use a polynomial expression to define the port profile instead of a simple radius. The purpose of this experiment is to determine the effect of flare rate on port performance to see if an optimum solution might exist by approaching it from a different angle. As well it was desired that all ports tune to the same frequency so that it would be a tightly controlled, legitimate comparison. This tuning requirement dictates that the ports would have different minimum throat diameters in order to achieve identical m_{ap}'s. Recall that all ports from the previous studies had identical minima and therefore tuned differently. A series of 7 ports was designed with ratios of maximum to minimum diameter that ranged from 1:1 to 2:1. All ports had the same physical length and a 15 mm radius was added to both ends of each port. For reference a straight port (port S) and an elliptical port (port EL) similar to the one cited by Granowski [9], were also included in the experiment. Figure 40 depicts the profile of the ports, and the following table completes the description of the ports:

Port Name	Physical Length (mm)	Minimum Diameter (mm)	Maximum Diameter (mm)	Max/Min Diameter	Max/Min Area	Tuning in 59 liter test box (Hz)
S	120	68.7	68.7	1.00	1.00	33.0
SR	120	66.1	66.1	1.00	1.00	32.9
A	120	64.4	72.3	1.12	1.26	33.0
B	120	62.9	79.2	1.26	1.59	33.1
C	120	61.8	87.4	1.41	2.00	33.2
D	120	60.9	96.7	1.59	2.52	33.4
E	120	60.1	107.0	1.78	3.17	33.5
F	120	59.5	119.0	2.00	4.00	33.6
EL	120	58.0	120.0	2.07	4.28	33.4

The ports were mounted in the bandpass enclosure described in Study #5. The experimental set up follows that of Study #5 except all ports were driven by a 33.0Hz sine wave with drive levels ranging from 1.12 VRMS to 50.79 VRMS.

Figure 41a. is a plot of THD versus SPL for ports S, SR, A, B and C. Figure 41b. shows the same data for ports C, D, E, F and EL. At low sound pressure levels any flare works significantly better than a traditional straight port and the more flare, the better. At medium SPLs there is a clear trend that is revealed in the data for the ports examined in Figure 41a. Here, performance is strongly related to flare rate; the ports with more flare have lower distortion. For the ports with significant flare, Figure 41b, the differences are more subtle. At high SPLs the performance gap closes even tighter with no clear winners, only losers, i.e.: here the straight port actually outperforms ports SR and A! Figures 41c. and 41d. plot odd harmonic distortion as a function of SPL for all 9 ports. At low and medium SPLs the trends are consistent with those in Figures 41a. and 41b. At high levels, however, ports C and D with a best fit NFR near 0.5 appear to have an edge.

This data leads us to the same conclusions found in study #5, namely that a generous flare, to a point, enhances port performance. There is some indication that too much flare is not necessarily a good thing. At medium SPLs ports C and D perform nearly as well as the ports with more generous flare and appear to have an edge at higher levels. These differences, however, are extremely subtle when one compares their performance to ports SR, S and A. Like the experiment with simple radii the flare rates that are in the middle range are the best, and an optimum solution was achievable. The ellipse also performed quite well suggesting that a different approach could be used to find an near optimum solution. The suggestion here is that there are probably an infinite number of profiles (all moderate in nature) that will perform well.

11. Study #9: Port Asymmetry

In the previous experiment we noted that at high SPLs ports C and D had the lowest odd harmonic distortion. In contrast, at high SPLs port C and D have more even harmonic distortion than the other ports, Figure 42a.

From our experience with transducers and amplifiers we tend to associate even harmonic distortion with asymmetry and odd harmonic distortion with symmetrical “clipping”. Could port C and D have hidden asymmetry? All the ports were surface mounted in the enclosure. This means that one end of the port has a baffle and the other end does not. Thus, all the ports were asymmetric. However, the ports with the most generous flare, ports F and EL, still have low even harmonic distortion at high SPLs. It appears that the maximum diameter of these ports is enough to “simulate” a mounting baffle on the inside edge of the port. If this is true then adding a simple flange to the inside of ports C and D should reduce even harmonic distortion. Figure 42b shows even harmonic distortion for ports C and D and the same ports with a 15mm (not very big) flange added to the inside of the port Cf & Df. Figure H shows the impact on THD. The flange did not effect odd harmonic distortion appreciably, but clearly the small flange improved the even order harmonic distortion dramatically. Figure 42c. shows that the THD has also come down. It is clear that when choosing a port flare of moderate rate an additional design feature that should be incorporated is a flange on the inside of the port.

12. Study #10: Thermal implication of port design and placement

In matters of the acoustical performance of a port, turbulence is the enemy. However, in matters of heat exchange turbulence is your friend. If the port mass acts as a slug of air during laminar flow, it could be argued that the same slug of air moves in and out of the box and that no effective exchange of air from inside to outside occurs. The inside of a loudspeaker enclosure heats up as the components radiate heat into the box; in fact, it is not unusual for high power designs to reach 200^{o} F inside the enclosure. Temperatures this high limit the life of all of the components significantly and it would therefore be desirable to keep the box as close to room temperature as possible. The ports in a vented box provide an ideal path for replacing the hot air in the box with cool ambient air, but if we have designed the port such that there is no net exchange, then the box will heat up and heat dissipation will be have to be through the walls. Turbulent air is extremely effective at dissipating heat as it rapidly mixes cool and warm air.

This line of thinking led the authors to speculate that smaller straight turbulent ports would have an advantage over well designed larger tapered ports. To prove this hypothesis an experiment was devised to test the heat dissipation of several port configurations. Figure 43a shows the six configurations tested. As well as trying flared vs straight we made the straight ports substantially smaller. We designed all ports to tune to about 25hz in a 12 ft^3 box with a single 18" driver. Experiments were run with one port and two ports. The condition with two ports placed one near the top and one near the bottom of the box, the idea being that with two ports in this configuration a convective "chimney effect" might provide additional cooling as cool air would come in the bottom and warm are exit the top. As well, to further take advantage of this idea a configuration was devised that had an asymmetrical port on the top and bottom with the bottom port oriented to cause preferential air flow in the inward direction and the upper port oriented to provide preferential flow in the outward direction.

The measurement setup is also pictured in figure 43a. A pink noise signal of 20 to 2,000 Hz was presented to the woofer. A broadband signal was used so that a large amount of heat would be generated but the port velocity in the case of the tapered ports would be low enough that they remain laminar, as only a small portion of the signal has energy near port tuning. The size of the smaller ports was chosen to ensure that they were in fact turbulent. The diameter of the tapered port was about 3.5 inches and the smaller ports were about 1.75 inches. The tapered ports were also much longer (to insure the same tuning). The amount of power to the system was monitored with a special device that also tracks voice coil temperature. A level of 250 real watts (true electrical power based on voltage and current, not DC resistance) was placed on the driver and the voice coil temperature and the inbox air temperature were monitored vs. time.

Figure 43b show the results of all six trials. One trial was done with the box completely sealed. The results clearly show that all of the ported conditions cool the box significantly over the sealed box. The rise in the voice coil temperature tracks the rise in

the box temperature except in the sealed box condition (which appeared to not have hit equilibrium and was still heating up after 3 hours). This would be expected. Interestingly, the conditions that cooled the box the most were the two iterations with the small turbulent ports. The trial with two small ports outperformed all other configurations tested. Clearly, the turbulent flow and the arrangement of the ports on the top and bottom both contributed to excellent heat exchange in the box. While the tapered performed poorly, it is a little surprising that the two asymmetrical tapered ports did not improve things as much as expected. Clearly the amount of DC flow due to the asymmetry was not substantial enough to create significant heat exchange through the box. By far, turbulence exchanges heat more effectively from the inside to the outside of the box than even large laminar ports. There may be a happy medium of running two asymmetrical ports slightly into turbulence that would find a balance of compression, distortion and heat dissipation.

13. General Conclusions

It should be clear based on the studies presented that the following design rules should be applied to design of loudspeaker ports:

1) Vast historical data and results herein suggest that the largest port area allowable by your design should be employed to keep air velocity down if low port compression and low distortion are desired. This is, however, in conflict with the solution for best heat exchange in the box.

2) **When designing a port for maximum acoustical output both the inlet and exit fluid dynamics should be balanced.** The geometry for best exit flow is *different* than that for inlet flow***. Inlet flow is best with a very large taper (NFR of 1.0). For exit flow a very narrow taper is best (NFR less than 0.5).*** **This points to an NFR of 0.5 as the optimum.**

3) Inlet head loss should be minimized. Use port profiles which do not have any sharp discontinuities**. This requires all port edges to have a blend radius of *at least* 20% of the minimum diameter** (as per figure 24).

4) For flared ports, choose an NFR to match the design application and intent. For lowest harmonic distortion at low levels, use NFR's near 1.0. At moderate levels, NFR's near 0.5 work best. At high levels, NFR's near 0 are desirable (though the above blend radius should still be used). **For the best compromise at all levels, NFR = 0.5 appears to be optimum.**

5) Roughening the port walls generally does **not** appear to be beneficial in the normal operating range of acoustic ports.

6) In designing a flared port, the closer to a simple radius that is used for the flare, the simpler and more accurate the end correction can be and the port tuning will be easy to calculate.

7) Maximally radiused ports have the best low level performance but have poor high level performance due to excessive turbulence within the port, near the ends, leading to compression and tuning shift due to the effective shortening.

8) Large ports with a taper designed to minimize turbulence will act poorly to exchange the air in the box and subsequently exchange heat. Ports that are in fact overdriven under maximum use and located at the top and bottom of the box would be preferred. Creating an asymmetry between the two is not largely useful although a compromise may exist.

9) There are *many* approaches to finding a port profile that will provide excellent performance.

14. Acknowledgements

Thanks to Harman International, Mark Gander, and John Vanderkooy

15 .References

1) H. D. Harwood, "Loudspeaker Distortion Associated with Low Frequency Signals." *J. Audio Eng. Soc.* Vol 20, No. 9. (November 1972).
2) R. Laupman, US Patent 4,213,515 "Speaker System," 1980 (filed Sept 12, 1978, awarded Jul. 22 1980)
3) J. Vanderkooy, "Loudspeaker Ports," presented at 103rd AES Convention, New York 1997
4) J. Vanderkooy, "Nonlinearities in Loudspeaker Ports," presented at 104th AES convention, Amsterdam 1998
5) J. Backman, "The Nonlinear Behaviour of Reflex Ports," presented at 98th AES convention, Paris
6) N. B. Roozen, J. E. M. Vaeland J. A. M. Nieuwendijk, etc. al, "Reduction of Bass-Reflex Port Nonlinearities by Optimizing the Port Geometry," presented at the 104th AES convention, Amsterdam, 1998
7) U. Ingard and H. Ising, " Acoustic Nonlinearity of an Orifice," *J. Acoustical Soc. Am.* Volume 42, No. 1 pp. 6-17 (1967).
8) J. Young, " An Investigation into the properties of Tubular Vents, as Used in a Helmholtz Resonator as Part of a Vented Box Loudspeaker System," Senior thesis, University of Sydney, School of Mechanical Engineering. December 1975.
9) B. Gawronski and G. Caron, US Patent 5,714,721 "Porting," (awared Feb. 3, 1998)
10) M. Polk and C Campbell, US Patent 5,517,573 "Ported Loudspeaker system and Method with Reduced Air Turbulence," (awarded may 14, 1996).
11) M. Goto, US Patent 4,987,601 " Acoustic Apparatus," (awarded Jan. 22, 1991)
12) S. Gahm, US patent 5,623,132 " Modular Port Tuning Kit," (awarded Apr. 22, 1997)

13) J. A. Pedersen and J. Vanderkooy, "Near-field Acoustic Measurements at High Amplitudes," presented at the 104th AES convention, Amsterdam, 1998
14) M.C.A.M Peters, A. Hirschberg, A. J. Reijnen, A. P. J. Wijnands, "Damping and Reflection coefficient measurements for an open pipe at low Mach and low Helmholtz numbers," J. *Fluid Mechanics*, vol 256, pp. 499-534,1993.
15) P. Merkli and H. Thomann, "Transition to turbulence in oscillating pipe flow." *J. Fluid Mechanics* vol 68, pp. 567-575, 1975
16) M. R. Gander, "Dynamic Nonlinearity and Power Compression in Moving Coil Loudspeakers," *J. Audio Eng. Soc*, Vol. 34 (September 1986)
17) C. Strahm, "Loudspeaker Enclosure Analysis Program," Manual, 1992
18) L. L. Beranek, *Acoustics*, American Institute of Physics. 1993.
19) L. Campos and F. Lau, "On sound in an inverse sinusoidal nozzle with low Mach number mean flow," *J. Audio Eng. Soc*, (July 1996)
20) K. Furukawa, US Patent 5,109,422, " Acoustic Apparatus," (awarded Apr. 28, 1992)
21) D. Y.Cheng, US Patent 5,197,509 "Laminar Flow Elbow system and Method," (awarded Mar. 30, 1993)
22) F.M. White, *Fluid Mechanics*, 3rd Ed. 1994
23) T. Maxworthy, "Some Experimental Studies of Vortex Rings," *J. Fluid Mechanics* vol. 81, 1977.
24) B. Seymour, "Nonlinear resonant oscillations in open tubes," *J. Fluid Mechanics* vol 60, 1973
25) A. Cummings and W. Eversman, "High amplitude acoustic transmission through duct terminations: Theory,". *Journal of Sound and Vibration*, vol 91, 1983
26) P.O.A.L. Davies, "Practical Flow Duct Acoustics," *Journal of Sound and Vibration* vol 124, 1988.
27) L. Van Wijngaarden, "On the oscillations near and at Resonance in open pipes," *Journal of Engineering Mathematics* Vol 2, No 3 1968
28) W. Chester, "Resonant oscillations in closed tubes," *Journal of Fluid Mechanics* vol. 18, (1963)
29) M. S. Howe, "The interaction of sound with low mach number wall turbulence, with application to sound propagation in turbulent pipe flow," *Journal of Fluid Mechanics*, Vol. 94, 1979.
30) S. W. Rienstra, "Small Strouhal number analysis for acoustic wave-jet flow-pipe interaction," *Journal of Sound and Vibration*, Vol. 86, 1983.
31) M. C. A. M. Peters, A. Hirschberg, " Acoustically induced periodic vortex shedding at sharp edged open channel ends: simple vortex models." *Journal of Sound and Vibration*, Vol. 161, 1993.
32) J. H. M. Disselhorst and L. Van Wijngaarden, "Flow in the exit of open pipes during acoustic resonance," *Journal of Fluid Mechanics* vol 99, 1980.
33) H. Levine and J. Schwinger, "On the Radiation of Sound from an Unflanged Circular Pipe," *Physical Review*, Vol 73, No. 4, 1948.

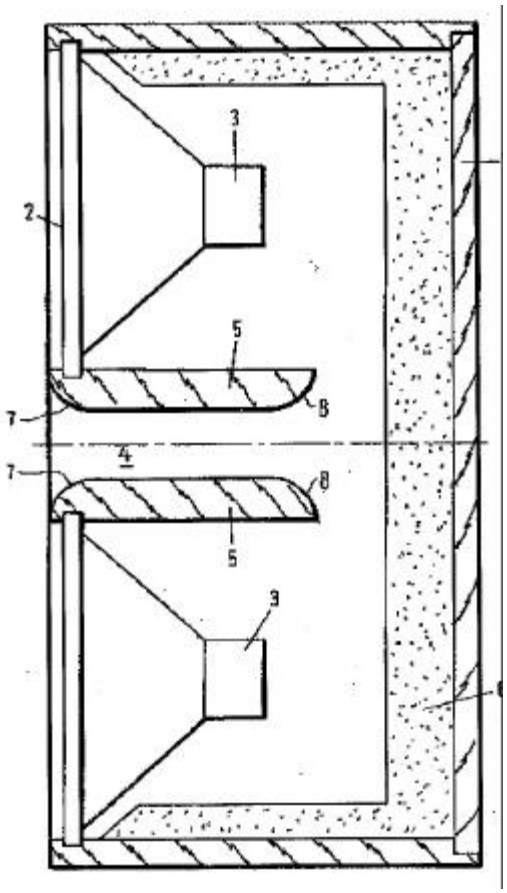

Figure 1. From Laupman [2] Patent # 4,213,515, early design with radii on both ends of a port. Filed in 1978.

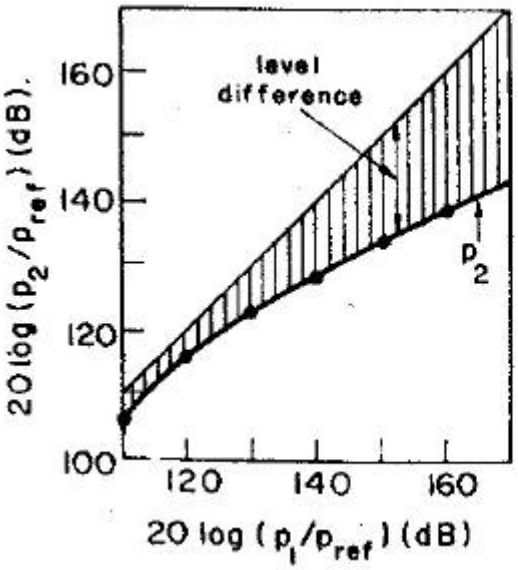

FIG. 10. SPL (p_2) transmitted through an orifice in a plate as a function of the driving sound pressure (p_1). Also shown, by the shaded portion, is the difference in level of p_1 and p_2.

Figure 2. From Ingard [7] pressure compression (reduction) through and orifice with increasing level.

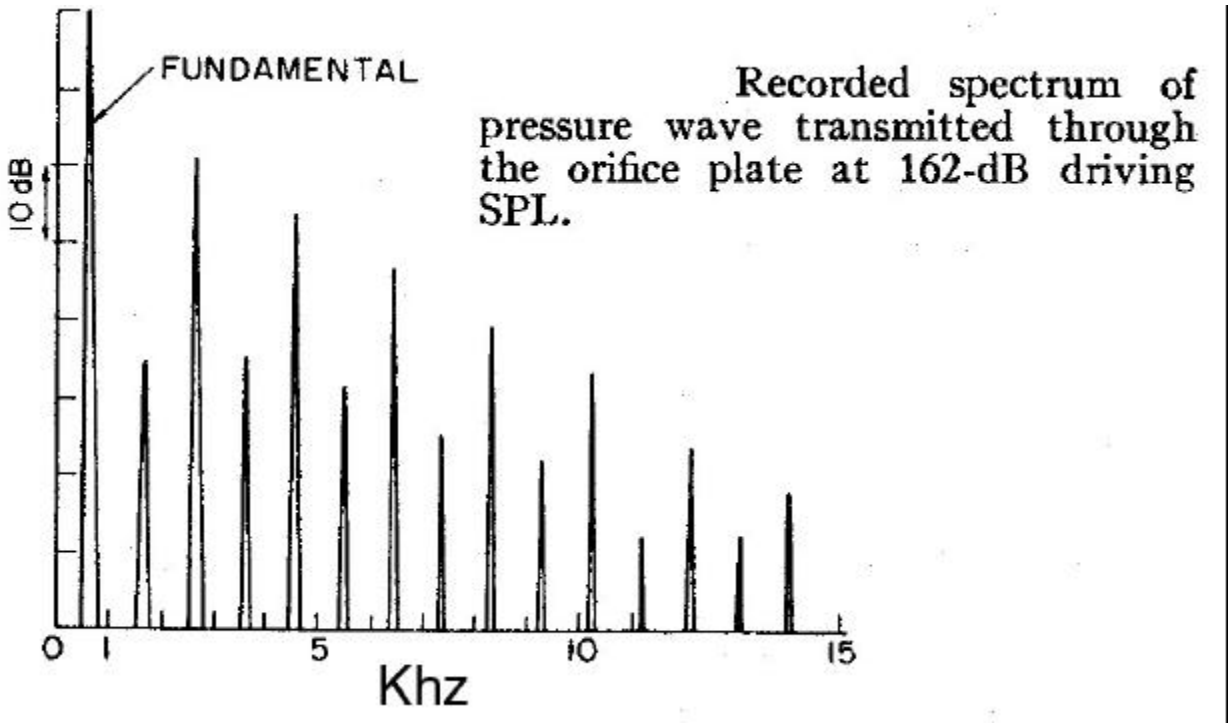

Recorded spectrum of pressure wave transmitted through the orifice plate at 162-dB driving SPL.

Figure 3a. From Ingard [7] harmonic content of orifice driven at very high level. Note predominance of odd order harmonics.

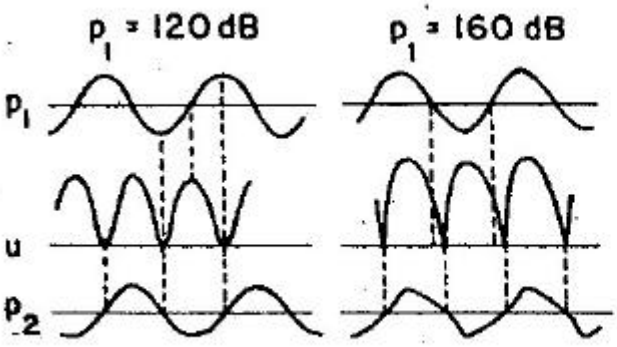

FIG. 8. Typical oscilloscope traces of the driving sound pressure p_1, orifice velocity u, and transmitted plane-wave pressure p_2, illustrating linear and nonlinear behavior.

Figure 3b. From Ingard [7] traces of pressure and velocity at low and high levels in an orifice. At low levels P1 and P2 are in quadrature. At high levels they are in phase. P1 would represent the pressure from the backside of the cone P2 the radiated sound form the port.

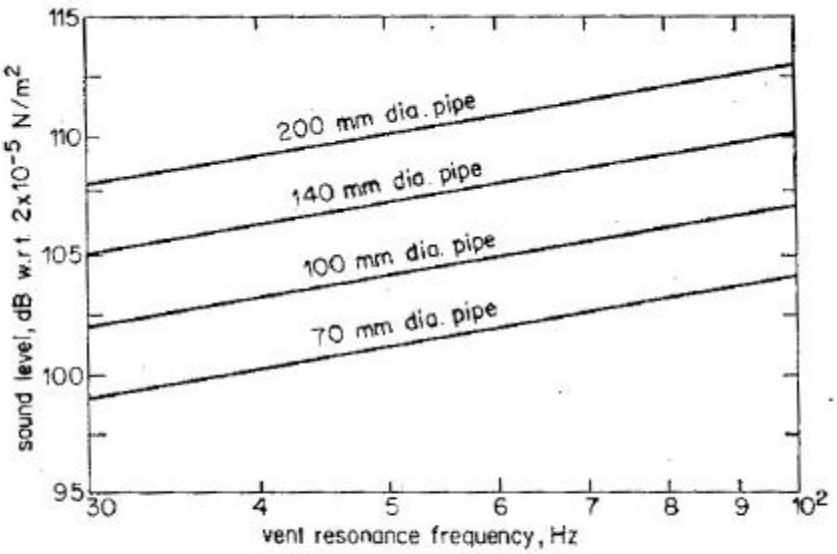

Fig. 12. Minimum program sound levels in room of 2000 ft³ (60 m³) for various-diameter long pipes and vent resonance frequencies before distortion is appreciable.

Figure 4. From Harwood [1] The important features of this data are that the larger the pipe the better, and doubling area improves performance by 10 dB. As well, lower tuning requires a larger pipe.

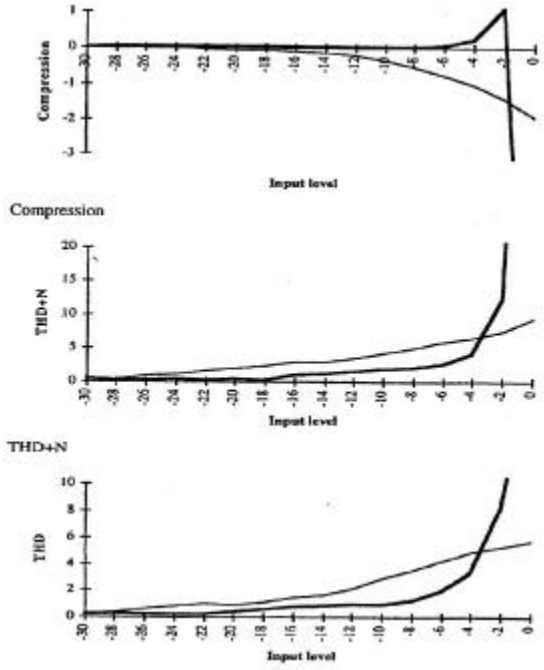

Figure 5 & 6. From Backman [5] The lighter trace represents a straight port, the heavier trace is a port with small radii at both ends.

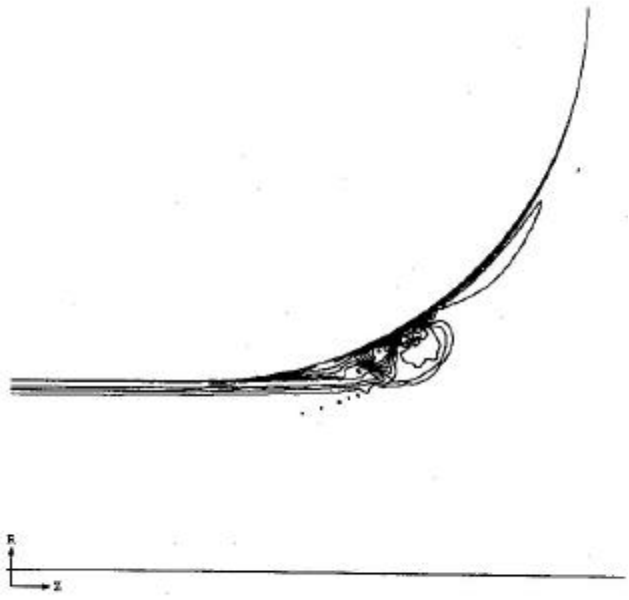

(a) time t=7 ms (maximum vorticity in vortex 0.2242E5 radians/s)

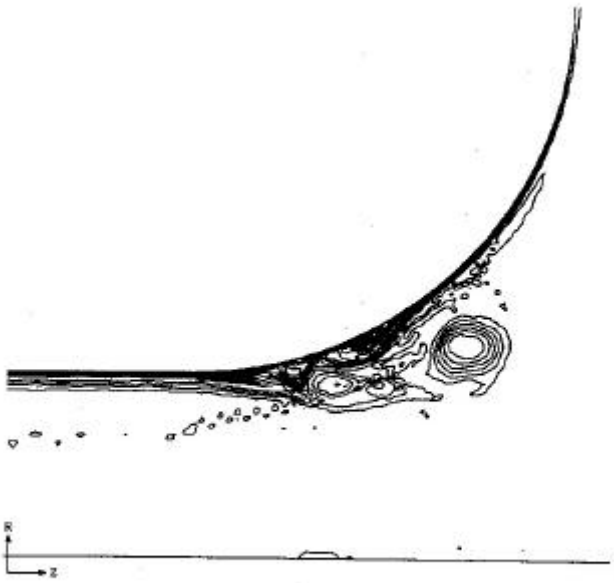

(c) time t=9 ms (maximum vorticity in vortex 0.1451E5 radians/s)

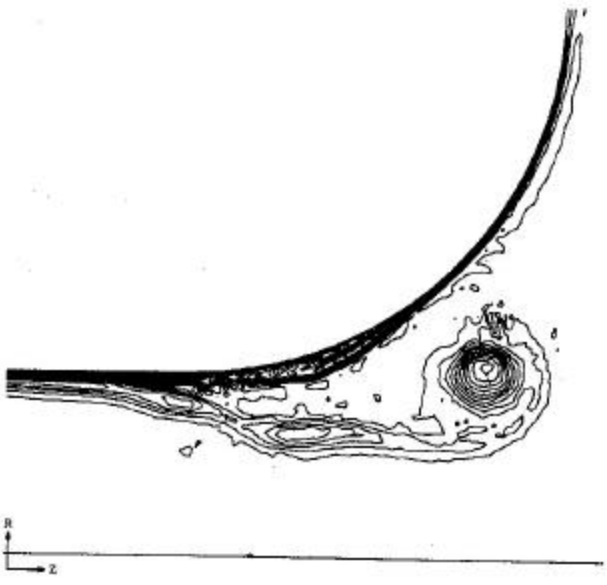

(a) time t=11 ms (maximum vorticity in vortex 0.132E5 radians/s)

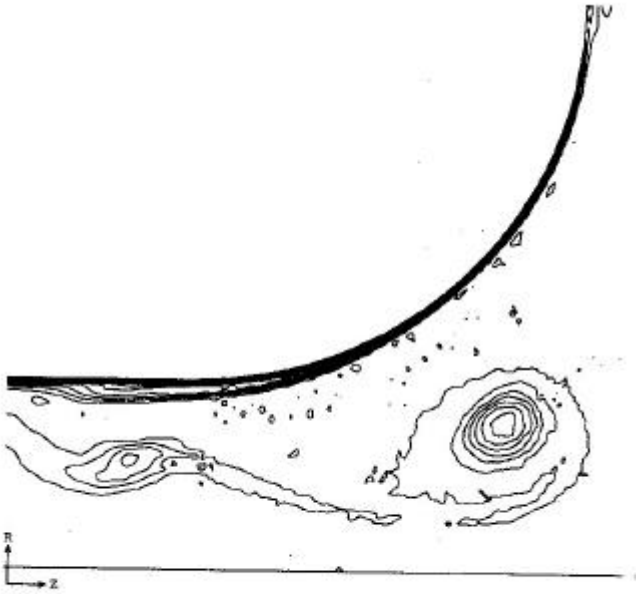

(c) time t=13 ms (maximum vorticity in vortex 0.9527E4 radians/s)

Figure 7. From Roozen [6] Vortex shedding in a highly radiused port on exit stroke. Note how early in the throat the shedding begins.

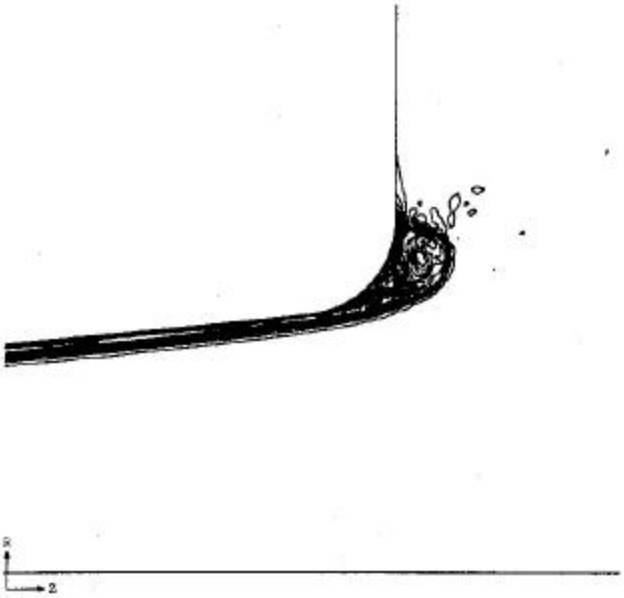

(a) time t=7 ms (maximum vorticity in vortex 0.1027E5 radians/s)

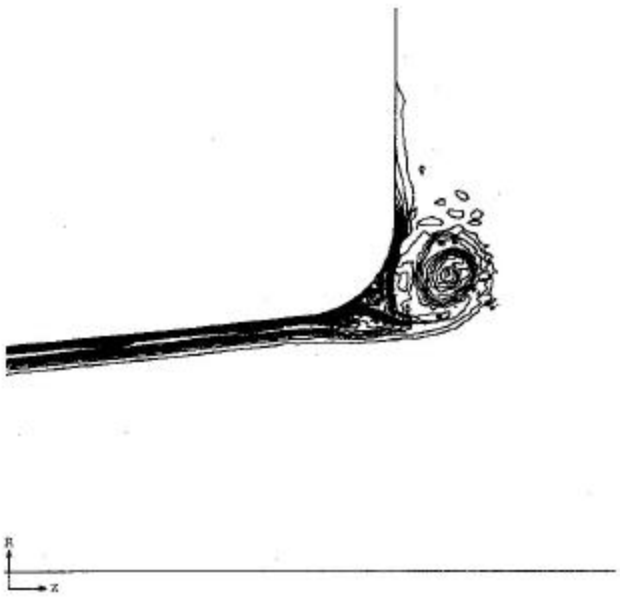

(c) time t=9 ms (maximum vorticity in vortex 0.8776E4 radians/s)

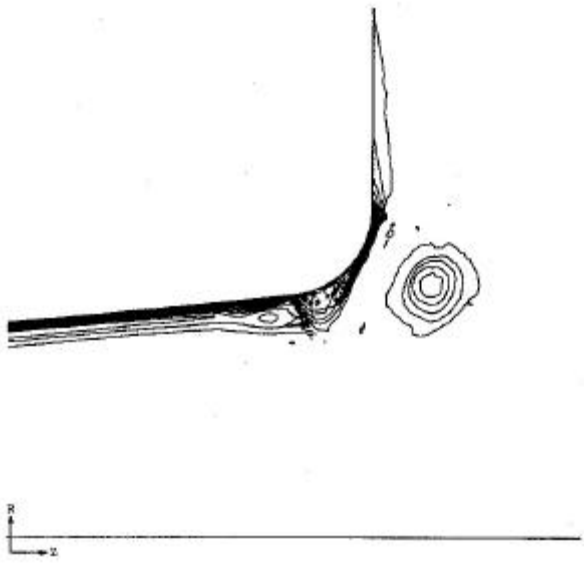

(a) time t=11 ms (maximum vorticity in vortex 0.717E4 radians/s)

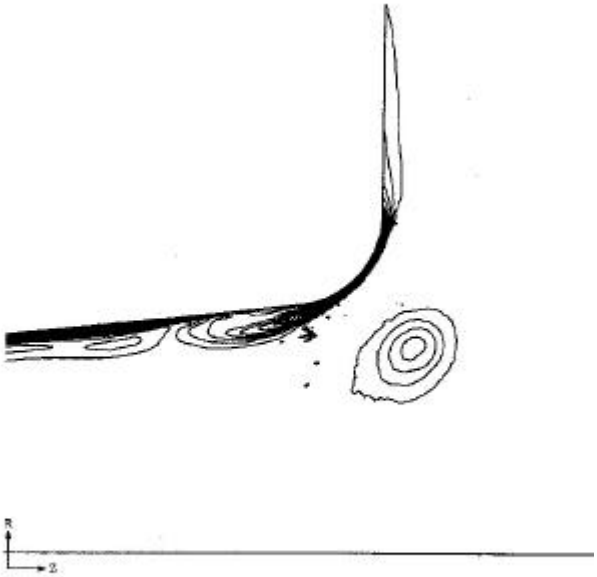

(c) time t=13 ms (maximum vorticity in vortex 0.5417E4 radians/s)

Figure 8. From Roozen [6] Vortex shedding from a very slow taper port.

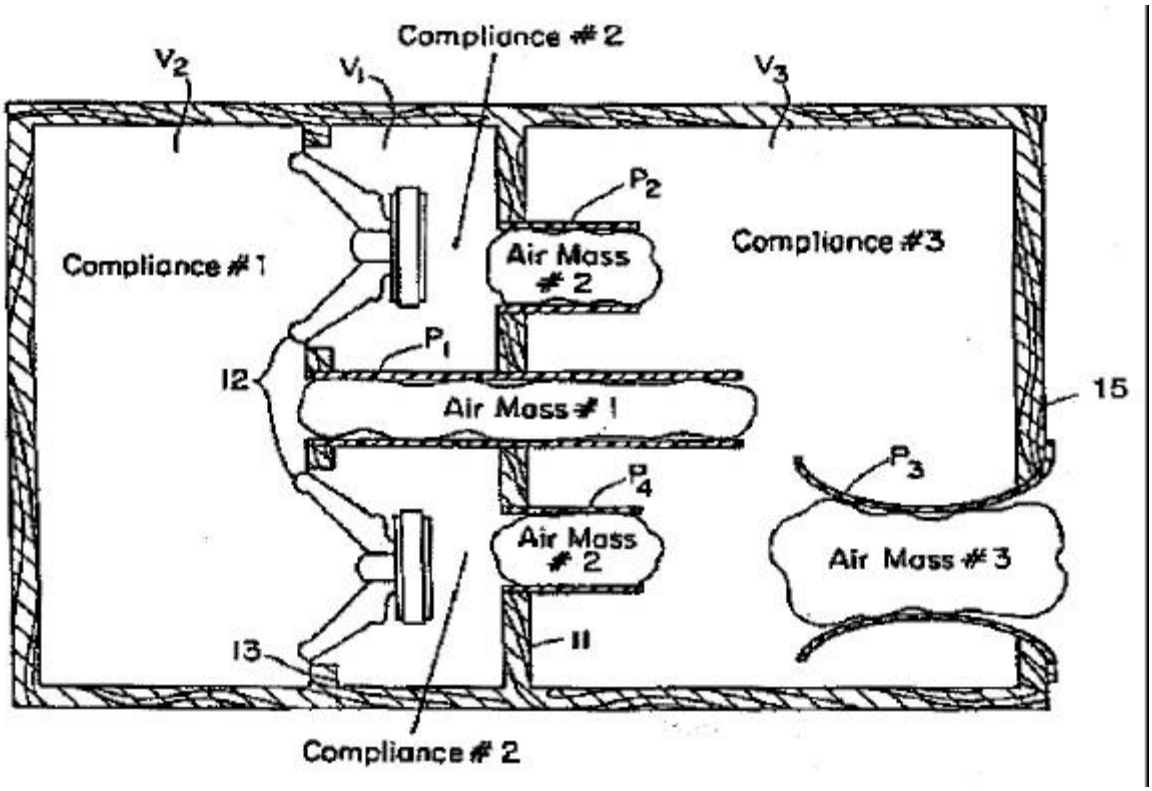

Figure 9. From Granowski [9] patent # 5,714,721. Port 3 is shown with an elliptical crossection. This is said to be optimum.

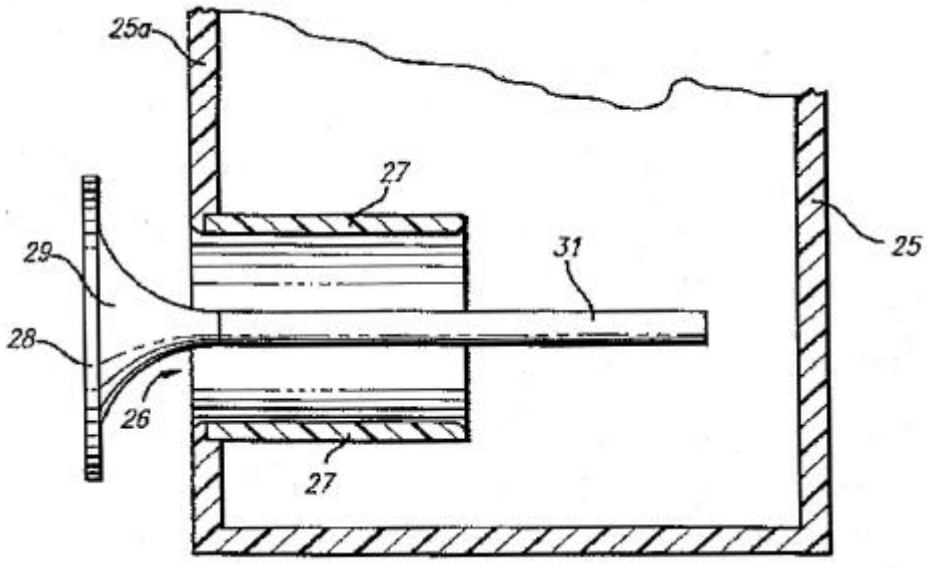

Figure 10. From Polk et al [10] patent # 5,517,573. The center fixture is said to improve aerodynamics and reduce air noise.

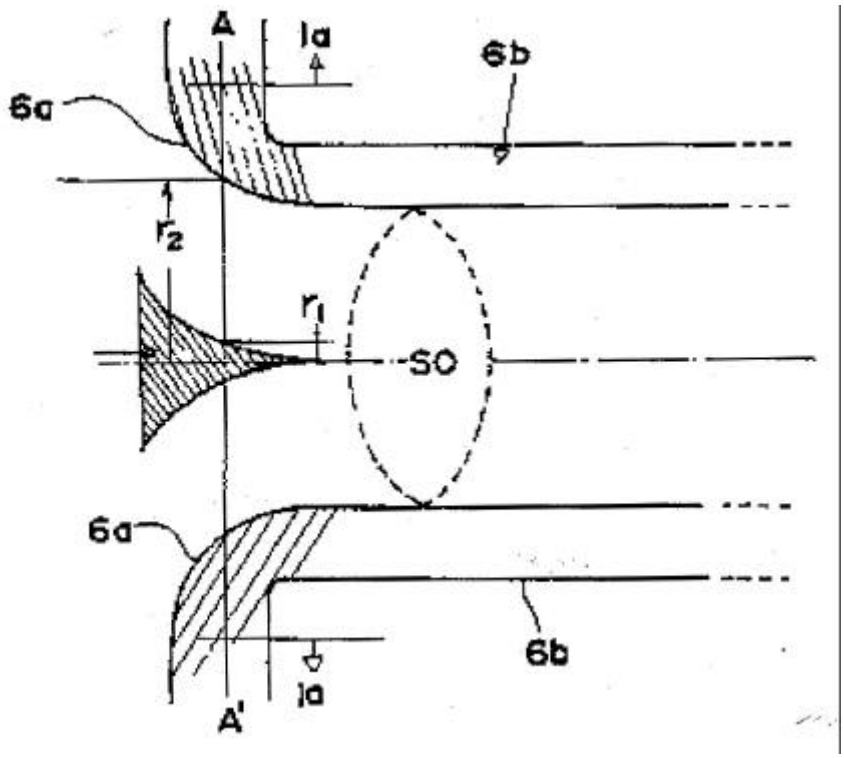

Figure 11. From Goto [11] patent # 4,987,601 a similar but earlier version of the Polk idea.

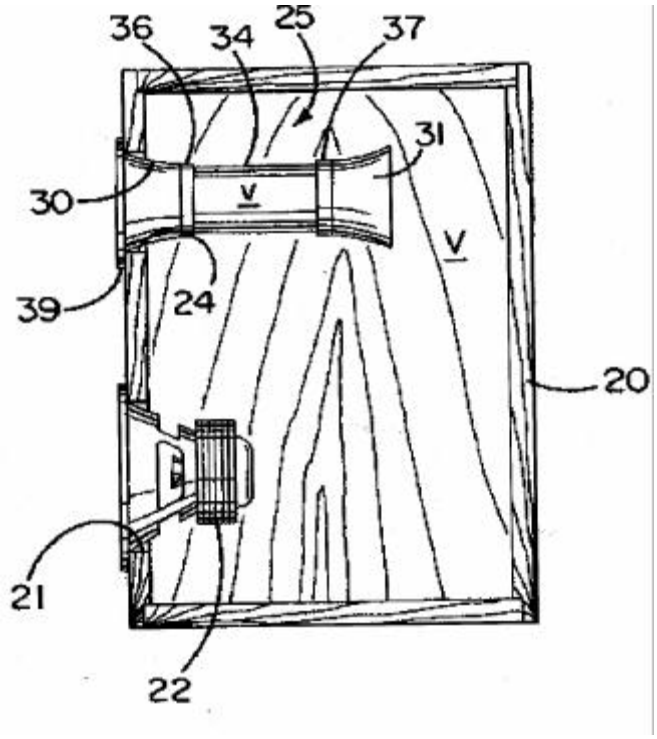

Figure 12. From Gahm [12] patent # 5,623,132. A modular design for adding radii to a straight port.

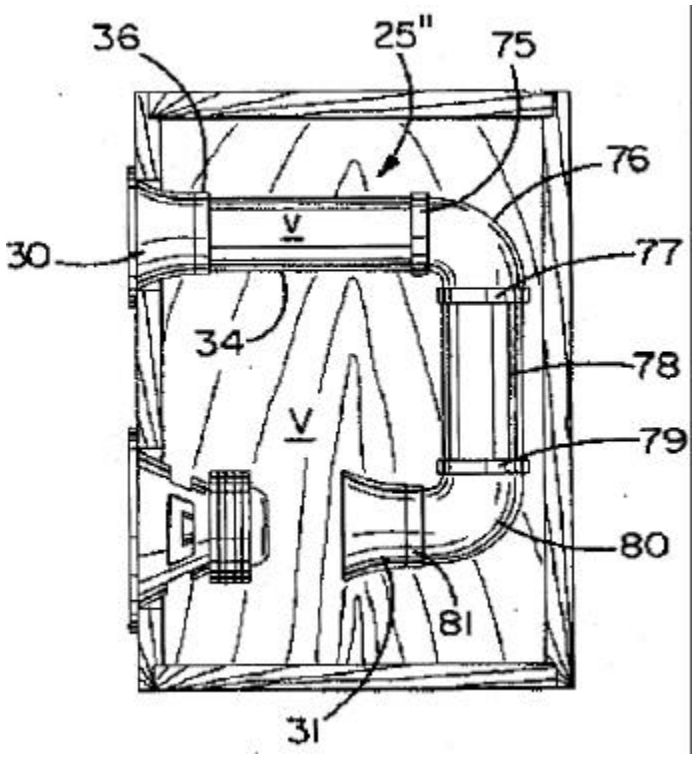

Figure 13. From Gahm [12] A further refinement of the modular port concept which utilizes the port to cool the transducer.

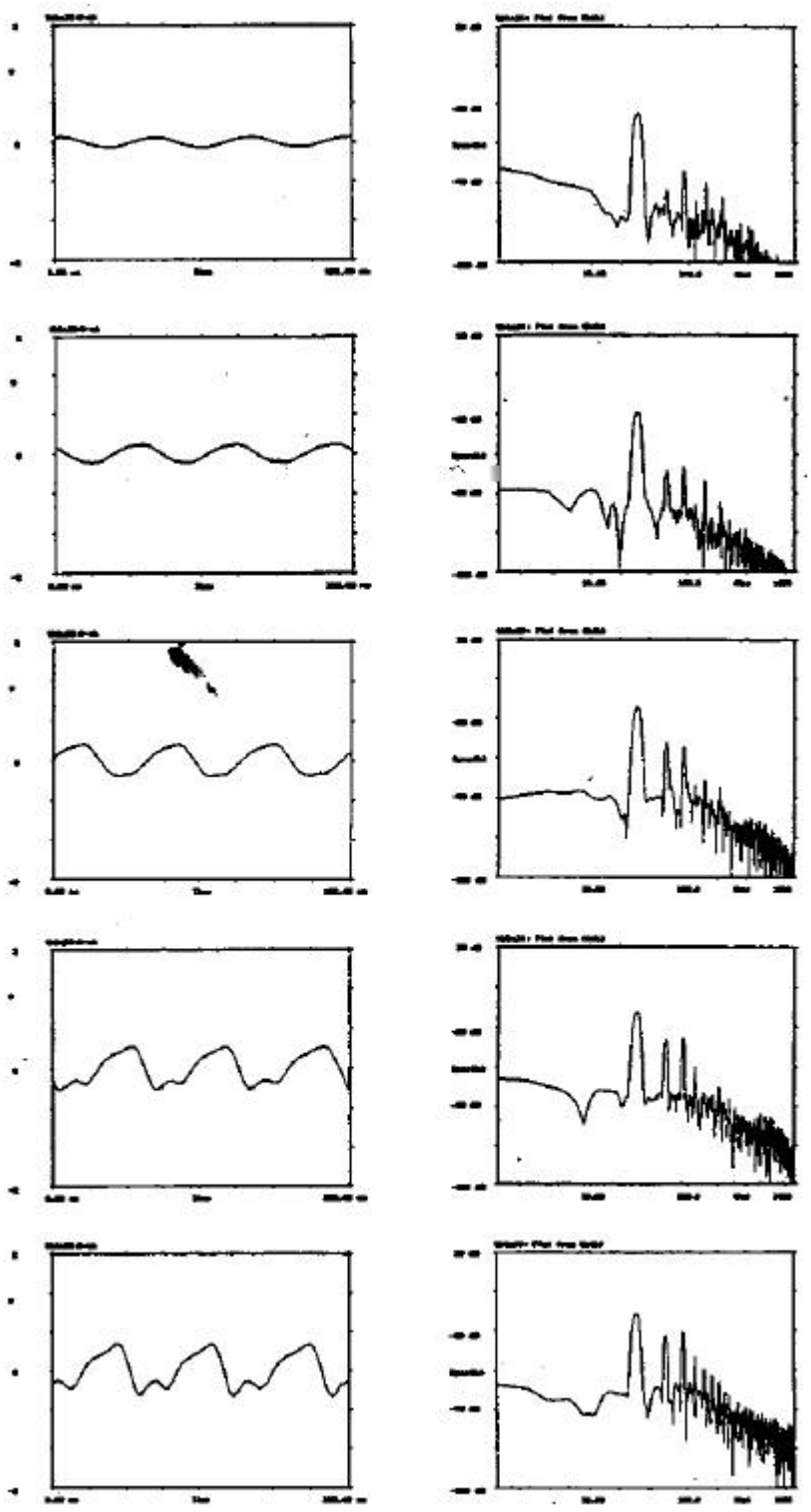

waveform FFT

Figure 14. from Vanderkooy [3] waveform data and FFT analysis at increasing levels from a straight flanged port. Note waveform is triangular and asymmetrical.

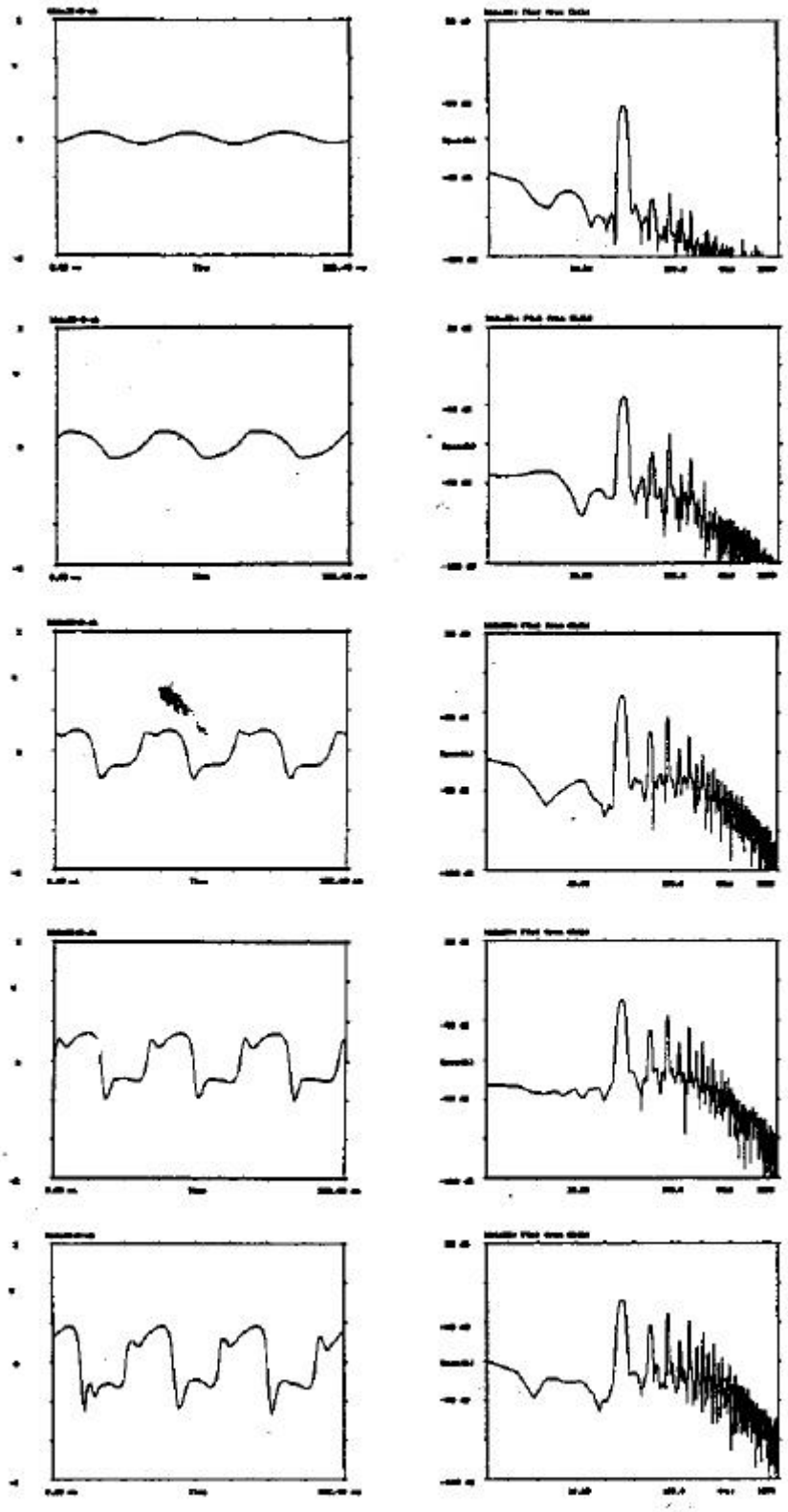

Figure 15. from Vanderkooy [3] waveform data and FFT analysis at increasing levels from a radiused (at both ends) flanged port. Note waveform approaches square wave.

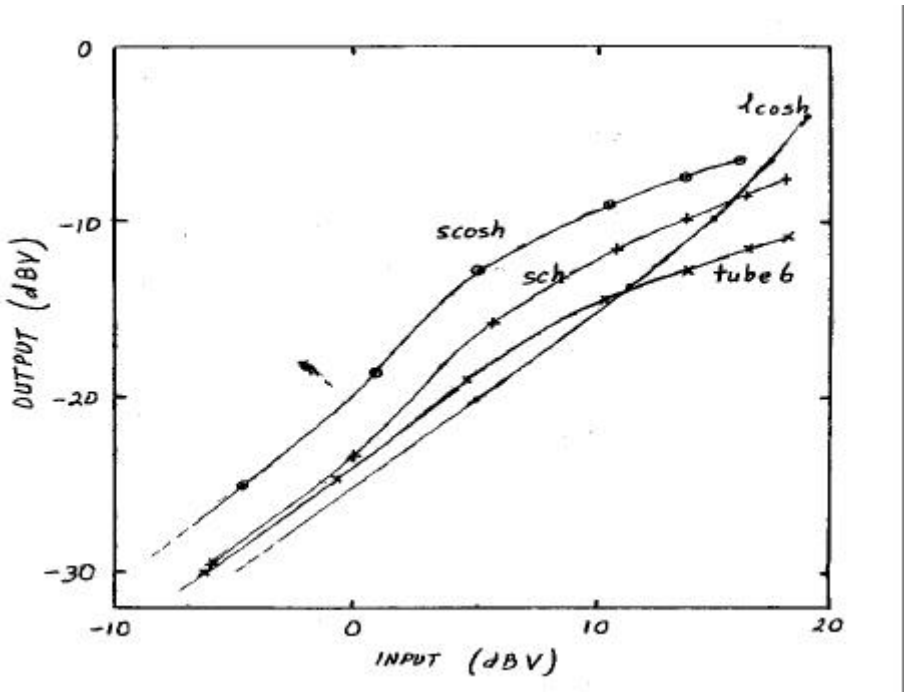

Figure 16. from Vanderkooy [3] Output vs. input of several flared ports. Note gain before compression.

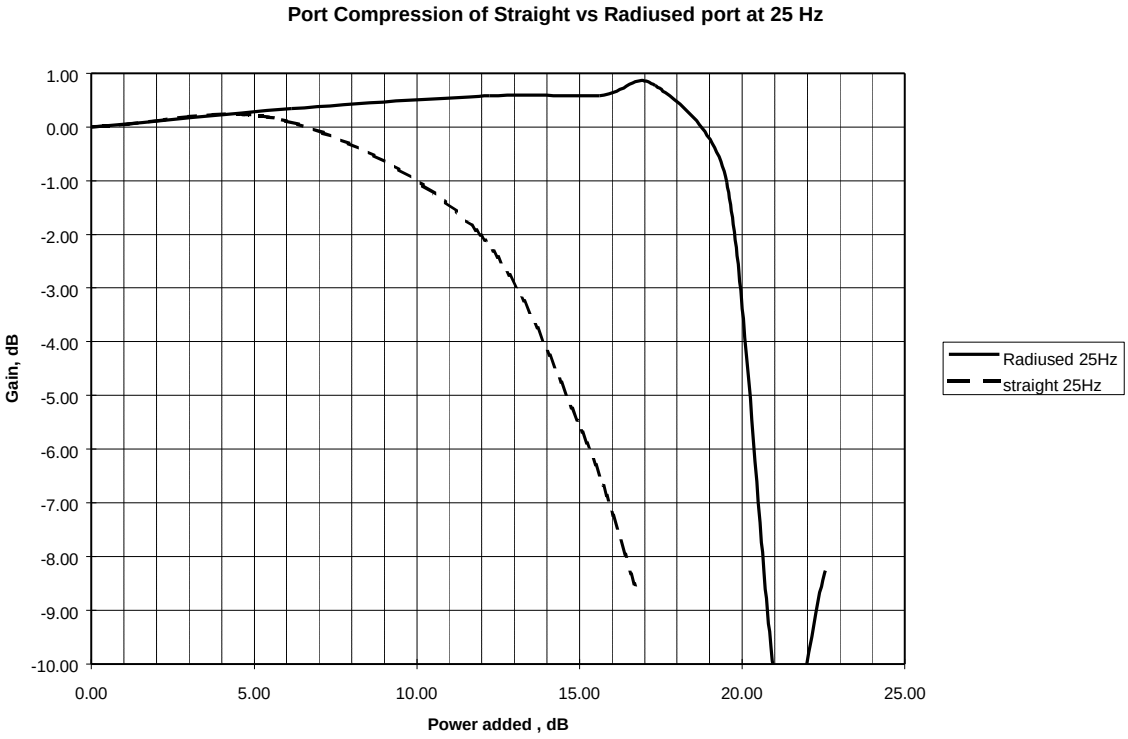

Figure 17. Compression of a 3” diameter 6” long port straight vs. highly radiused port at 25 Hz. Note gain before compression.

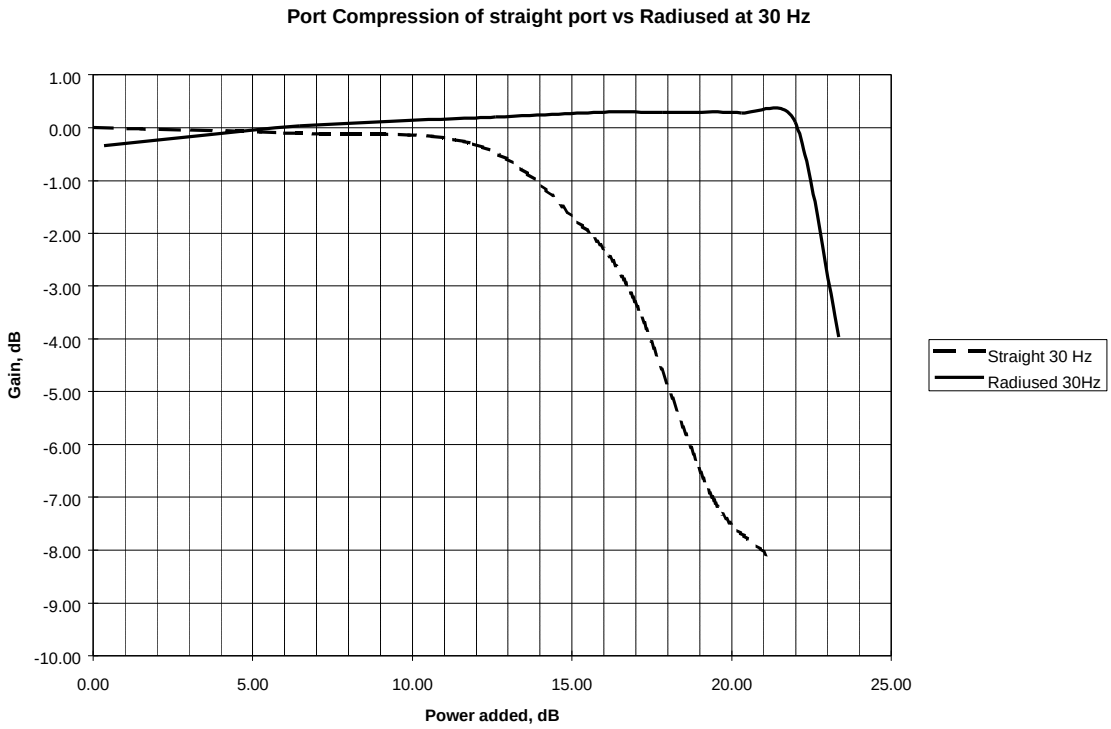

Figure 18. Compression of a 3” diameter 6” long port straight vs. highly radiused port at 30 hz

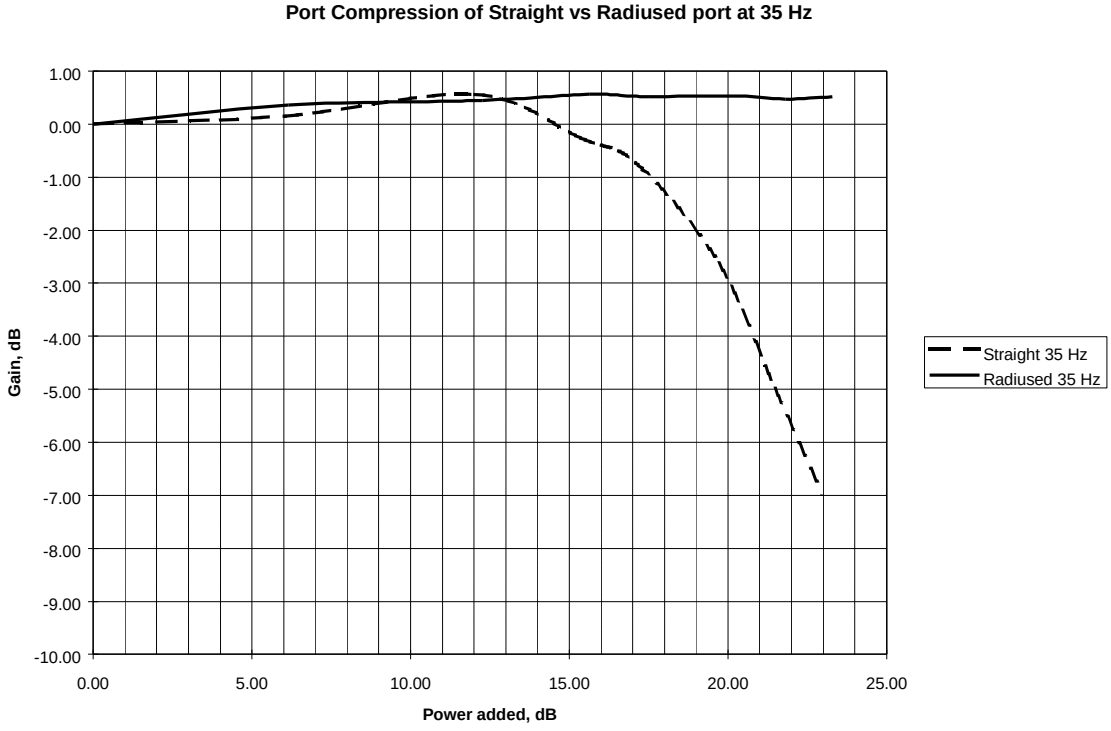

Figure 19. Compression of a 3” diameter 6” long port straight vs. highly radiused port at 35 hz. Note velocity is too low to compress the radiused port at 35hz.

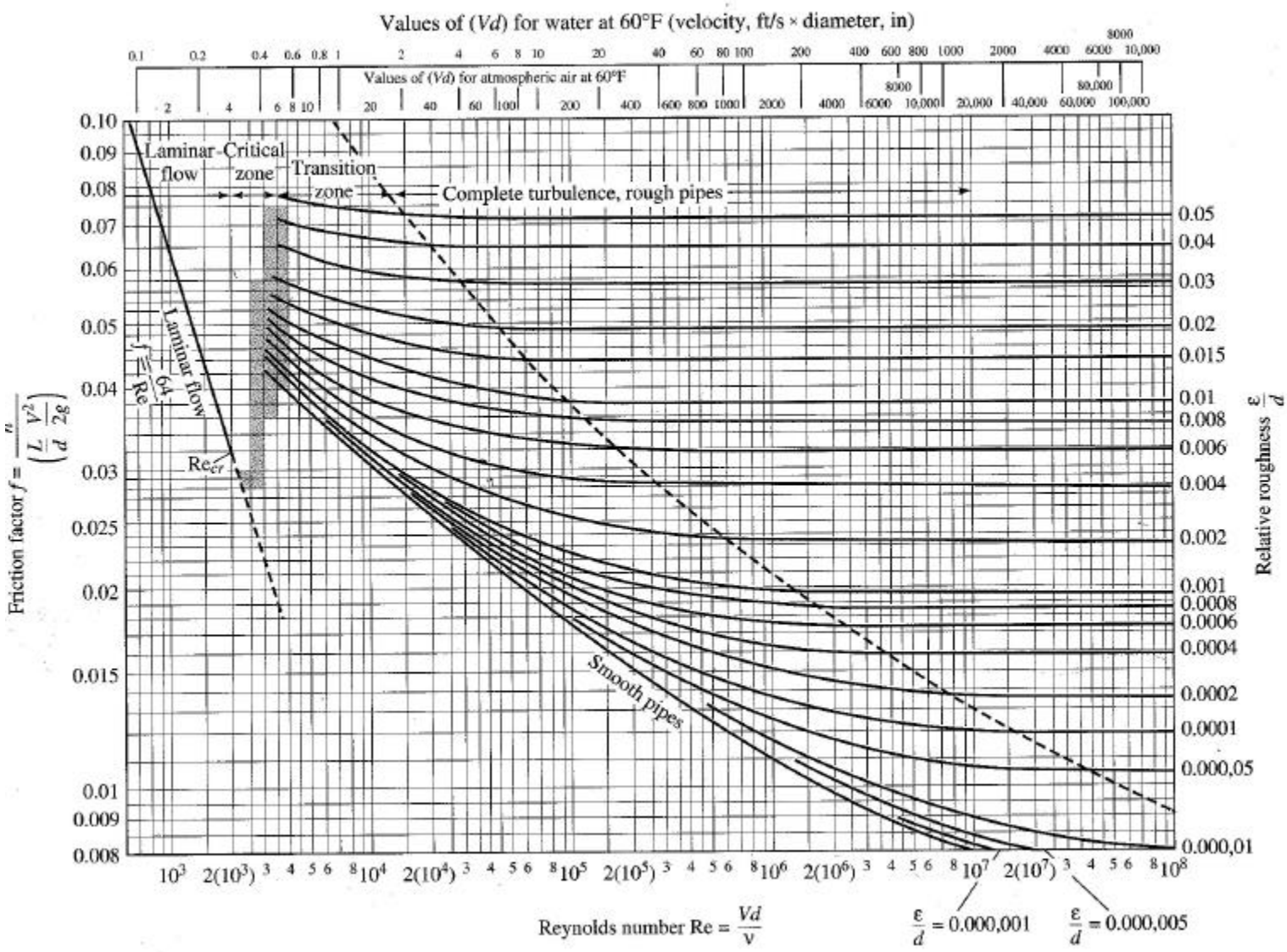

Figure 20. The Moody Chart. Shown is the relationship between Reynold's number, turbulence, and roughness (from ref [22])

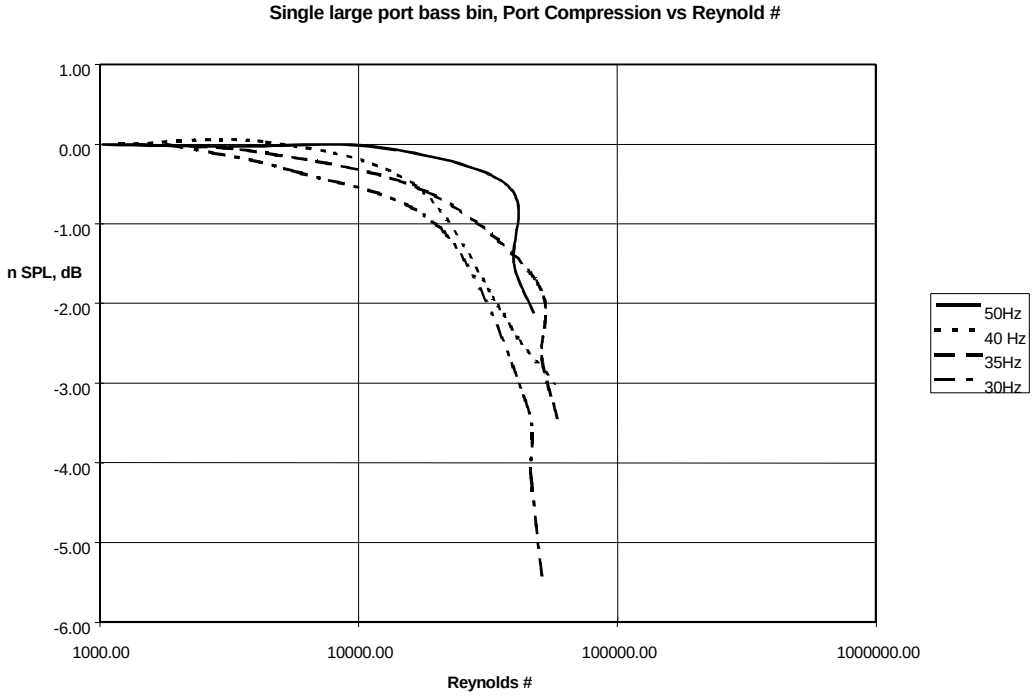

Figure 21. Port Compression vs. Reynold's number in a double 18" subwoofer. 10 ft^3 tuned to 45hz with a single rectangular port.

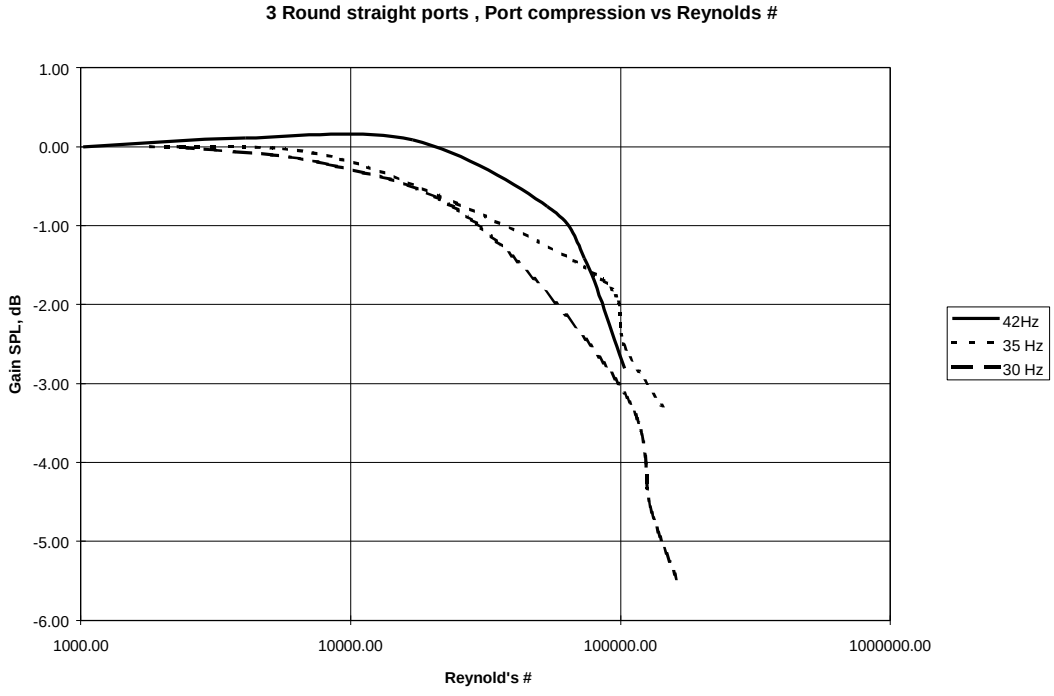

Figure 22. Port Compression vs. Reynold's number in a double 18" subwoofer. 12 ft^3 tuned to 35 Hz with 3 round ports.

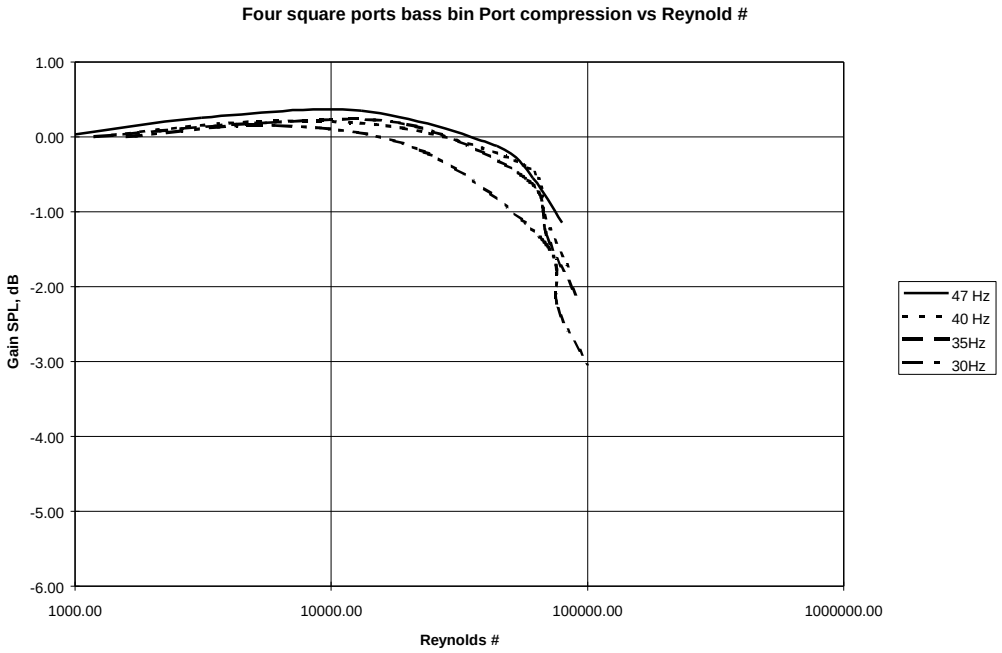

Figure 23. Port Compression vs. Reynold's number in a double 18" subwoofer. 12 cu ft tuned to 39 Hz with 4 square ports.

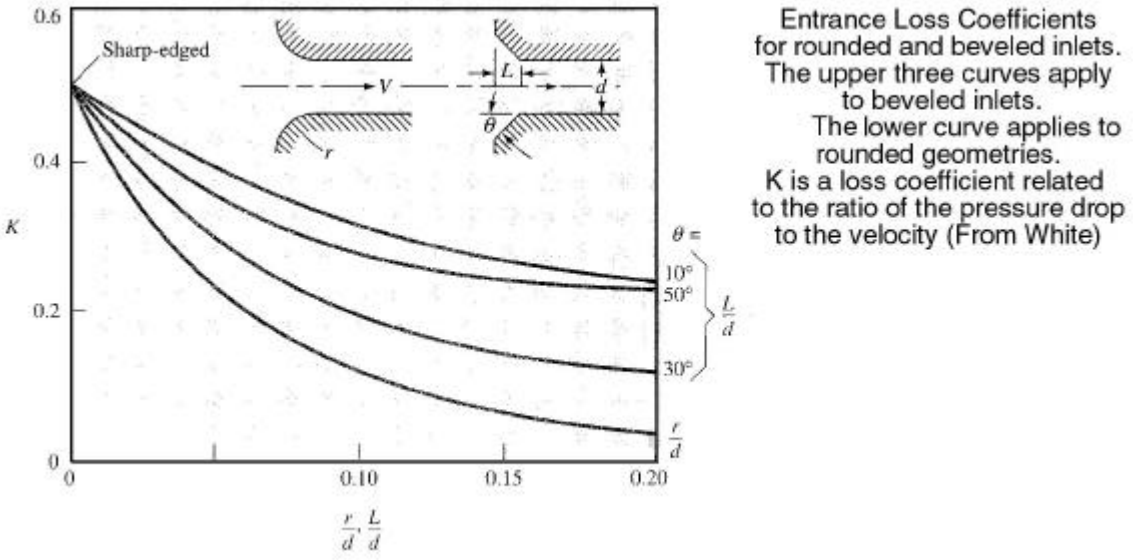

Figure 24. Loss factor vs inlet geometry. **Note r/d= .2 yields a nearly lossless inlet.**

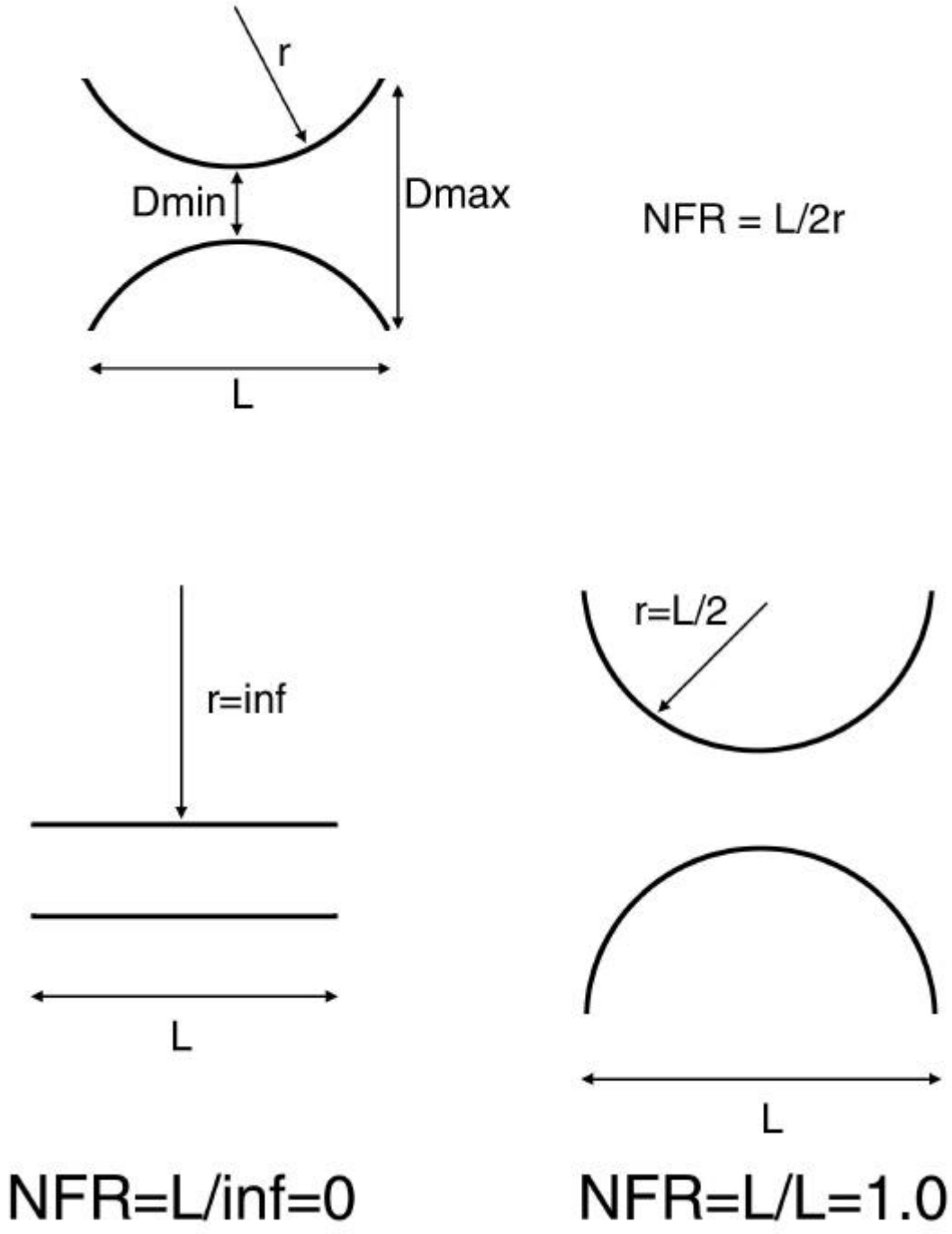

Figure 25a. Simple radiused port nomenclature

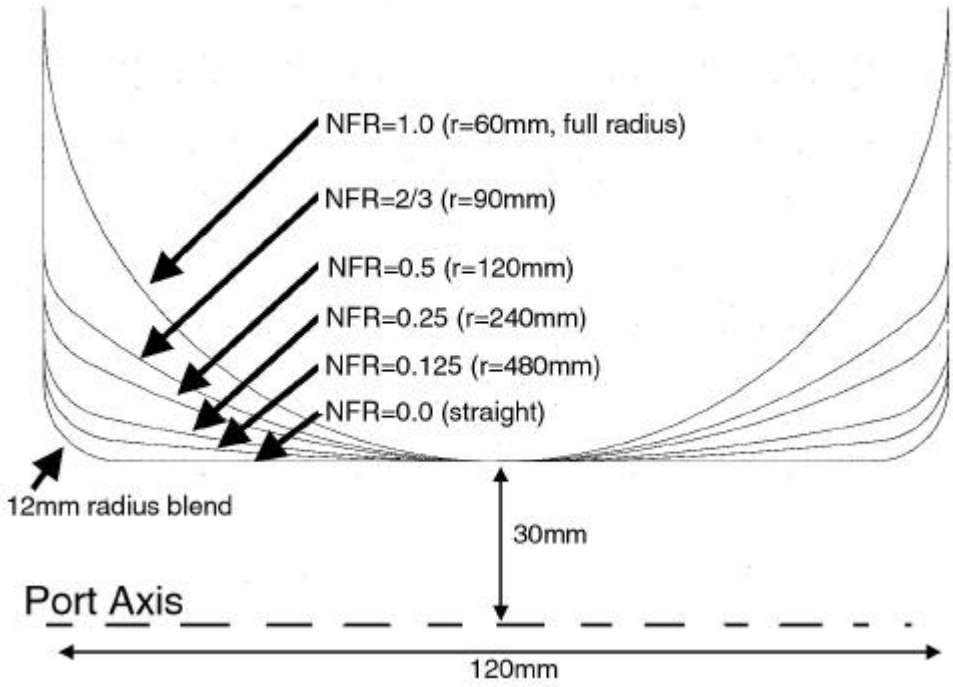

Figure 25b. Port profiles for study

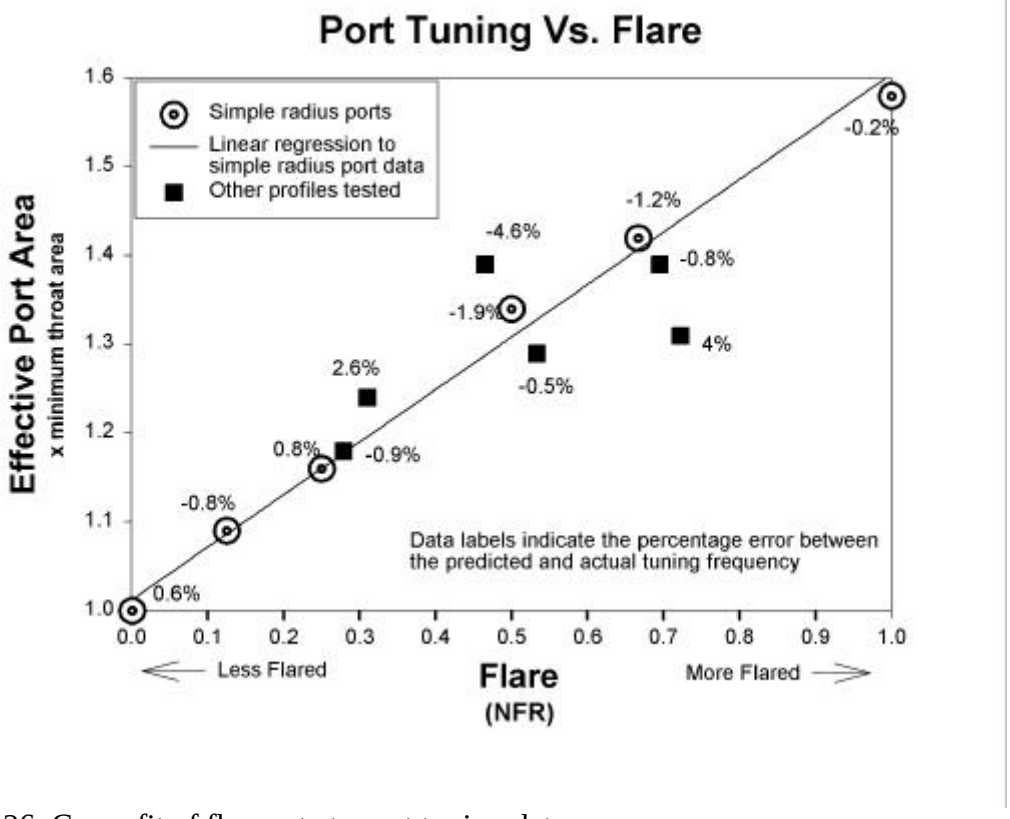

Figure 26. Curve fit of flare rate to port tuning data.

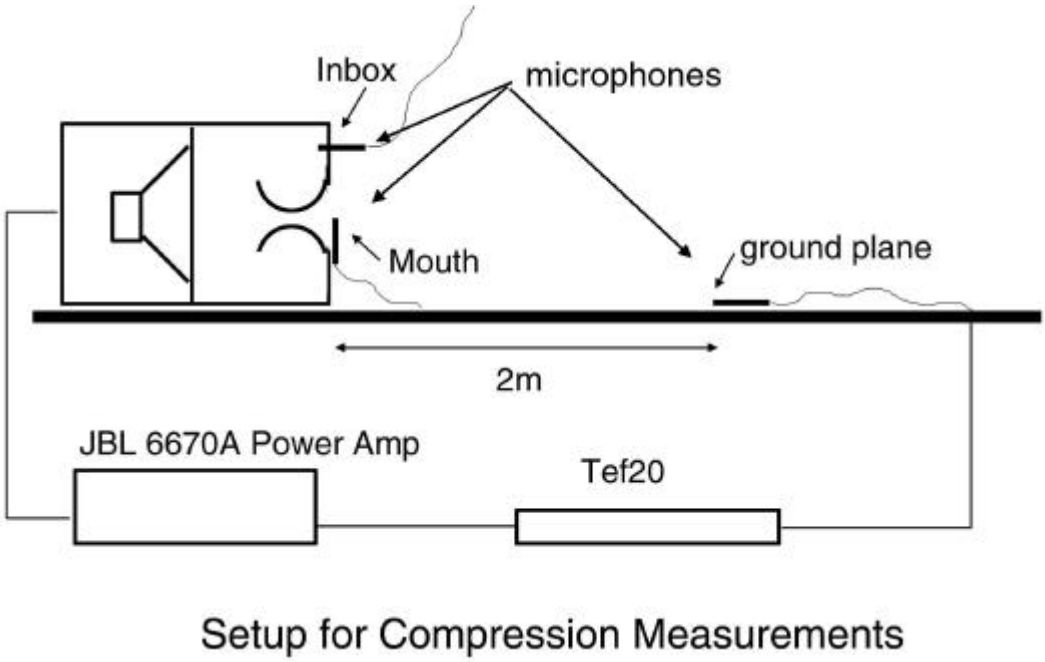

Figure 27 . Bandpass speaker for compression testing.

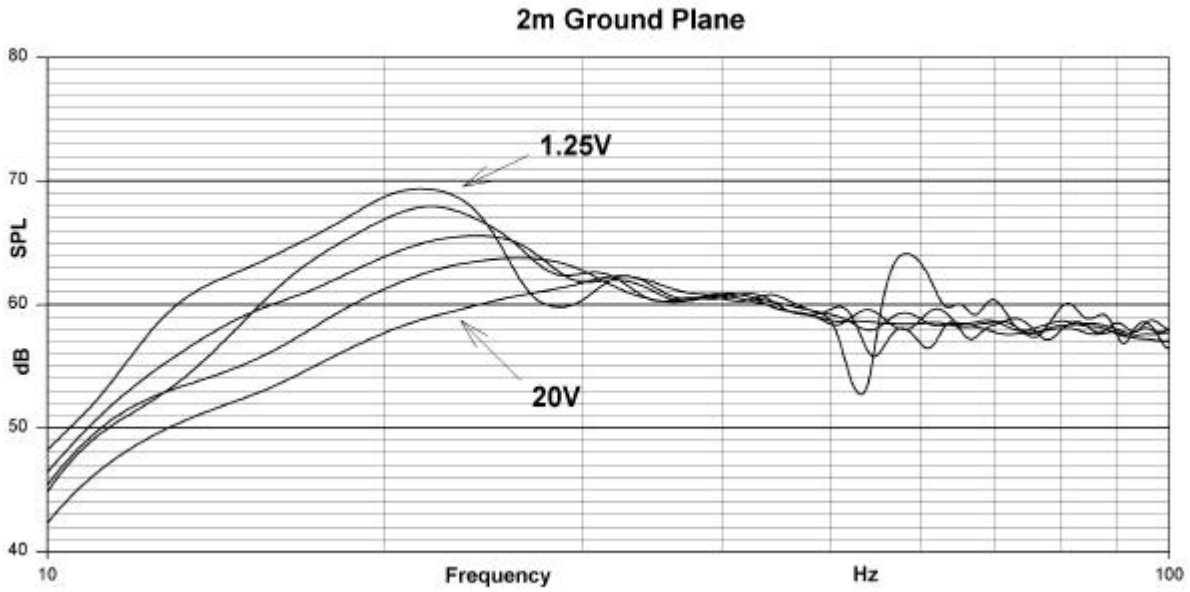

Figure 28a Compression measurement of a port at 2m ground plane. 6dB voltage increments from 1.25 to 20 volts. Each progressive curve has been lowered 6dB. All curves overlap at upper frequencies no thermal compression is seen.

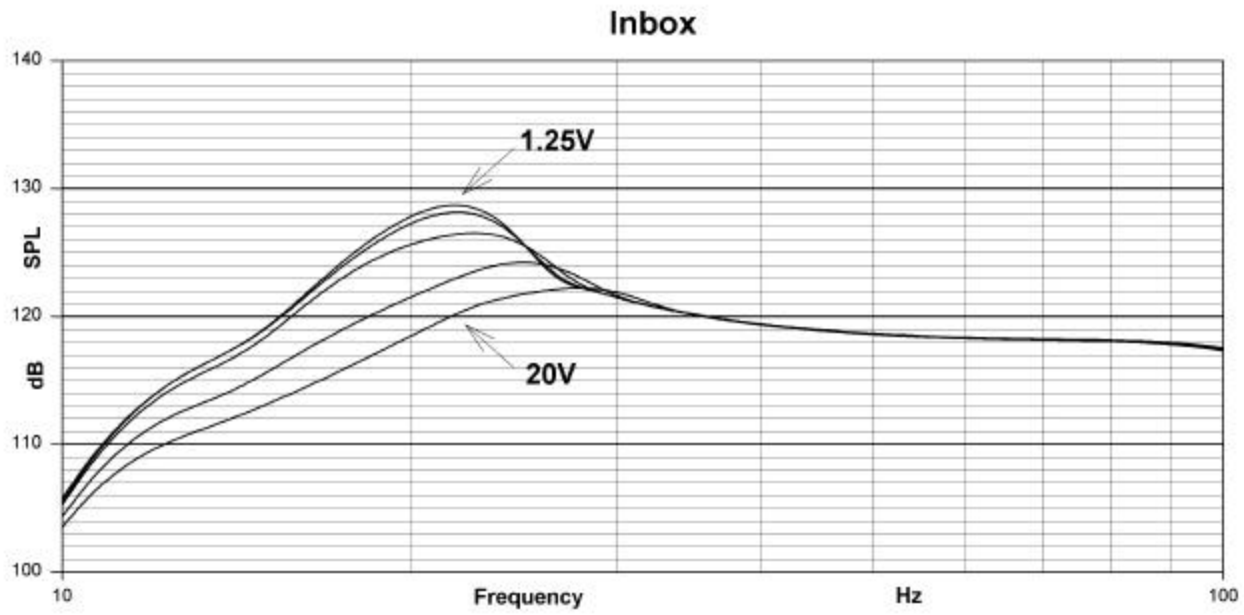

Figure 28b Same measurement as 28a with a microphone placed in the box.

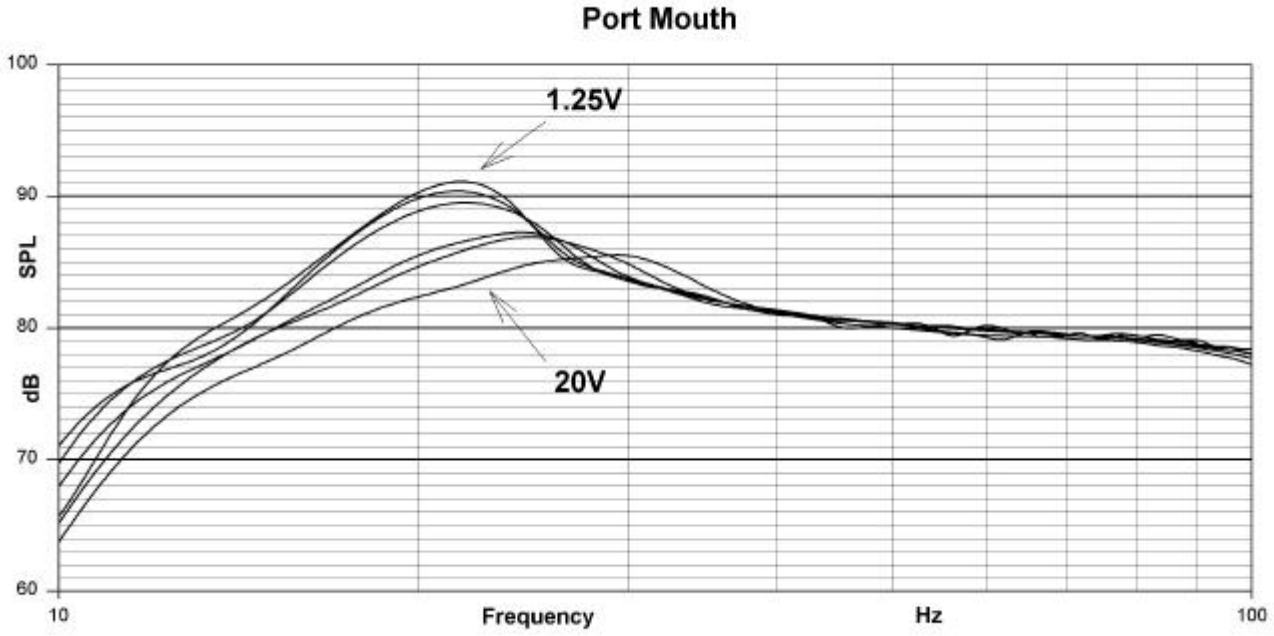

Figure 28c Same as 28a, 28b with microphone at the mouth of the port transverse in the baffle plane.

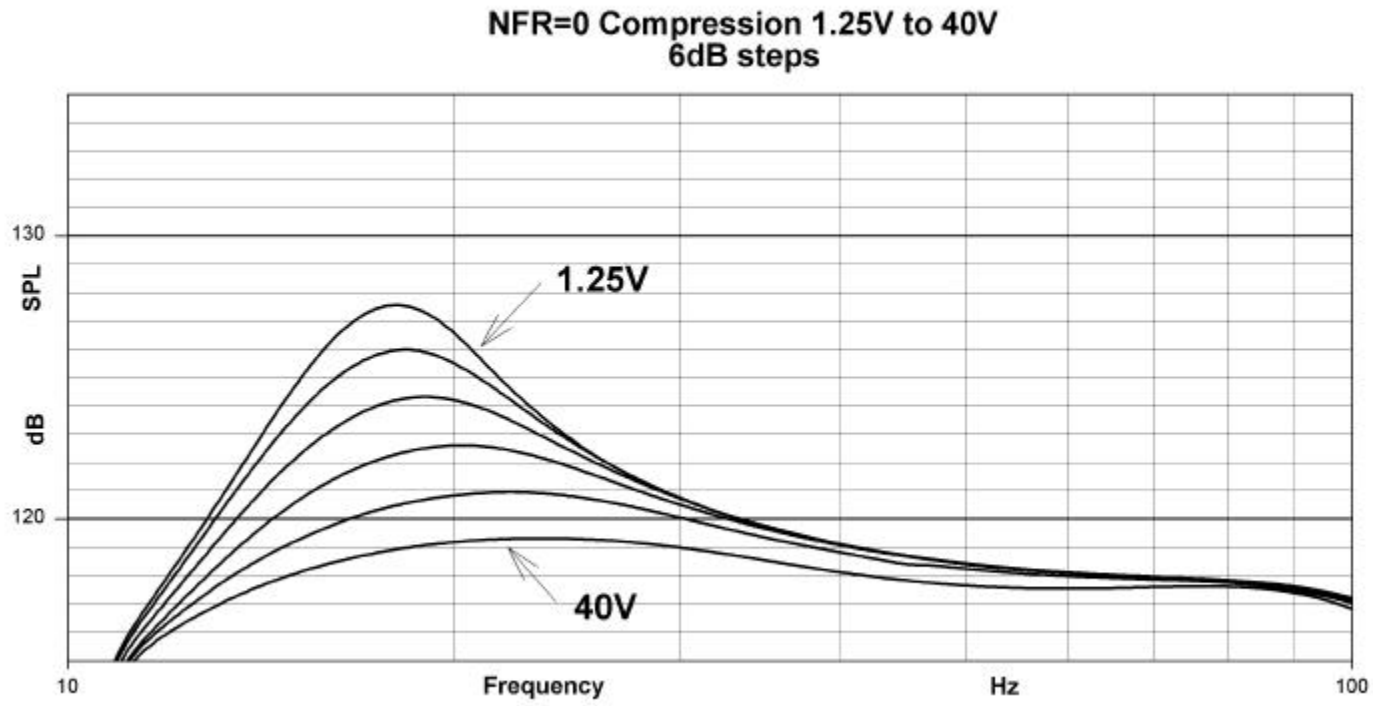

29a. Port compression measured in the box for a port with NFR of 0.0

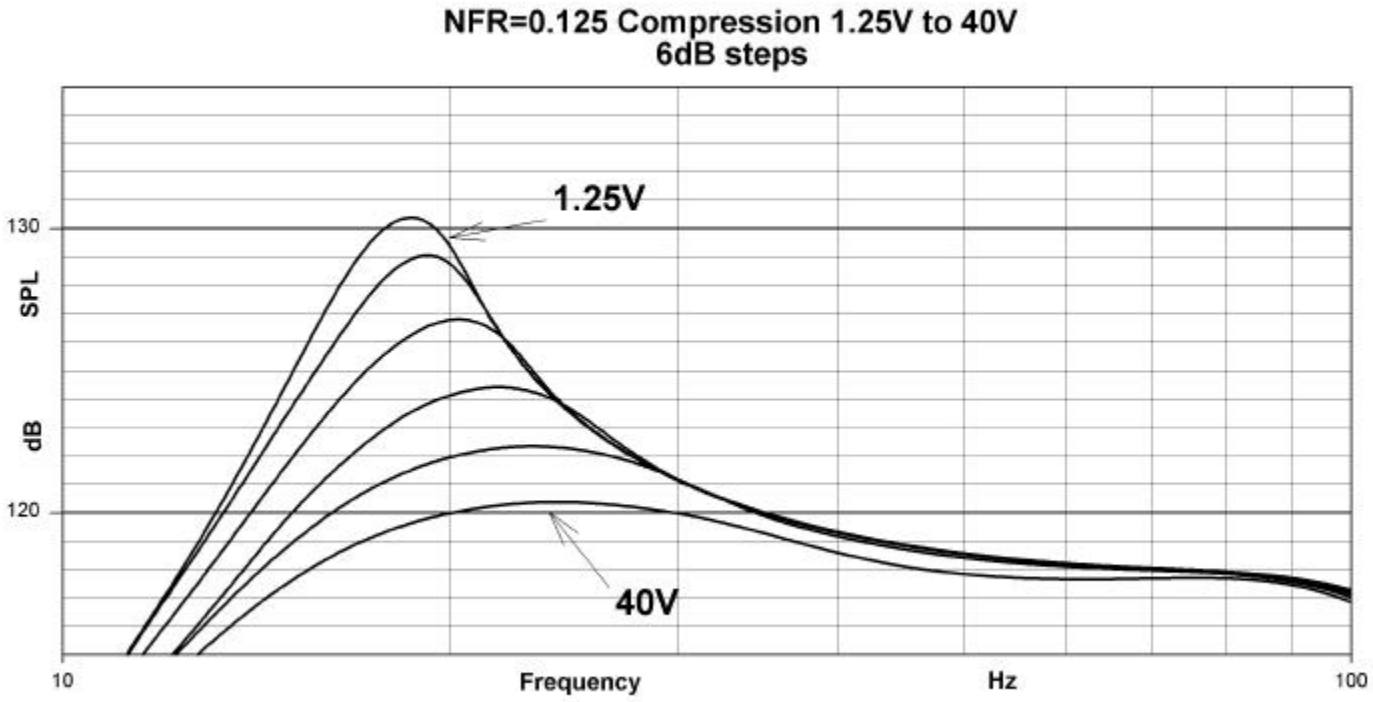

29b. Port compression measured in the box for a port with NFR of 0.125

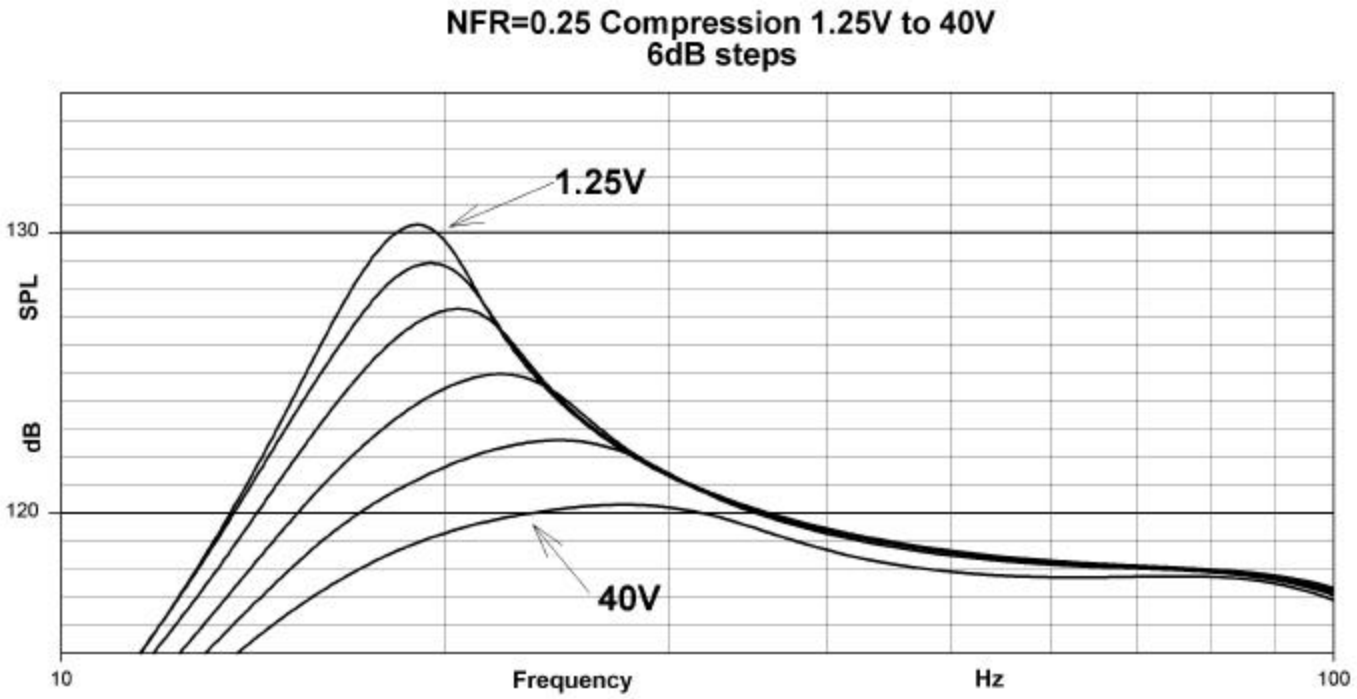

29c. Port compression measured in the box for a port with NFR of 0.25

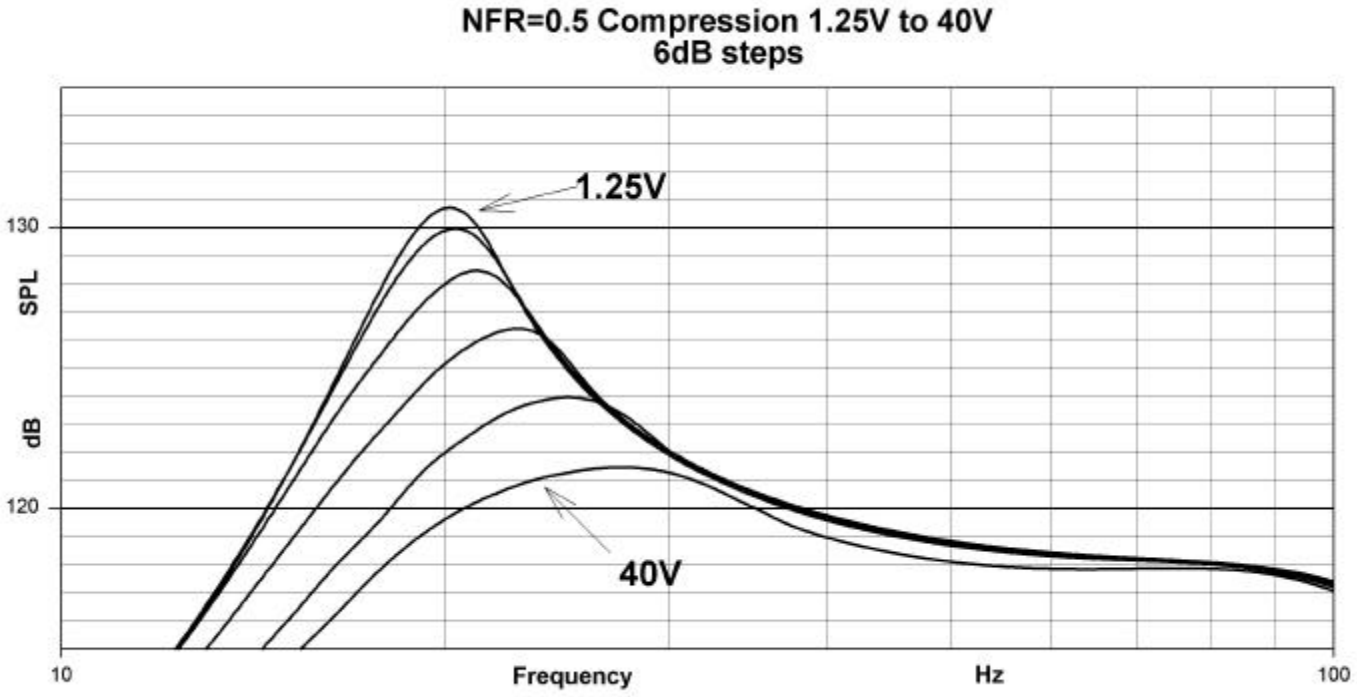

29d. Port compression measured in the box for a port with NFR of 0.5

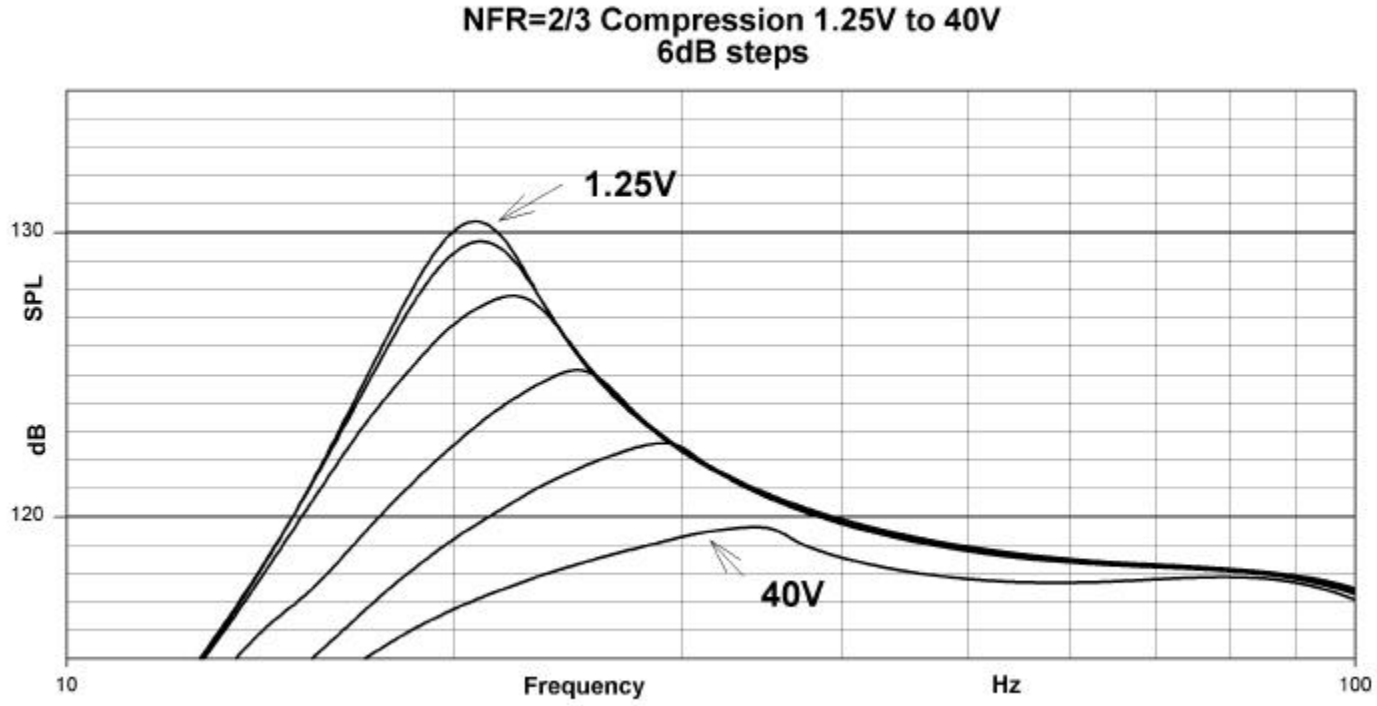

29e. Port compression measured in the box for a port with NFR of 0.66

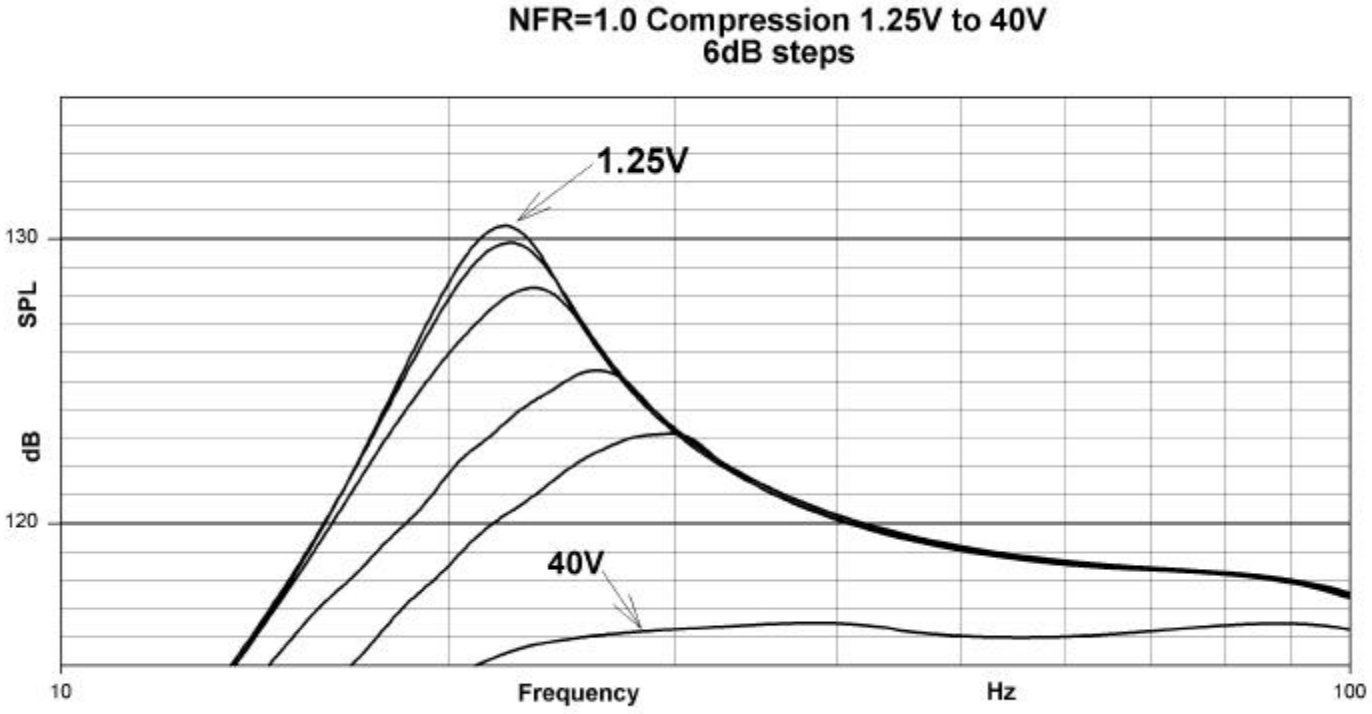

29f. Port compression measured in the box for a port with NFR of 1.0

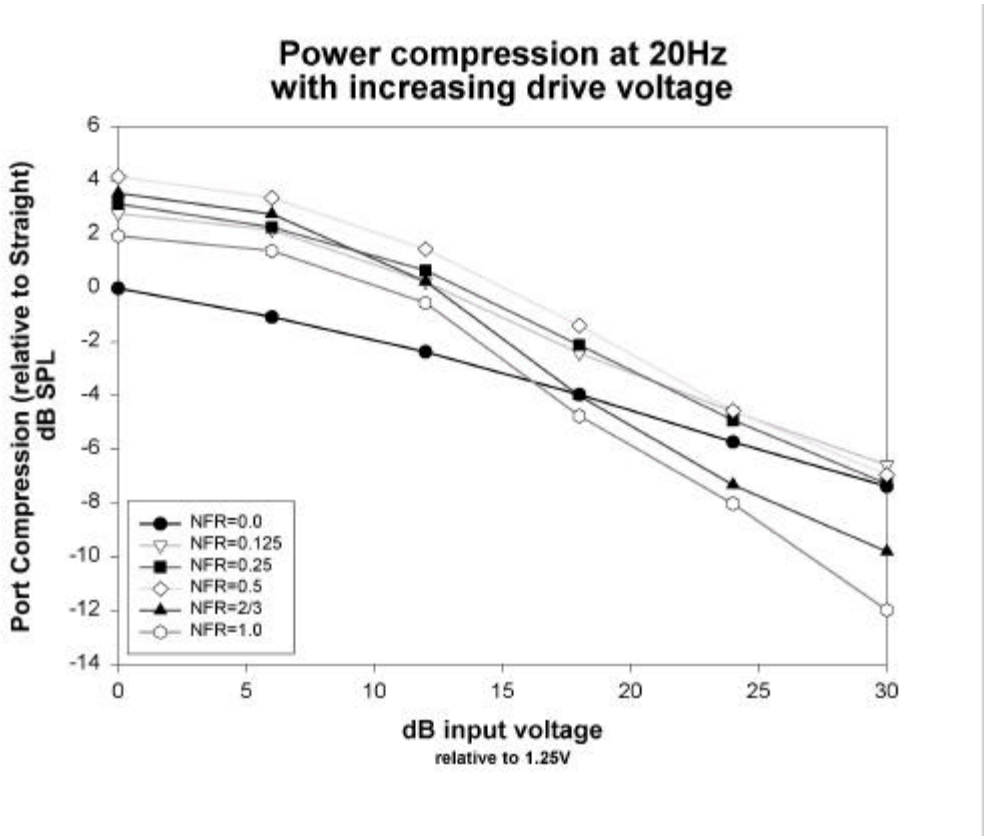

Figure 30a. Port Compression vs Level at 20Hz for simple radius ports, Note NFR of .5 is best of all.

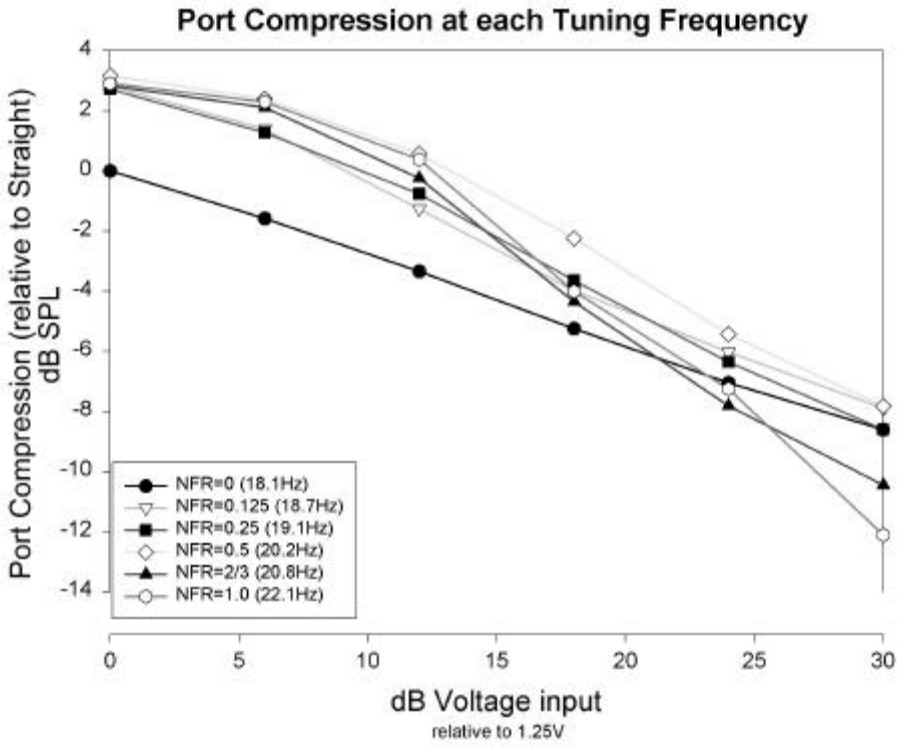

Figure 30b. Port compression at port tuning for simple radius ports. Note NFR of 0.5 is best.

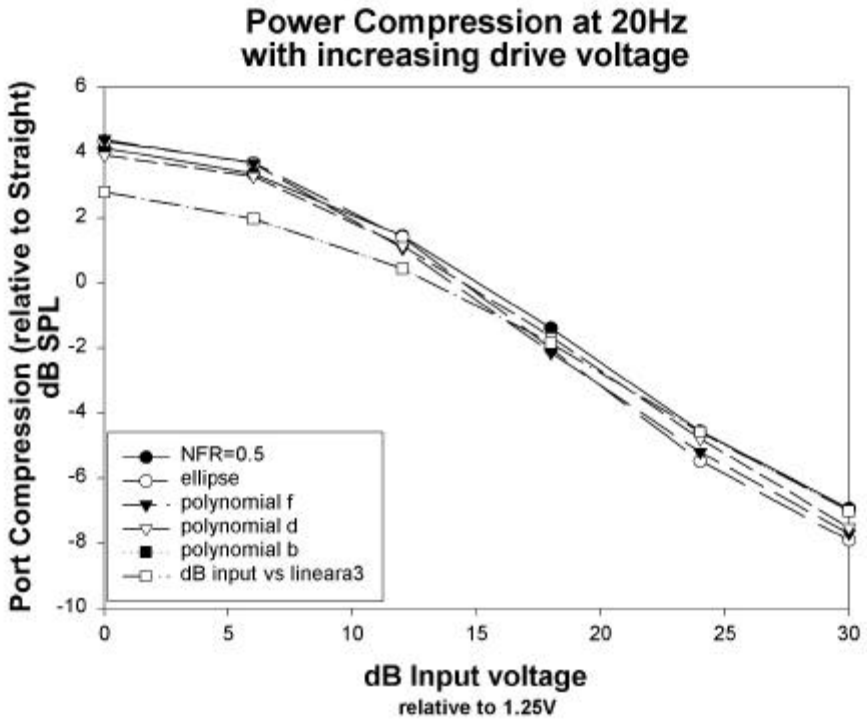

Figure 30c. Port Compression for other profiles. Polynomial ports are described in section 10, study #8 (NFR=0.5 plotted for reference)

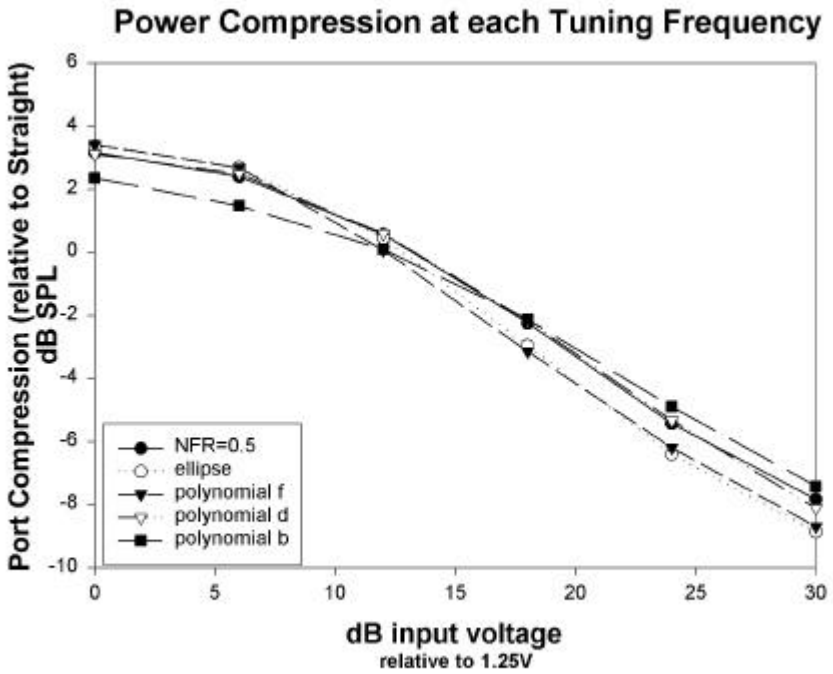

Figure 30d. Port Compression at tuning for other profiles. Polynomial profiles are discussed in section 10, study #8. (NFR=0.5 plotted for reference.)

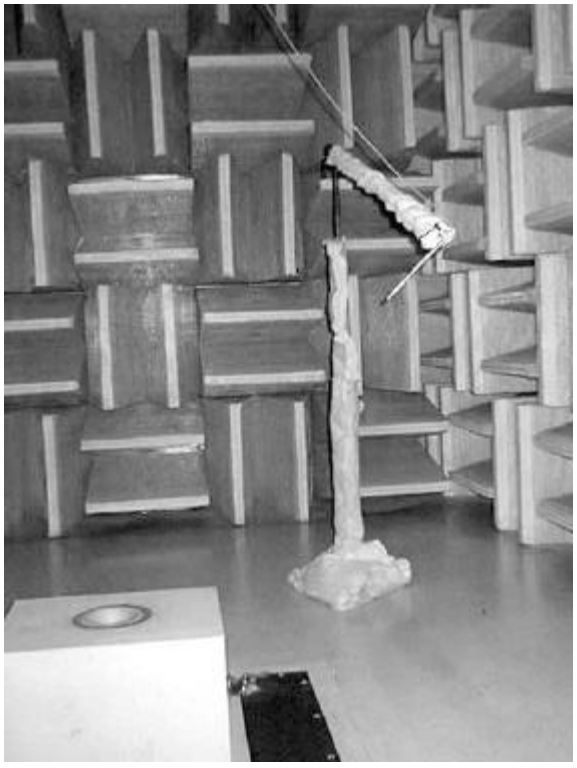

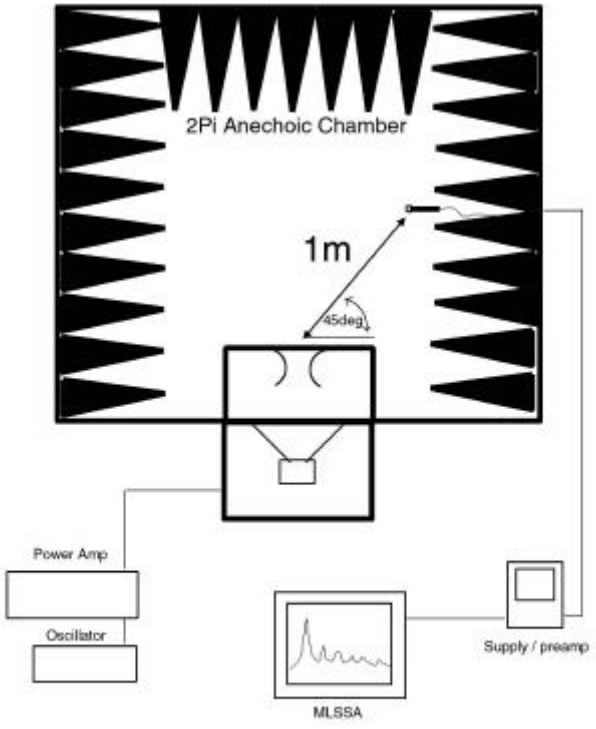

Distortion Measurement Setup

Figure 31.

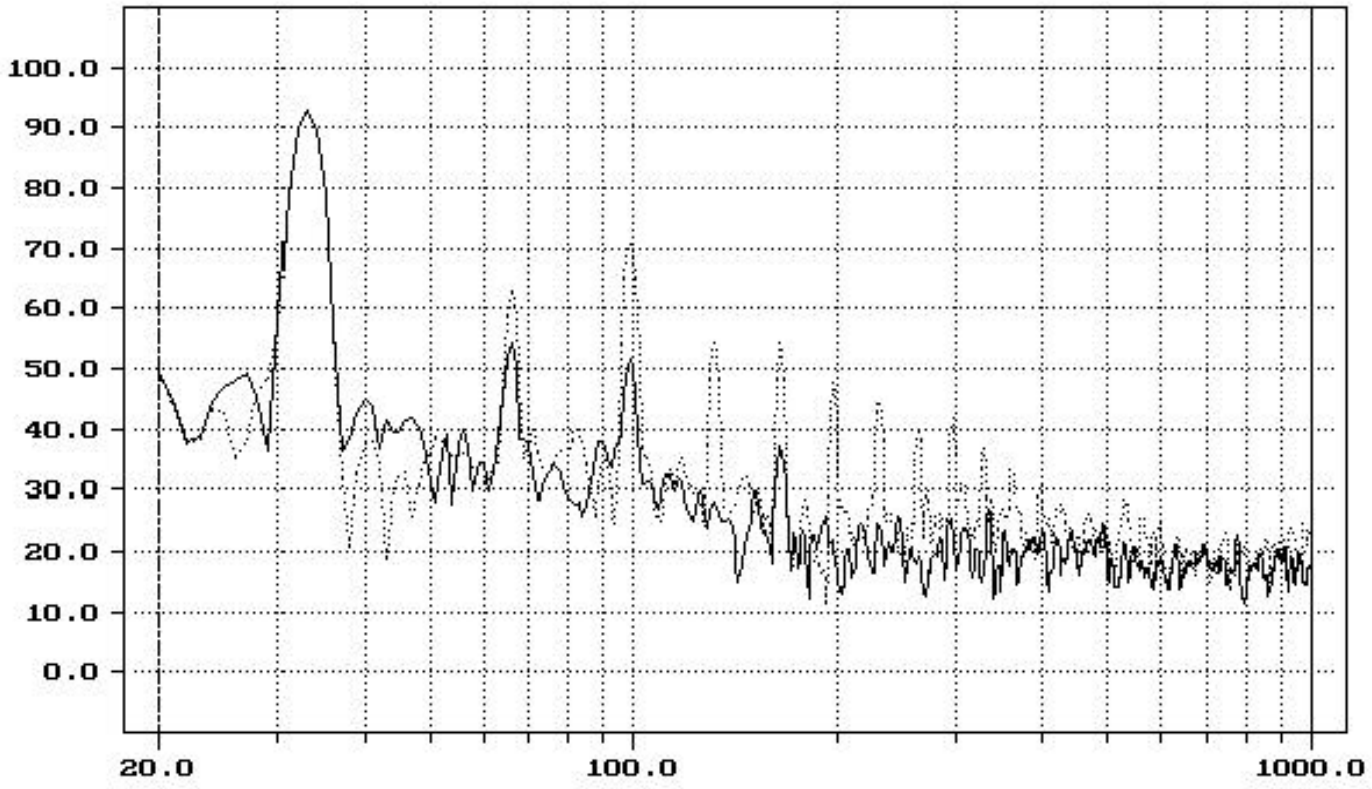

Figure 32a. Spectra of worst port (straight profile, dotted curve) and one of the best ports (solid curve) at 93dB fundamental of 33Hz, showing that a THD measurement captures the differences. The noise is well below the harmonics therefore the level of harmonics represent a good measure of the performance.

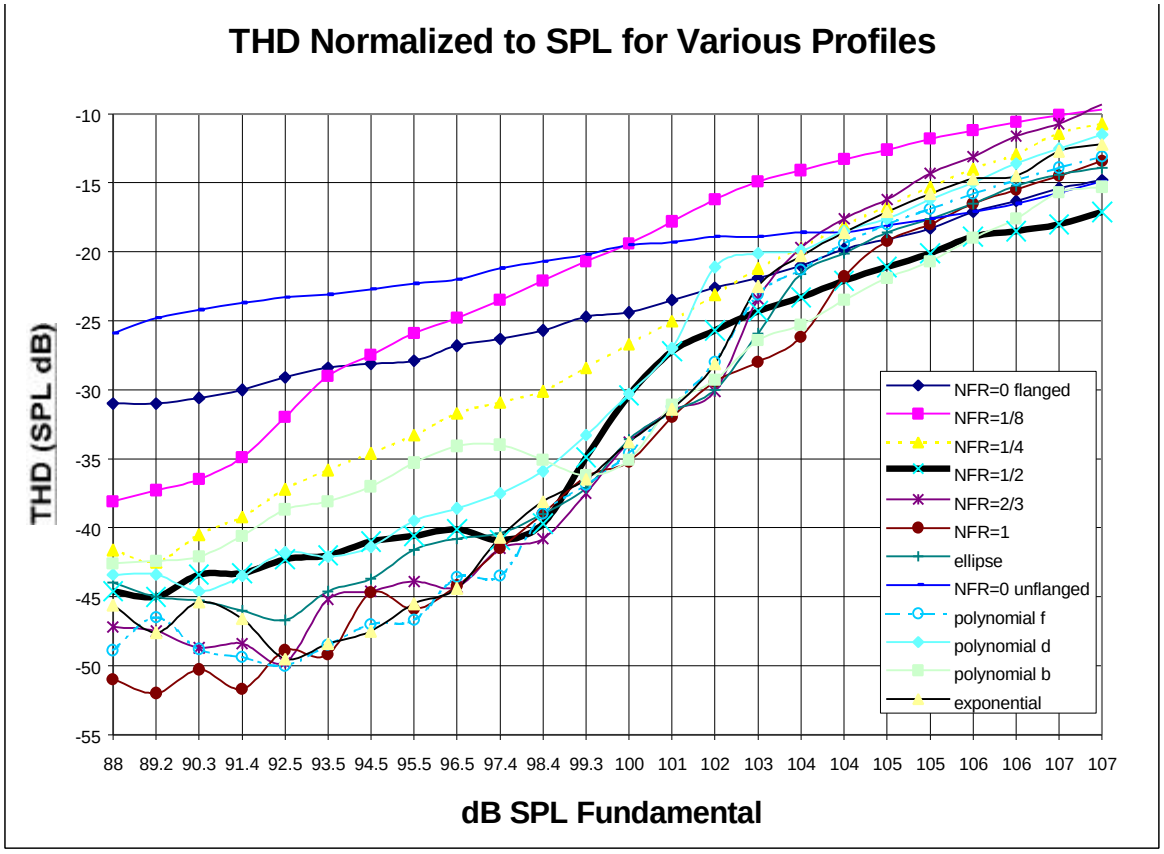

Figure 32b. THD for all port tests vs. fundamental at increasing levels

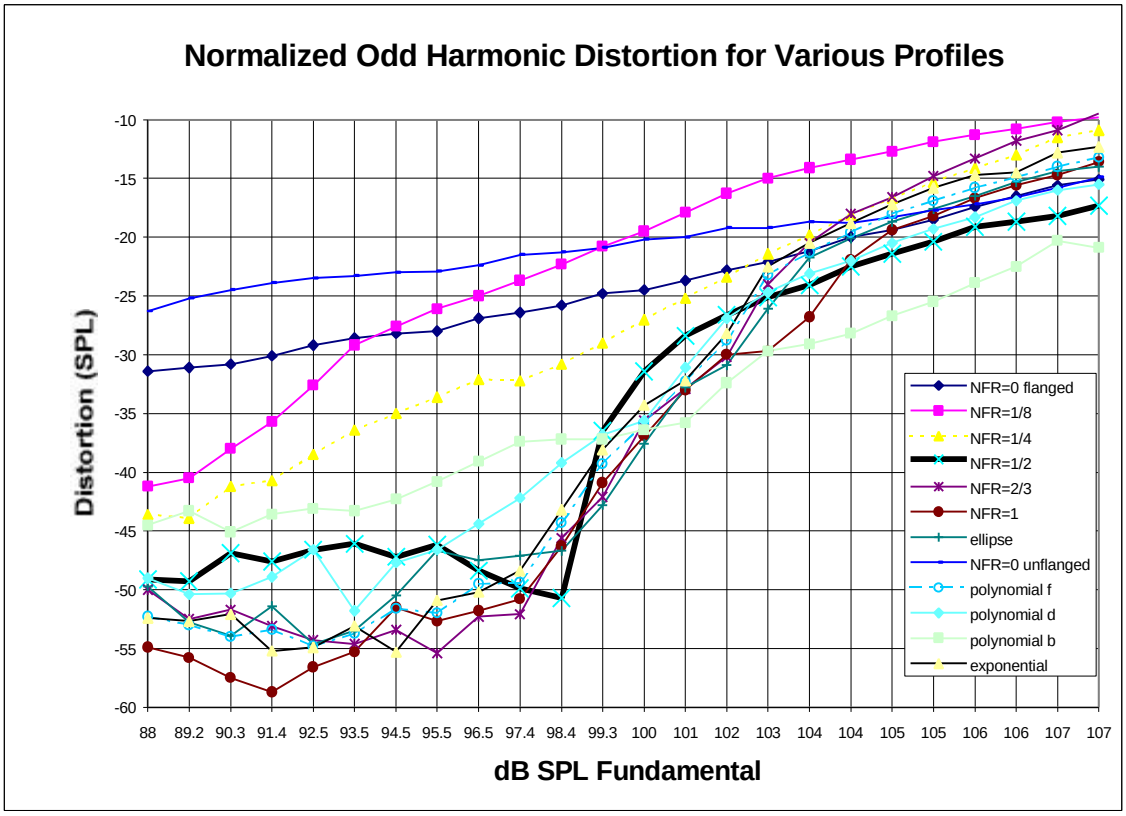

32c. Odd harmonics of all ports tested with increasing level

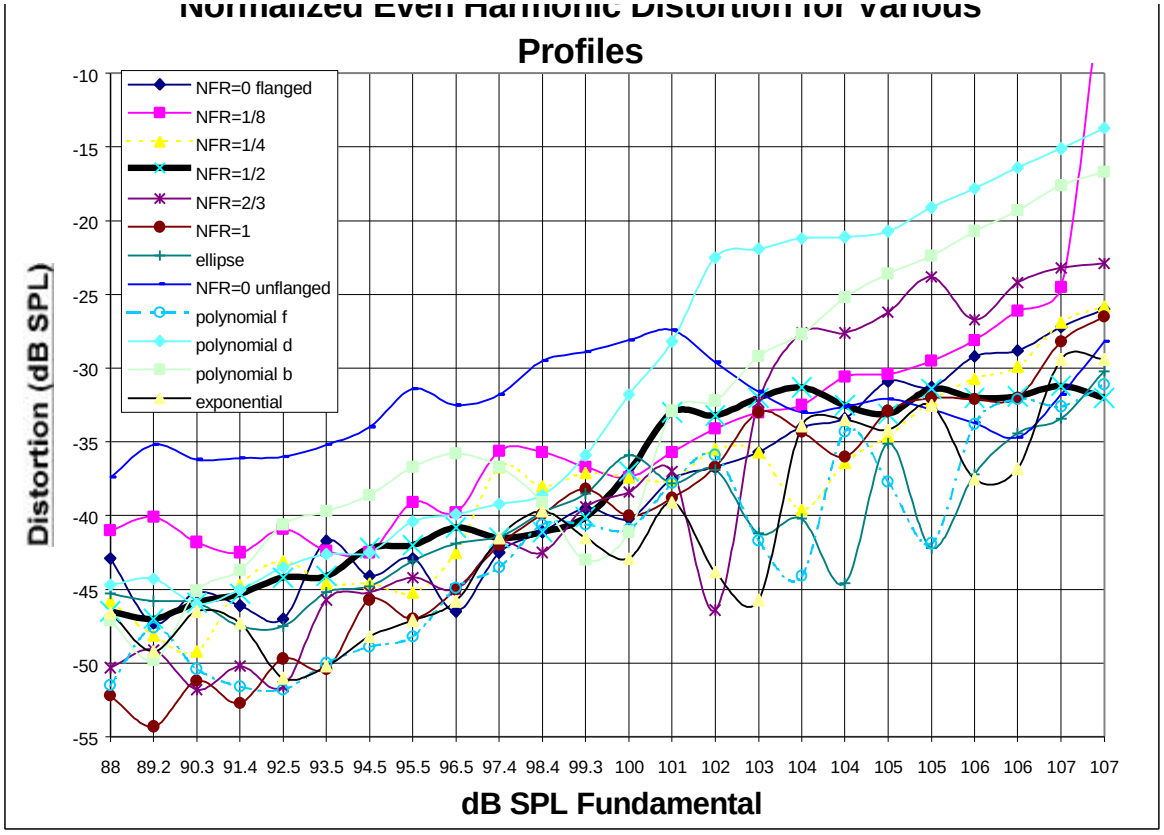

Figure 32d. Even order harmonics

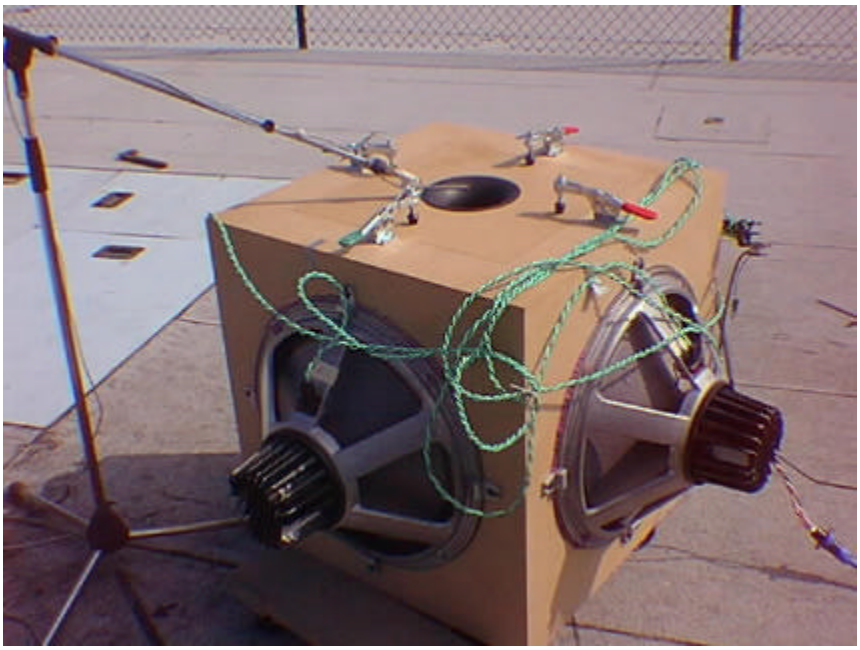

Figure 33. Setup for velocity measurements

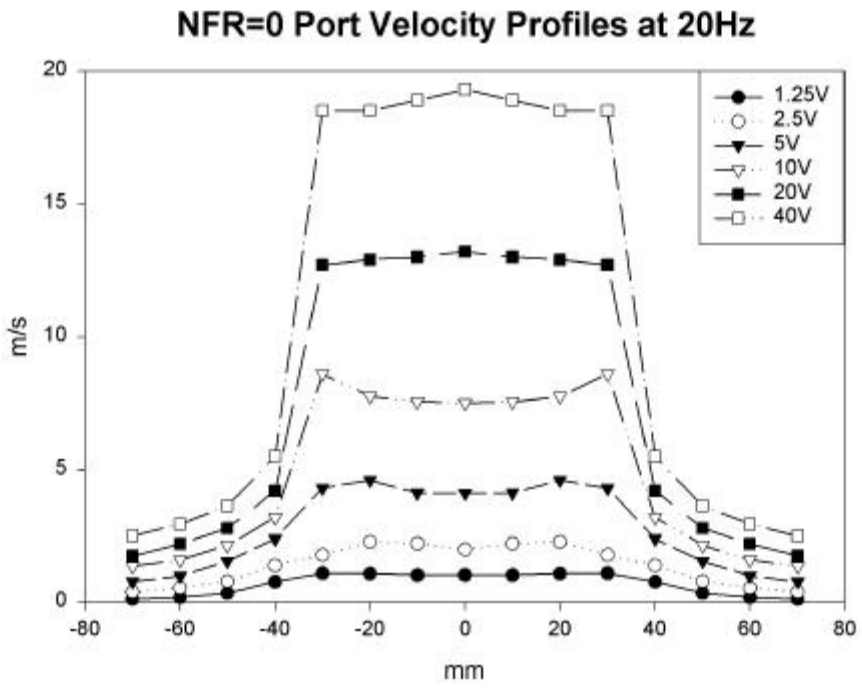

Figure 34a. NFR =0.0. Note the higher velocity at the edges of the port on the 10V measurement.

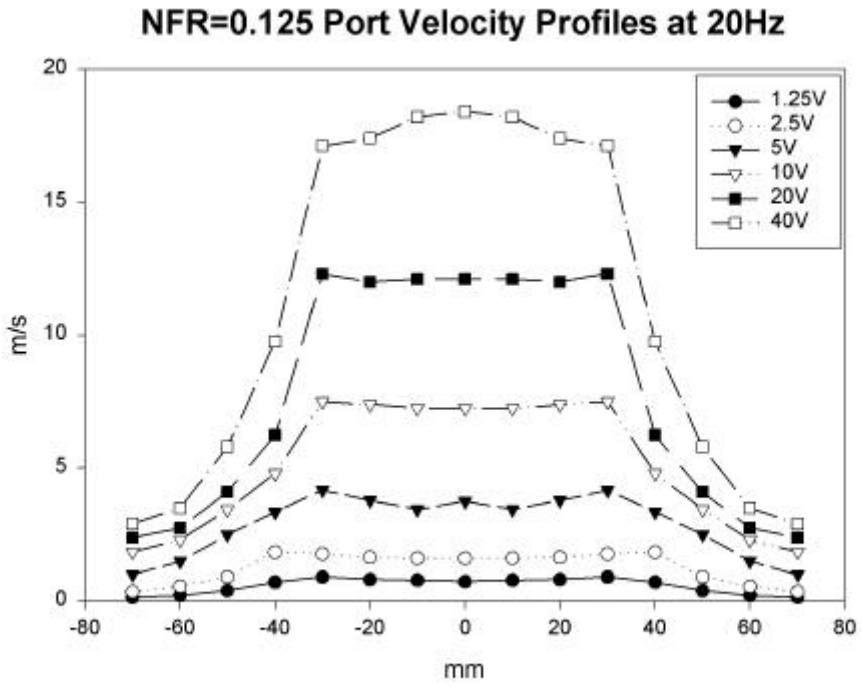

Figure 34b. NFR=0.125 The 5 V measurement shows the rise in velocity at the edges.

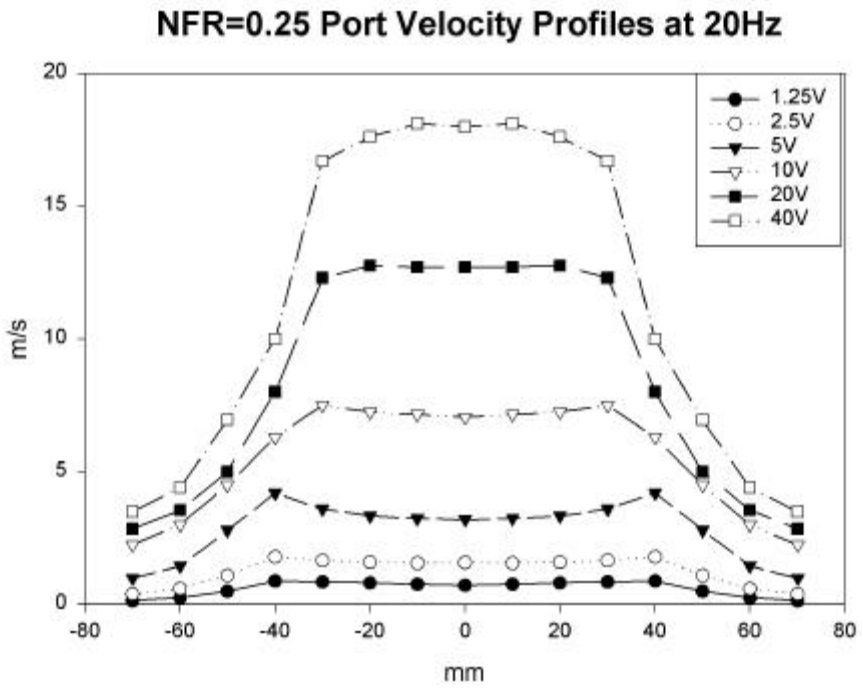

Fig 34c. NFR=0.25, 5V measurement shows rise in velocity at edges.

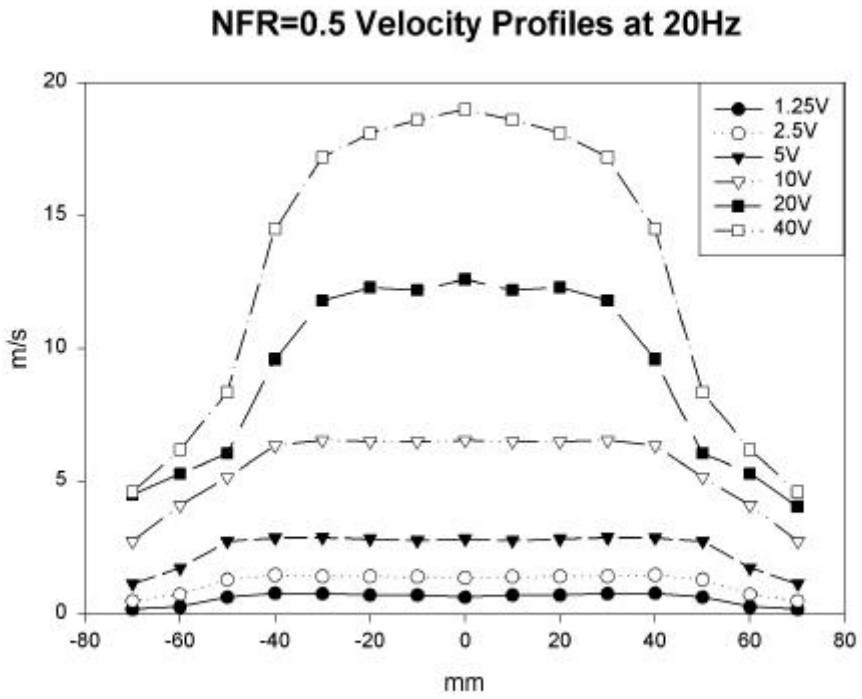

Fig 34d. NFR=0.5, Ports with NFR of .5 or higher don't have higher velocity at port edges

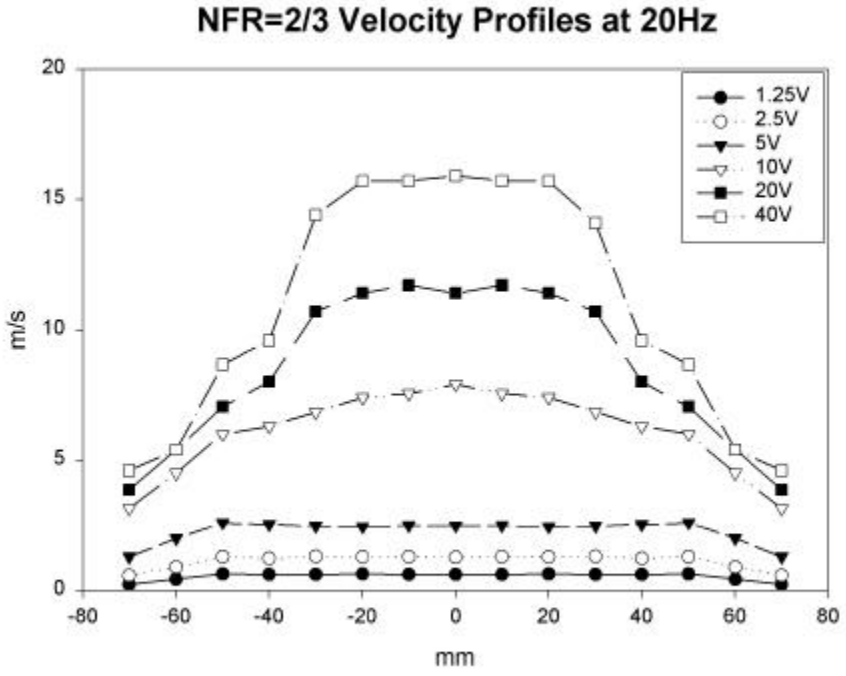

Figure 34e NFR = 2/3

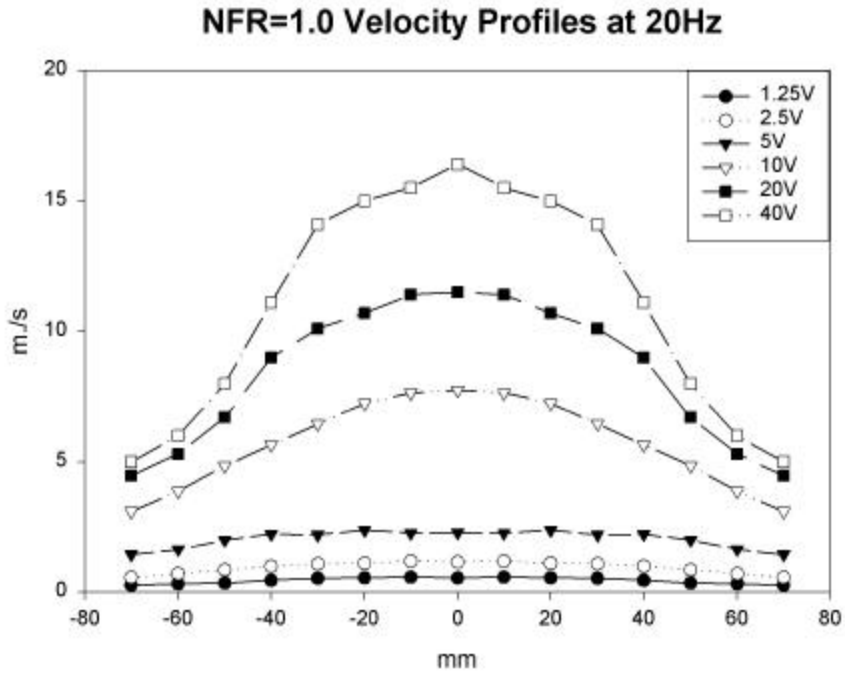

Fig 34f. NFR=1.0

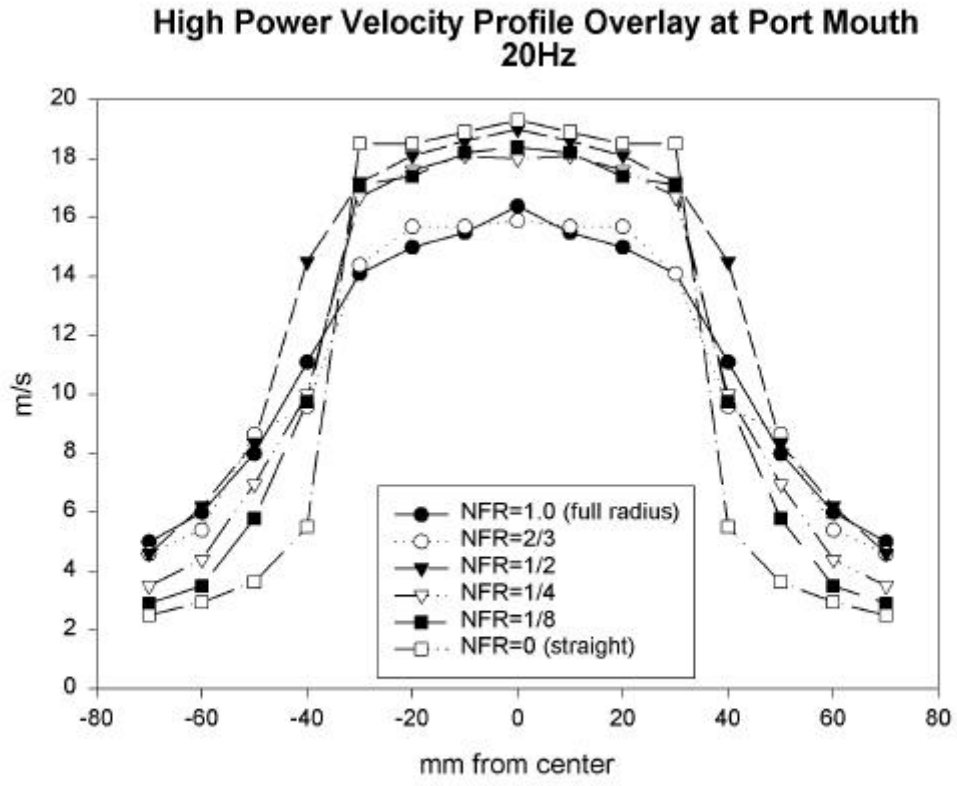

Figure 35. Velocity profiles at very high level for all ports in study

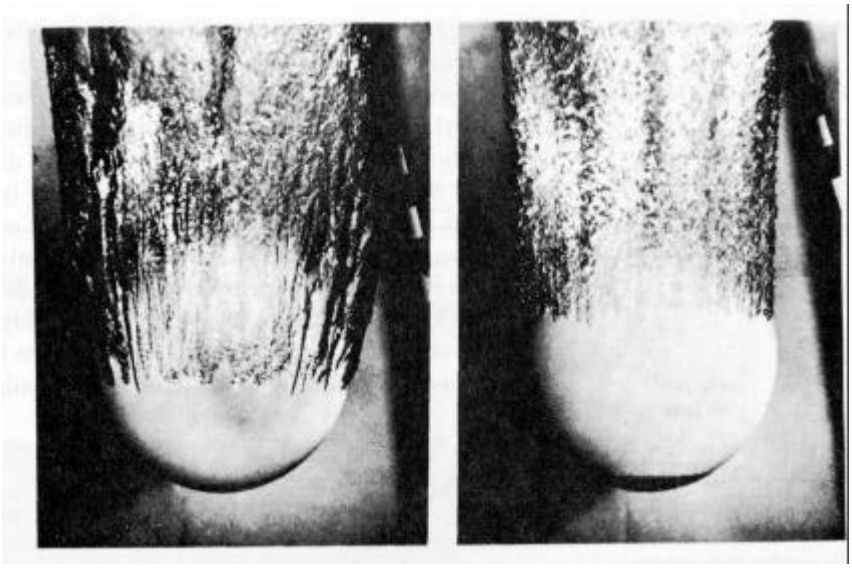

a. smooth b. textured at bottom

Figure 36. Wake of a bowling ball as a function of texturing leading surface.

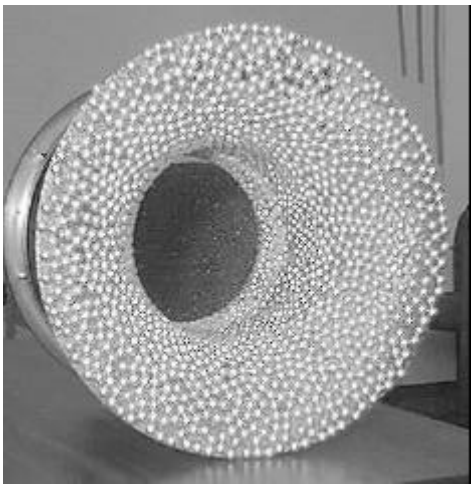

Figure 37. Example of a port used for roughness study

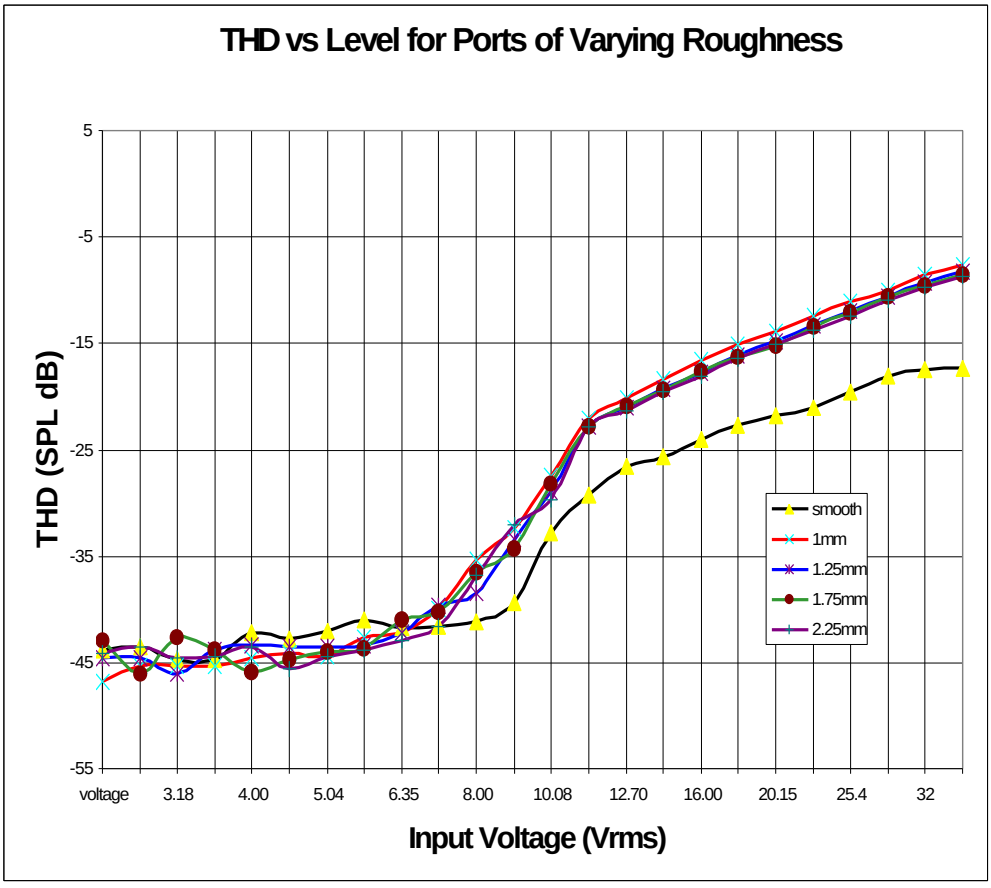

Figure 38a. THD of ports in Roughness study

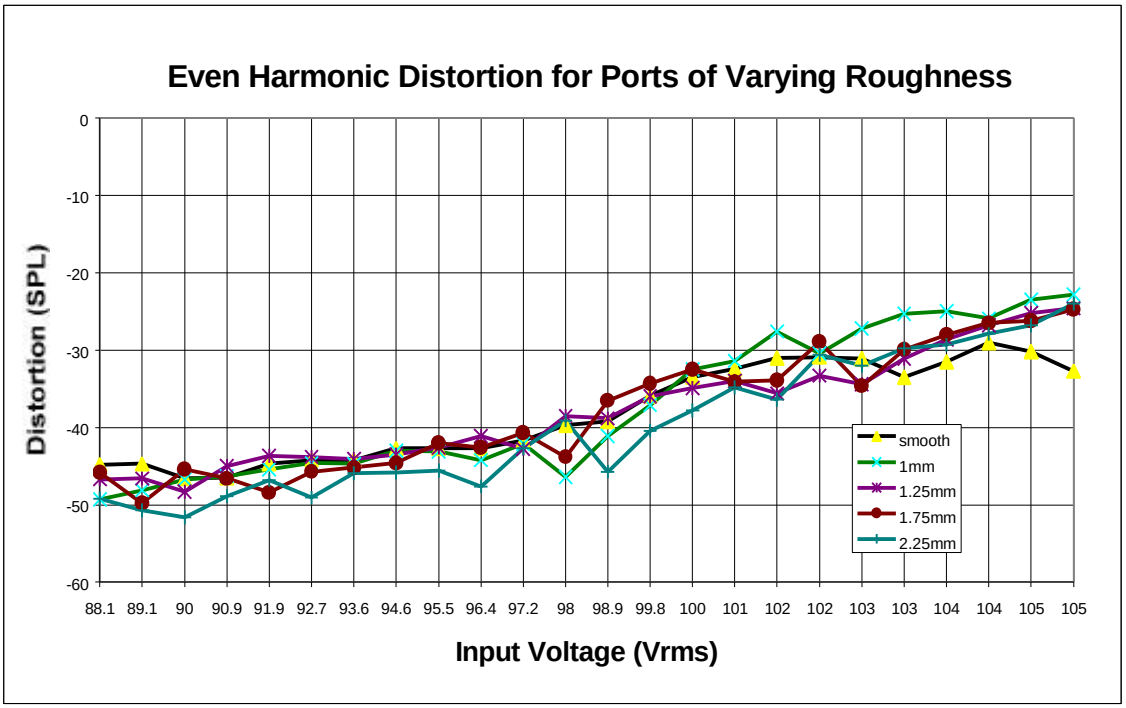

Figure 38b. Even order harmonic distortion for ports in roughness study

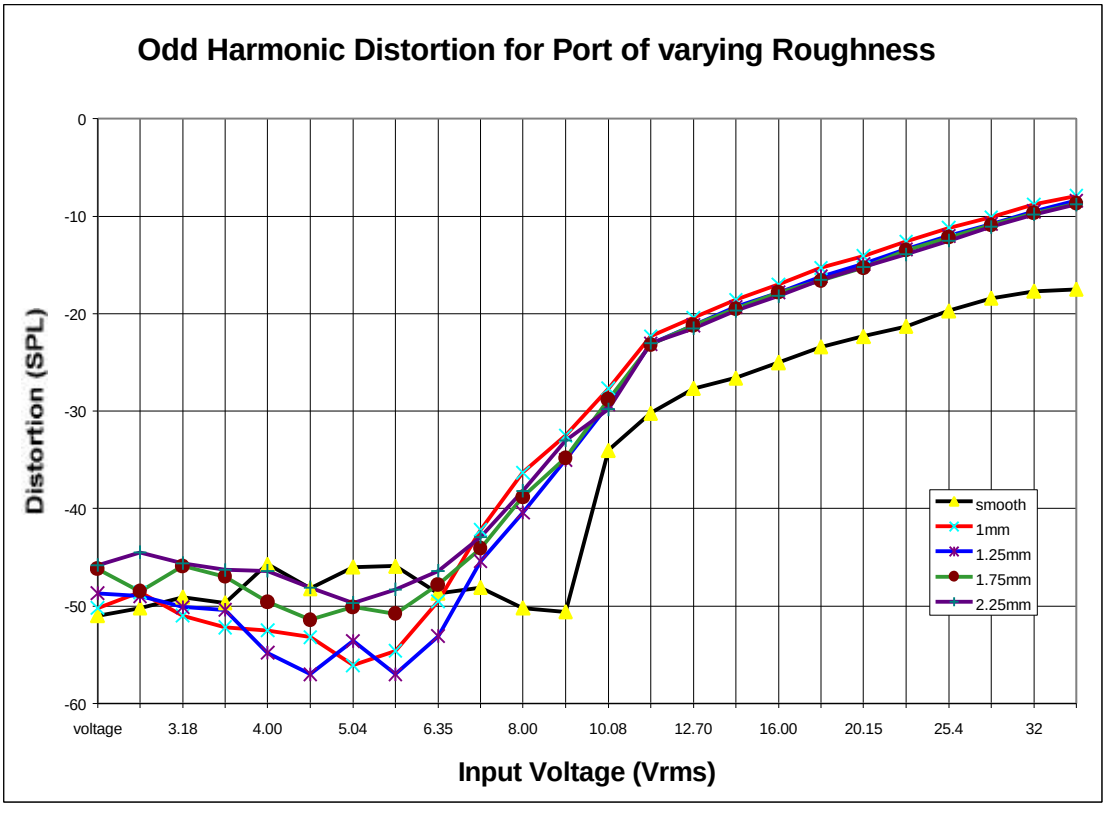

Figure 38c. Odd order harmonic distortion

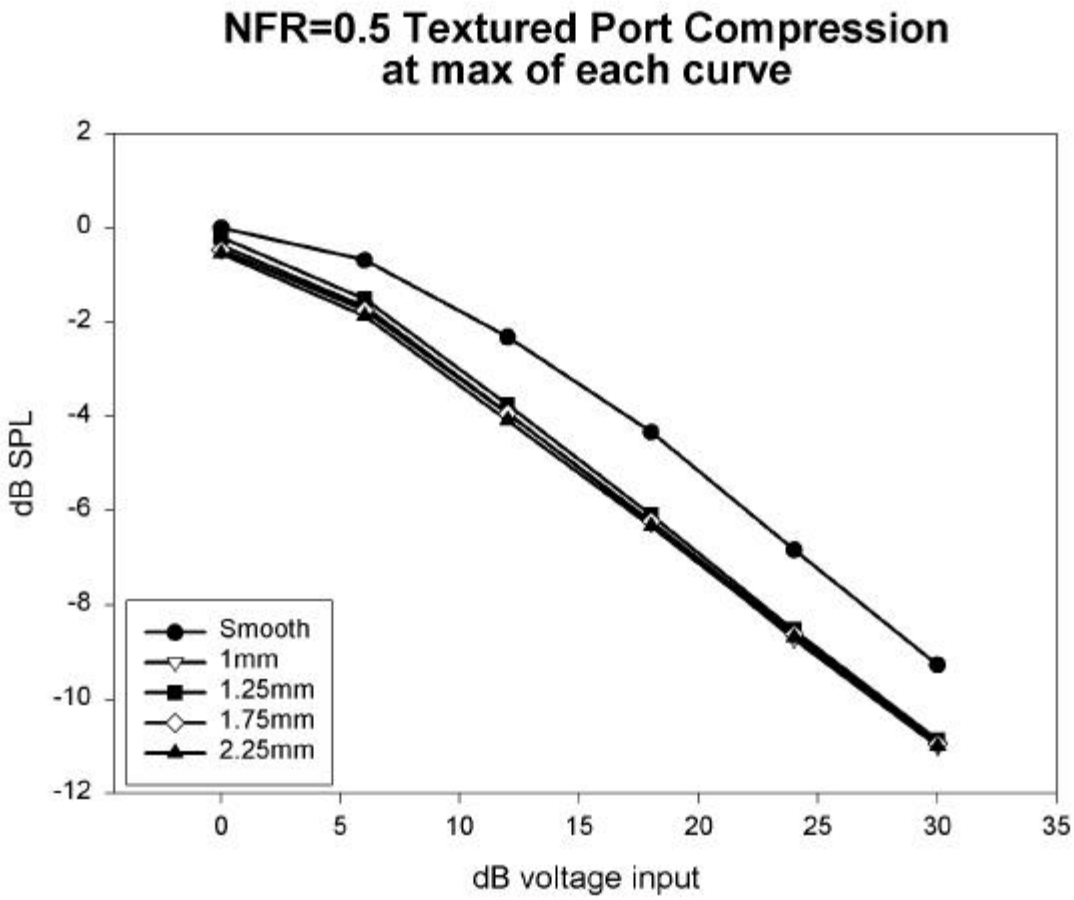

Figure 39. Port Compression of ports in Roughness study

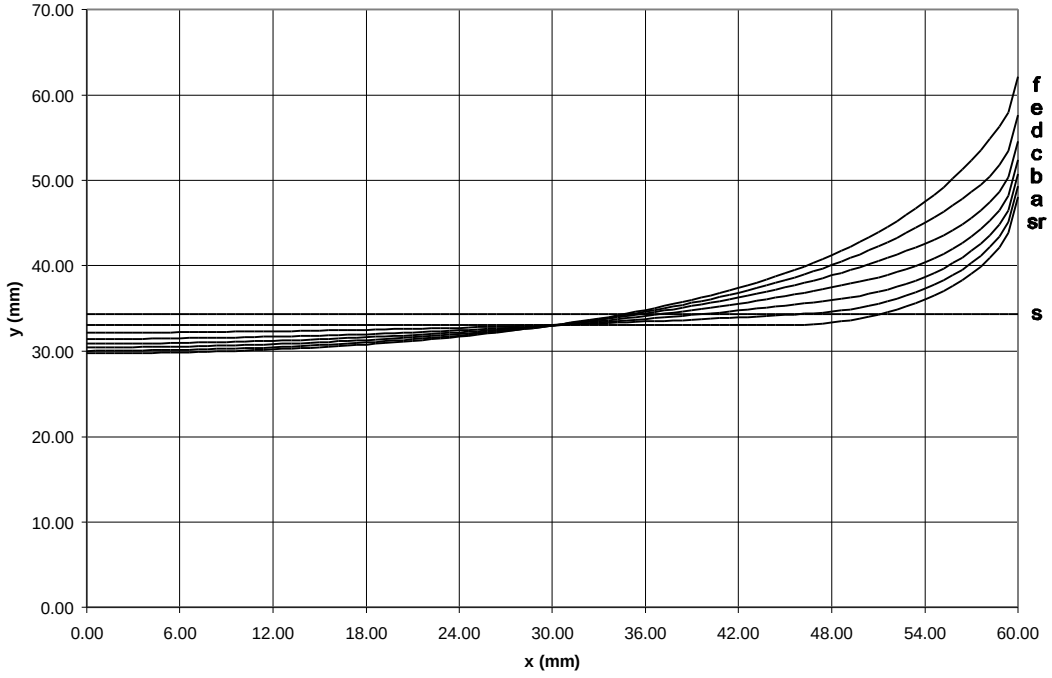

Figure 40. Port profiles.

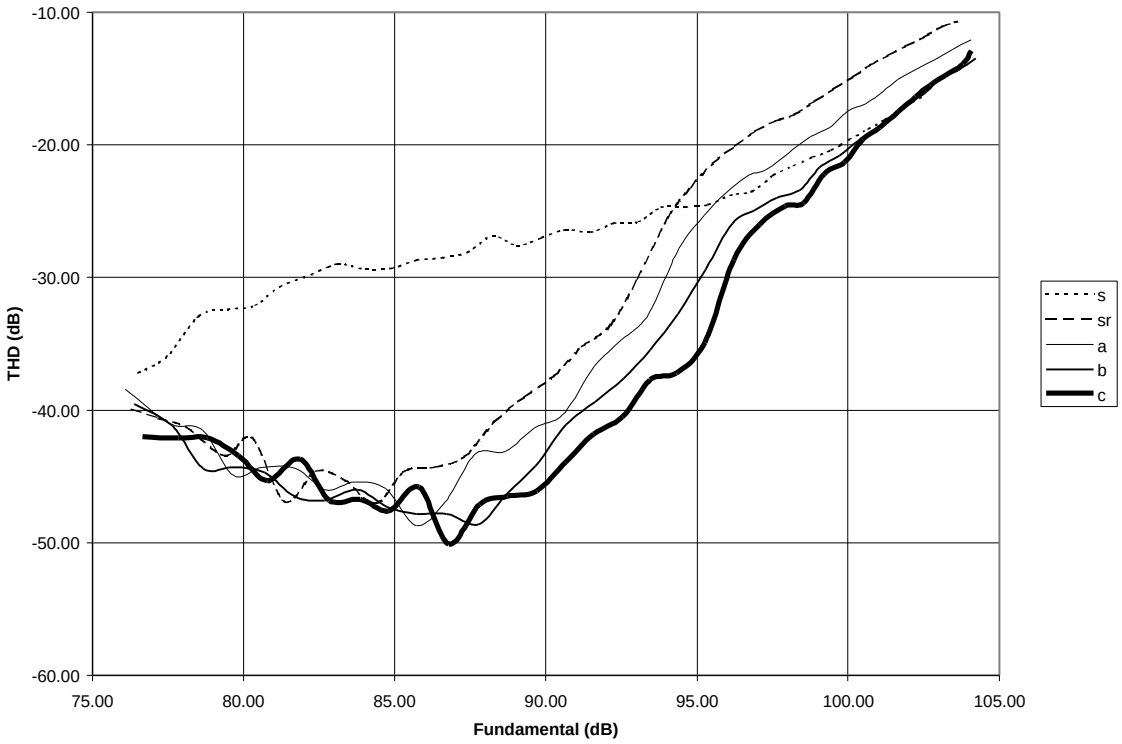

Figure 41a. THD vs. Fundamental SPL for ports s, sr, a, b and c.

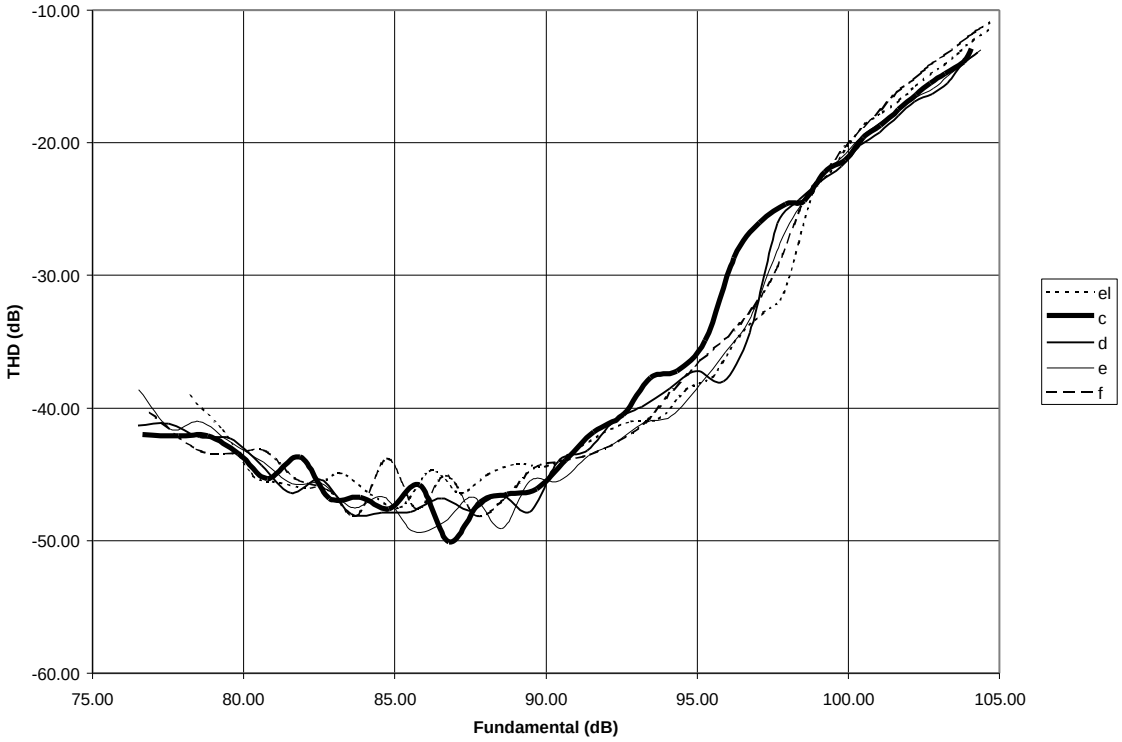

Figure 41b: THD vs Fundamental SPL for ports c, d, e, f and el.

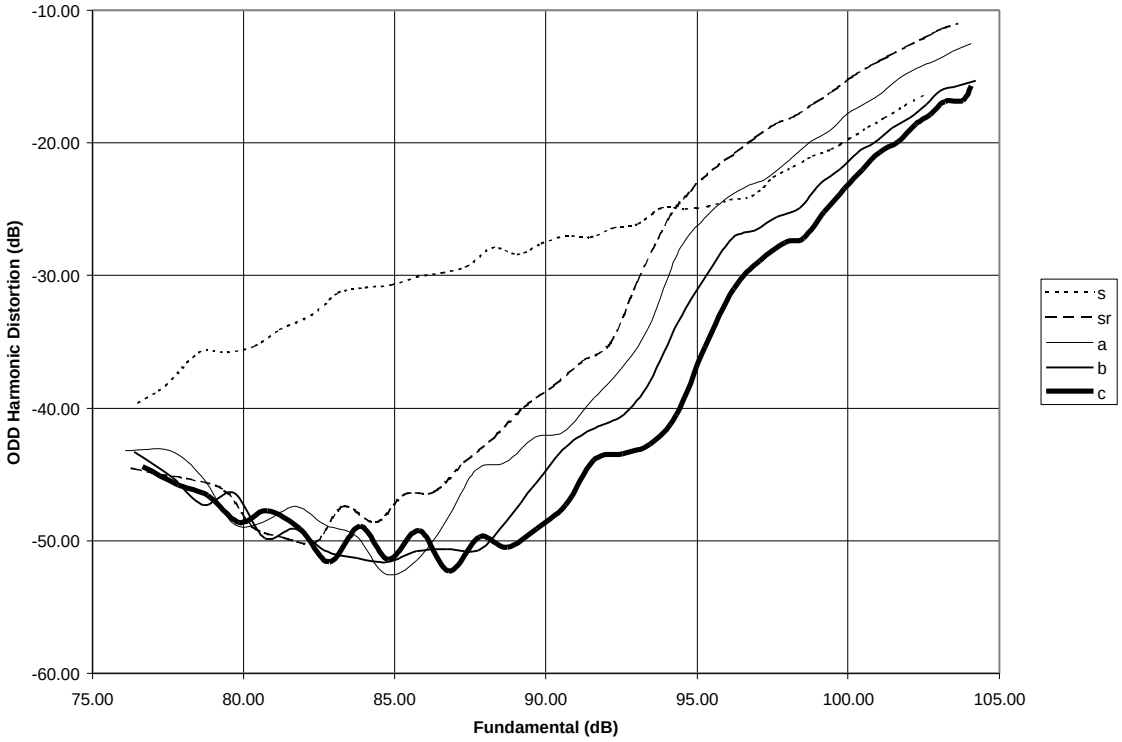

Figure 41c. Odd Harmonic Distortion vs Fundamental SPL for ports s, sr, a, b and c.

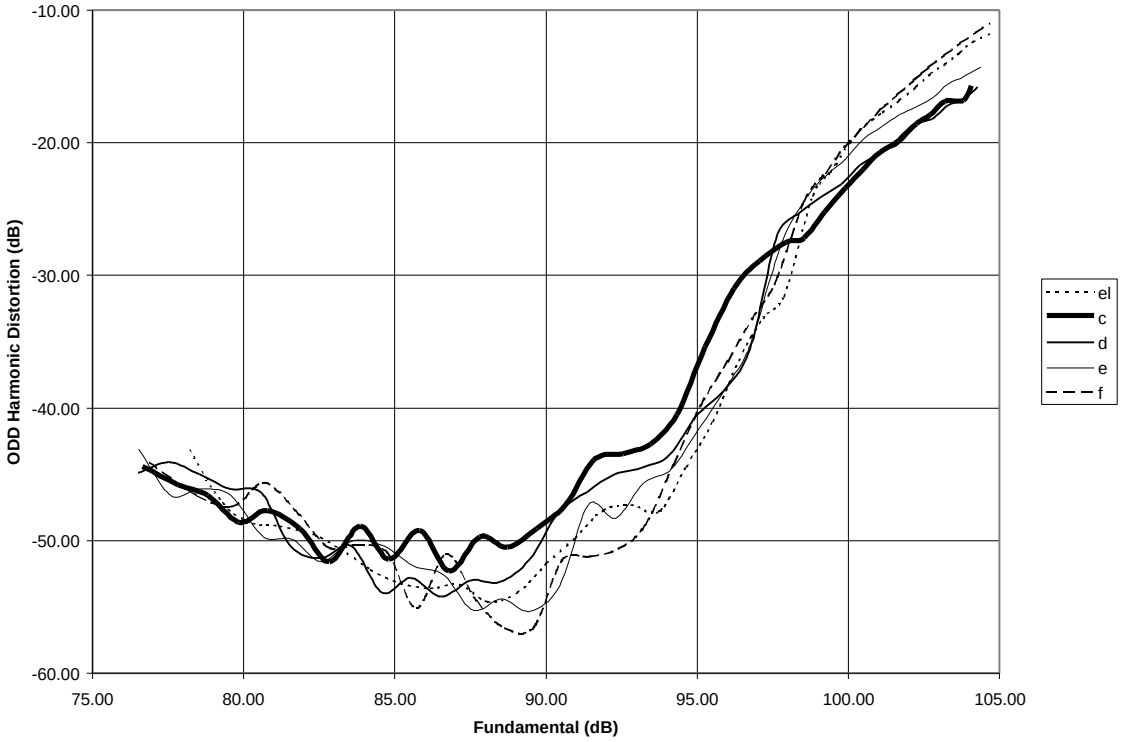

Figure 41d. Odd Harmonic Distortion vs. Fundamental SPL for ports c, d, e, f and el.

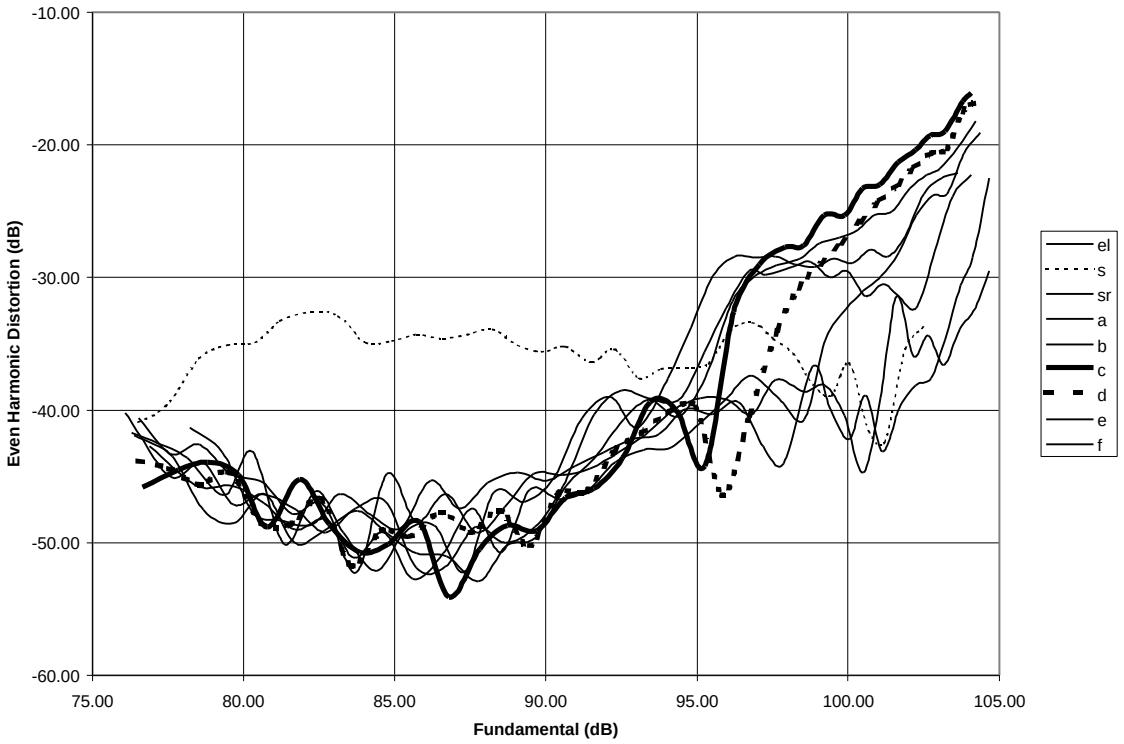

Figure 42a. Even Harmonic Distortion vs. Fundamental SPL for all 9 ports.

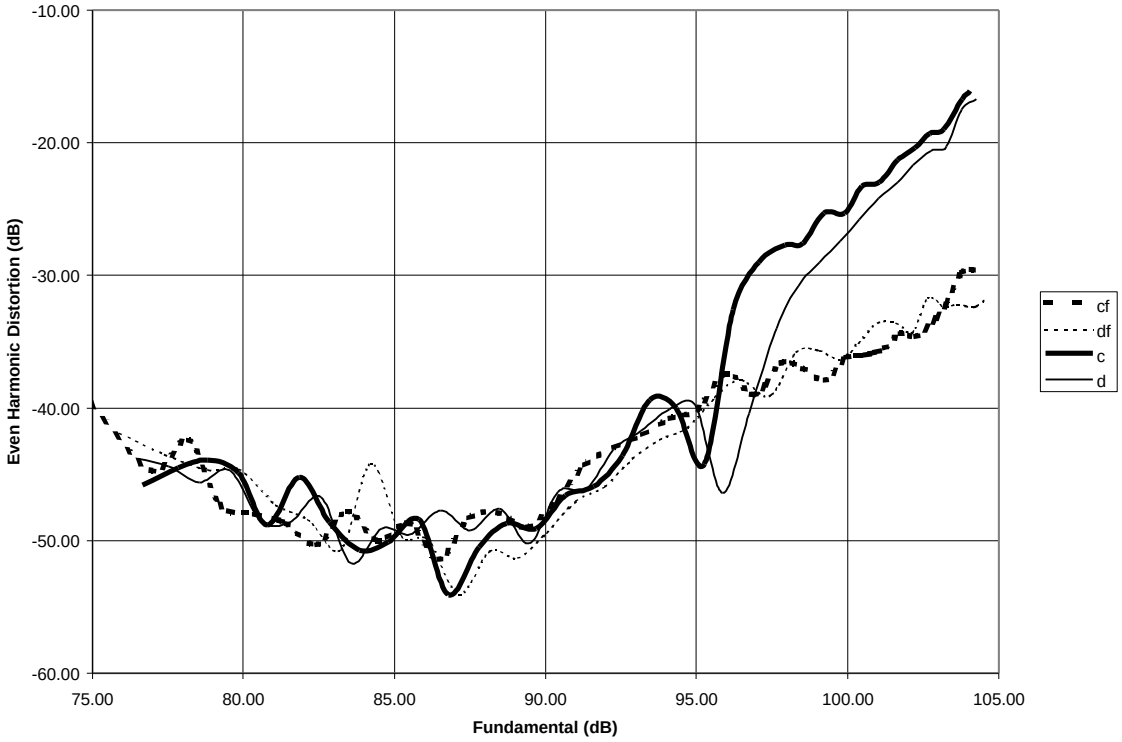

Figure 42b. Even Harmonic Distortion vs. Fundamental for ports c, d, cf and df.

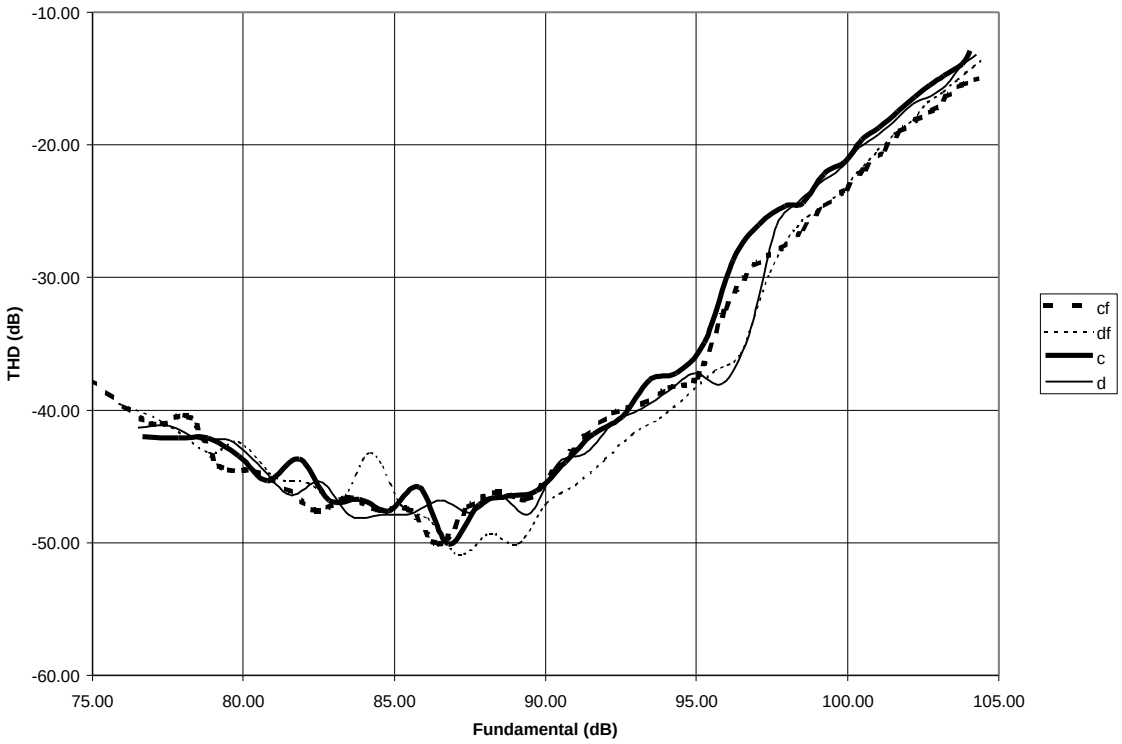

Figure 42c. THD vs. Fundamental SPL for ports c, d, cf and df.

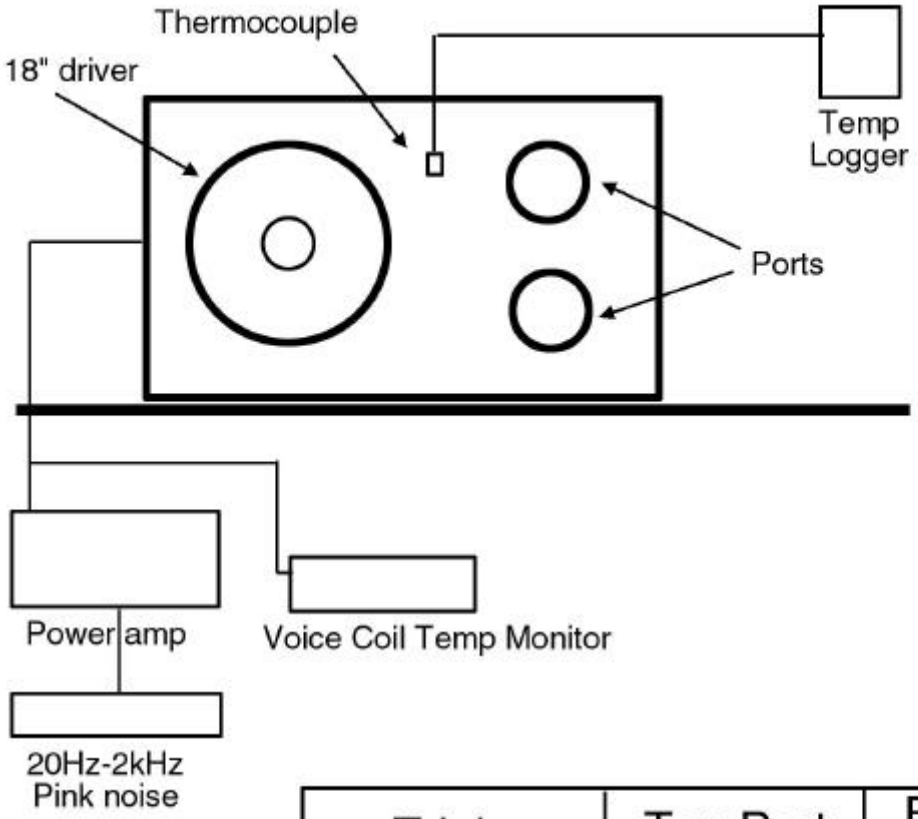

Trial	Top Port	Bottom Port
Sealed	X	X
2 double flared	) (	) (
1 double flared	) (	X
2 small holes	⊓	⊓
1 small hole	⊓	X
innie/outie	⊓	)

Figure 43a. Setup for Thermal experiment

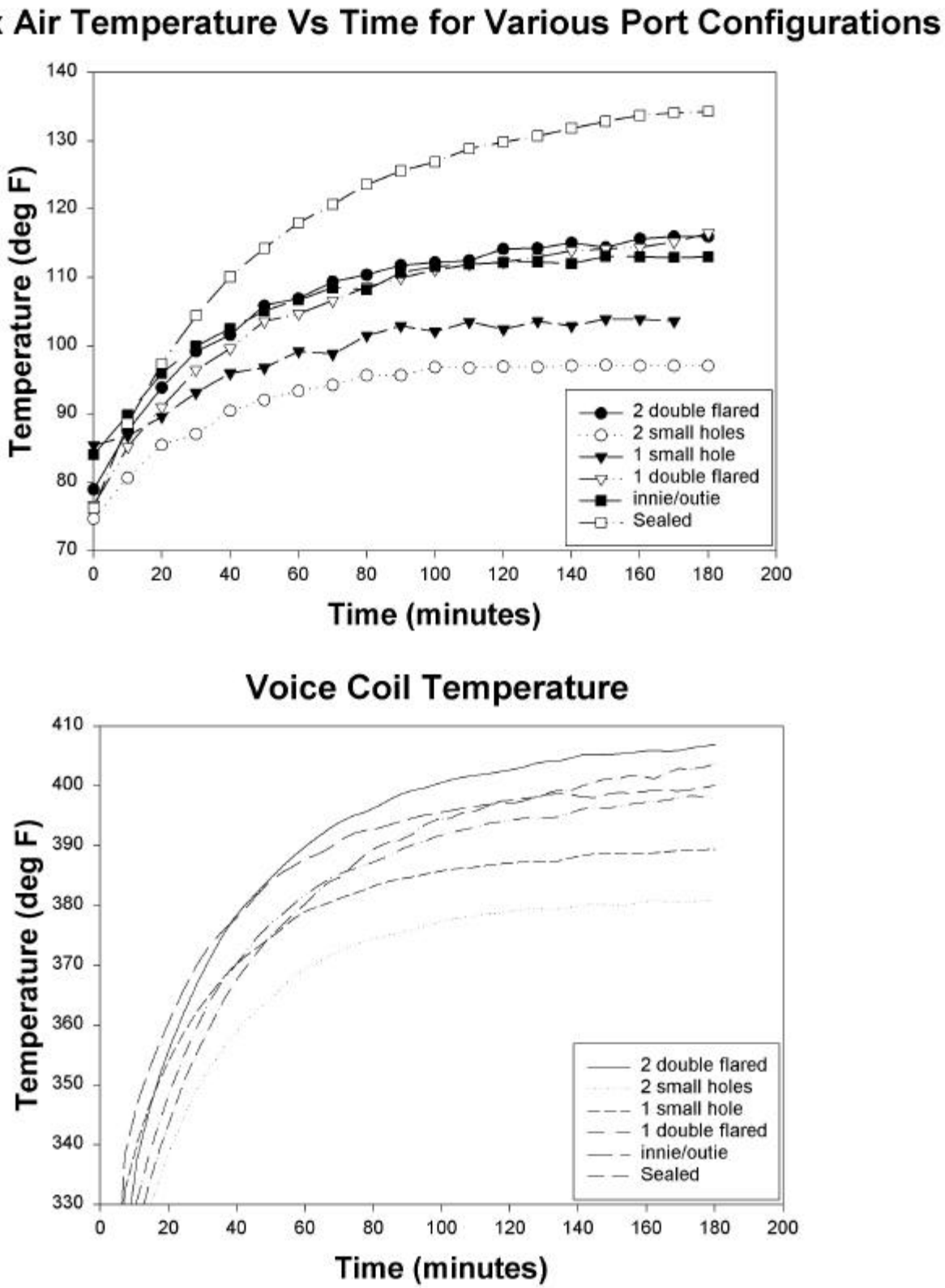

Figure 43b. Thermal repercussions of port placement and geometry